

UNIVERSITY OF CALGARY

Emulsion Layer Growth in Asphaltene/Solids-Stabilized Water-in-Oil Emulsions

by

Michaela McGurn

A THESIS

SUBMITTED TO THE FACULTY OF GRADUATE STUDIES
IN PARTIAL FULFILMENT OF THE REQUIREMENTS FOR THE
DEGREE OF MASTER OF SCIENCE

GRADUATE PROGRAM IN CHEMICAL ENGINEERING

CALGARY, ALBERTA

AUGUST, 2017

© Michaela McGurn 2017

Abstract

The effect of inorganic, coarse solids on emulsion layer stability and growth was investigated. Factors including solids type (kaolin and silica), size, concentration, and wettability were considered. Model asphaltene-stabilized water-in-oil emulsions were prepared from water and organic phase consisting of solids, asphaltenes, heptane, and toluene. In batch experiments, coalescence rates were determined from the change in emulsion height over time as the emulsion coalesced. In continuous experiments, emulsion layer growth was measured for emulsions in a continuous separator. A material balance/coalescence rate based model was developed and fit to the data. Coarse solids at low concentrations destabilized emulsions in batch separations but, above a threshold concentration, solids increased emulsion stability. In continuous separations, even at feed concentrations below the threshold, solids accumulated in the emulsion until the threshold was reached and stable emulsions were formed. The performance of continuous separations cannot be predicted from batch tests.

Acknowledgements

I would like to thank my supervisor Dr. Harvey Yarranton, lab manager Elaine Baydak, and my fellow members of the Asphaltene and Emulsion Research group for their continued support, guidance and encouragement throughout my M.Sc. studies.

I am grateful to Suncor and Shell for providing bitumen samples for the experimental work. Special regards are extended to Dr. Danuta Sztukowski and Vieman Ali-Marcano for their valuable and insightful comments in the completion of this thesis.

Lastly, I would like to extend my heartfelt thanks to my family, my parents Stephen and Karen McGurn and my sisters Leah and Tess, without whose support this thesis would not have been possible. Most importantly, I dedicate this thesis to my grandmother, Anne Morris, who passed away during my studies at the University of Calgary. May she always be loved and remembered.

Table of Contents

Abstract	ii
Acknowledgements	iii
Table of Contents	iv
List of Tables	vii
List of Figures	ix
List of Symbols, Abbreviations and Nomenclature	xv
CHAPTER 1: INTRODUCTION.....	1
1.1 Thesis Objectives	3
1.2 Thesis Structure	4
CHAPTER 2: LITERATURE REVIEW	6
2.1 Emulsions.....	6
2.1.1 Emulsion Destabilization.....	7
<i>Flocculation</i>	8
<i>Sedimentation/Creaming</i>	9
<i>Coalescence</i>	9
<i>Ostwald Ripening</i>	10
<i>Phase Inversion</i>	11
2.1.2 Emulsion Stabilization.....	11
2.1.3 Emulsion Stabilizers: Surfactants.....	12
2.1.4 Emulsion Stabilizers: Solids.....	14
<i>Effect of Solids Wettability</i>	14
<i>Effect of Initial Particle Location</i>	16
<i>Effect of Solids Size, Shape, and Concentration</i>	16
2.1.5 Emulsion Stabilizers in Crude Oils	18
2.1.5.1 Asphaltenes	19
2.1.5.2 Inorganic Solids	21
2.1.6 Other Factors in Emulsion Stability	24
<i>Droplet Size Distribution</i>	24
<i>Dispersed Phase Volume Fraction</i>	24
2.1.7 Demulsification	25
<i>Chemical Treatment</i>	25
<i>Thermal Treatment</i>	26
<i>Mechanical Treatment</i>	26
<i>Electrical Treatment</i>	26
2.2 Emulsion Layers in Water/Oil Separation Processes	27
2.2.1 Settling in Liquid-Liquid Dispersions	27
<i>Batch Dispersions</i>	28
<i>Continuous Dispersions</i>	29
2.2.2 Mathematical Models	30
2.2.2.1 Hindered Settling and Coalescence Model	30
2.2.2.2 Material Balance Model.....	32
2.3 Rag Layers in Heavy Oil and Oil Sands Processes	33
2.4 Chapter Summary	37

CHAPTER 3: EXPERIMENTAL METHODS.....	39
3.1 Materials	39
3.1.1 Asphaltenes.....	39
3.1.2 Solids	41
3.2 Emulsion Separation Experiments.....	41
3.2.1 Apparatus.....	42
3.2.1.1 Apparatus Cleaning.....	46
3.2.2 Preparation of Bulk Phases.....	47
3.2.3 Batch Experiment	47
3.2.4 Continuous Experiment	48
3.2.5 Decay Experiment	49
3.2.6 Emulsion Layer Water Volume Fraction in Continuous Separation.....	50
3.2.7 Solids Content in Emulsion Layer from Continuous Separations.....	51
3.3 Property Measurements	51
3.3.1 Particle Size Distribution.....	51
3.3.2 Wettability of Solids.....	53
3.3.2.1 Contact Angle Measurement	53
3.3.2.2 Film Flotation Method.....	54
3.3.3 Drop Size Distribution.....	55
CHAPTER 4: MODELING	56
4.1 Batch Model.....	56
4.2 Continuous Growth and Decay Model	59
4.2.1 Decay Model	59
4.2.2 Continuous Model	60
4.2.3 Combined Continuous and Decay Model.....	61
CHAPTER 5: RESULTS AND DISCUSSION	64
5.1 Asphaltene-Stabilized Emulsions	64
5.1.1 Modeling the Experimental Data.....	64
<i>Batch Separation Experiments.....</i>	<i>65</i>
<i>Continuous Separation Experiments</i>	<i>67</i>
5.1.2 Effect of Experimental Variables on Emulsion Stability	70
5.1.2.1 Effect of Asphaltene Source on Emulsion Stability	70
5.1.2.2 Effect of Asphaltene Concentration.....	72
5.1.2.3 Effect of Solvent Type.....	74
5.1.2.4 Effect of Drop Size Distribution/Mixing Conditions	76
5.1.2.5 Effect of Water Volume Fraction	78
5.1.3 Prediction of Continuous Behaviour from Batch Model Parameters.....	81
5.1.4 Selection of Base Case Emulsion for Solids Addition	85
5.2 Solids-Stabilized Emulsions	85
5.2.1 Solids Properties.....	86
<i>Surface Wettability.....</i>	<i>86</i>
<i>Particle Size Distribution.....</i>	<i>87</i>
5.2.2 Effect of Solids Addition in the Batch Experiment.....	88
5.2.2.1 Effect of Solids Type, Size, and Contact Angle	90
5.2.3 Effect of Solids Addition in the Continuous Experiment.....	95

5.2.4 Prediction of Continuous Behaviour in the Presence of Solids.....	99
CHAPTER 6: CONCLUSIONS AND RECOMMENDATIONS.....	101
6.1 Asphaltene-Stabilized Emulsions	101
6.2 Solids-Stabilized Emulsions	102
6.3 Recommendations.....	102
REFERENCES.....	104
APPENDIX A:Water Volume Fraction in the Batch Experiment.....	117
APPENDIX B: Effect of CSS and SAGD Asphaltene Concentration.....	124
APPENDIX C:Error Analysis	126
C.1 Error Analysis Theory.....	126
C.1.1 Error in Repeated Measurements.....	126
C.1.2 Average Absolute Relative Deviation	127
C.2 Emulsion Layer Height	127
C.2.1 Batch Experiment	127
<i>Asphaltene-Stabilized Emulsions</i>	127
<i>Solids-Stabilized Emulsions</i>	129
C.2.2 Continuous Experiment	130
C.2.3 Decay Experiment.....	131
C.3 Solids Contact Angle Measurements	132
<i>Kaolin</i>	132
<i>Silica</i>	133
C.4 Water Volume Fraction in the Continuous Experiment.....	133
C.5 Particle Size Distribution	134
C.6 Droplet Size Distribution.	134

List of Tables

Table 3.1 Solids free C7-asphaltene and toluene-insoluble (TI) contents of OS, CSS, and SAGD bitumen.....	40
Table 5.1 Model parameters used for batch and continuous experiments for water-in-toluene emulsions stabilized by asphaltene extracted from OS bitumen. The measured emulsion layer growth rate, dh/dt , for the continuous experiment is also tabulated.	67
Table 5.2 Model parameters used for batch and continuous experiments for water-in-toluene emulsions stabilized by asphaltene extracted from OS, CSS, and SAGD bitumen.....	70
Table 5.3 Model parameters used for batch and continuous experiments for water-in-toluene emulsions stabilized by OS/SAGD asphaltene blends.....	72
Table 5.4 Model parameters used for batch and continuous experiments for water-in-toluene emulsions stabilized by OS asphaltene at concentrations between 0.5 and 10 g/L.	74
Table 5.5 Model parameters used for batch and continuous experiments for water-in-50/50 heptol emulsions stabilized by asphaltene extracted from OS, CSS and SAGD bitumen....	76
Table 5.6 Model parameters used for batch and continuous experiments for water-in-toluene emulsions stabilized 1.5 g/L OS, CSS, and SAGD asphaltenes at a mixing speed of 10,000 rpm.	78
Table 5.7 Model parameters used for batch water-in-toluene emulsions stabilized by 0.5 g/L OS asphaltenes and prepared with initial water volume fractions ranging from 0.25 to 0.85.....	80
Table 5.8 Model parameters used for batch water-in-toluene emulsions stabilized by 1.5 g/L OS asphaltenes and prepared with initial water volume fractions ranging from 0.25 to 0.80.....	80
Table 5.9 Model parameters used for batch experiments for water-in-toluene emulsions stabilized 1.5 g/L OS asphaltenes and 12 μm kaolin particles (contact angle of 80°) at solids concentrations from 0.05 to 20 g/L.....	90
Table 5.10 Model parameters used for batch experiments for water-in-toluene emulsions stabilized 1.5 g/L OS asphaltenes and 12 μm kaolin particles (contact angle of 50°) at solids concentrations from 1 to 20 g/L.....	91
Table 5.11 Model parameters used for batch experiments for water-in-toluene emulsions stabilized 1.5 g/L OS asphaltenes and 12 μm kaolin particles (contact angle of 125°) at solids concentrations from 0.05 to 20 g/L.....	91
Table 5.12 Model parameters used for batch experiments for water-in-toluene emulsions stabilized 1.5 g/L OS asphaltenes and 32 μm silica particles (contact angle of 75°) at solids concentrations from 0.05 to 20 g/L.....	92

Table 5.13 Model parameters used for batch experiments for water-in-toluene emulsions stabilized 1.5 g/L OS asphaltenes and 32 μm silica particles (contact angle of 115°) at solids concentrations from 0.25 to 20 g/L.....	92
Table 5.14 Model parameters used for batch experiments for water-in-toluene emulsions stabilized 1.5 g/L OS asphaltenes and 18 μm silica particles (contact angle of 75°) at solids concentrations from 0.05 to 20 g/L.....	93
Table 5.15 Model parameters from continuous experiments for water-in-toluene emulsions stabilized by 1.5 g/L OS asphaltenes and 12 μm kaolin particles (contact angle of 80°).....	97
Table 5.16 Model parameters from continuous experiments for water-in-toluene emulsions stabilized by 1.5 g/L OS asphaltenes and 32 μm silica particles (contact angle of 75°).	97
Table 5.17 Calculated kaolin concentrations in the continuous phase of the emulsion layer for the continuous experiment water-in-toluene emulsions stabilized by 1.5 g/L OS asphaltenes and 12 μm kaolin particles with a contact angle of 80° or 32 μm silica particles with a contact angle of 75°.....	99
Table B.1 Model parameters used for batch experiments for water-in-toluene emulsions stabilized by CSS and SAGD asphaltene at concentrations between 0.5 and 5 g/L.....	125
Table C.1 Error analysis for emulsion layer height in the batch experiment for a water-in-50/50 heptol emulsion stabilized by 1.5 g/L CSS asphaltenes	128
Table C.2 Error analysis for emulsion layer height in the batch experiment for a water-in-toluene emulsion stabilized by 0.25 g/L kaolin (80° contact angle).....	129
Table C.3 Error analysis for emulsion layer height in the continuous experiment for a water-in-toluene emulsion stabilized by 0.25 g/L kaolin (80° contact angle).	130
Table C.4 Error analysis for emulsion layer height in the decay experiment for a water-in-toluene emulsion stabilized by 0.25 g/L kaolin (80° contact angle).....	131
Table C.5 Error analysis for contact angle measurements for kaolin-50/50 heptol-water systems, where the kaolin has been treated with 0.02-1 g/L OS asphaltenes.	132
Table C.6 Error analysis for contact angle measurements for silica-50/50 heptol-water systems, where the silica has been treated with 0.02-1 g/L OS asphaltenes.....	133
Table C.7 Error analysis for the water volume fraction in the emulsion layer.	133
Table C.8 Error analysis for the particle size distributions.....	134
Table C.9 Error analysis for the droplet size distributions.	134

List of Figures

Figure 2.1 Schematic representation of emulsion breakdown processes.....	8
Figure 2.2 Schematic representation of the three step coalescence process.....	10
Figure 2.3 Surfactant structures for water continuous phases below CMC adsorb as monomers at interface or above CMC as micelles.	13
Figure 2.4 Position of spherical water-wet, bi-wettable and oil-wet solids at the oil water interface.....	15
Figure 2.5 Positioning of fine and coarse solids in an emulsion.....	18
Figure 2.6 Proposed archipelago structure of an asphaltene molecule with an elemental formula of $C_{420}H_{496}N_6S_{14}O_4V$, an H/C ratio of 1.18 and a molecular weight of 6191 g/mol (Spiecker <i>et al.</i> , 2003).....	20
Figure 2.7 Role of solids in the stabilization of water-in-oil emulsions: a) solids adsorbed on the interface, b) solids trapped between droplets.....	21
Figure 2.8 Conceptual model of bitumen solids.	23
Figure 2.9 Flocculation (I), sedimentation (II) and dense-packed (III) zones in a steady-state closed packed dispersion where the dense phase is the dispersed phase.....	28
Figure 2.10 Non steady-state batch dispersion containing sedimentation and dense-packed zones over time..	29
Figure 2.11 Rag layer formation in oil sand separation vessels.....	35
Figure 3.1 Emulsion preparation apparatus: a) Teflon disc (lid); b) Teflon baffles; c) overhead mixer; d) beaker; e) beaker setup assembled with all parts from (a) to (d).	43
Figure 3.2 Schematic diagram of the continuous apparatus setup: 1) feed emulsion tubing; 2) emulsion layer; 3) oil recycle tubing; 4) separator with water jacket; 5) pump; 6) water recycle tubing; 7) Teflon baffle; 8) Teflon disc (lid); 9) impeller; 10) water-in-oil emulsion; 11) beaker; 12) water bath.....	44
Figure 3.3 Schematic diagram of the separator used in continuous experiments: 1) feed port; 2) separator overflow exit; 3) water jacket; 4) oil exit valve; 5) oil exit; 6) glass emulsion feed tube; 7) feed outlet; 8) free oil phase; 9) water jacket outlet; 10) emulsion layer; 11) centerline; 12) free water phase; 13) water jacket inlet; 14) water exit valve; 15) water exit.....	45
Figure 3.4 Dimensions of the 250 mL glass separator used in continuous experiments.	46
Figure 3.5 Batch experiment schematic of the emulsion beaker at different time steps.....	48

Figure 3.6 Schematic representation of the emulsion layer height over time during the continuous and the decay experiment: 1) original separator; 2) continuous experiment begins with pump turned on and emulsion feed into separator; 3) emulsion layer growth in separator; 4) pump turned off at beginning of decay experiment; 5) emulsion layer coalesces into free water and oil layers.....	50
Figure 3.7 Drop shape analyzer equipped with camera measures the solid-water-heptol contact angle of compressed solids through the water phase.	54
Figure 3.8 Film floatation method to measure relative wettability of coarse solids through critical surface tension.	55
Figure 4.1 Material balance on the dispersed water in the emulsion layer over time in the batch experiment.....	57
Figure 4.2 Material balance on the free water in the batch experiment.....	59
Figure 4.3 Material balance on the dispersed water in the emulsion layer in the continuous experiment.....	61
Figure 4.4 Division of emulsion into individual layers in combined continuous and decay model.....	62
Figure 4.5 Block flow diagram of the algorithm for the numerical model.....	63
Figure 5.1 Emulsion and the water layer heights over time for a batch experiment performed at 60°C and 1000 rpm with an overhead mixer. The emulsion was prepared with an initial water volume of 0.50. The organic phase consisted of 1.5 g/L OS asphaltenes in toluene..	65
Figure 5.2 Water volume fractions over time for a batch experiment performed at 60°C and 1000 rpm with an overhead mixer. The emulsion was prepared with an initial water volume of 0.50. The organic phase consisted of 1.5 g/L OS asphaltenes in toluene.....	67
Figure 5.3 Continuous experiment emulsion layer heights over time for a W/O emulsion stabilized by OS asphaltenes at 60°C. The emulsion was prepared with an initial water volume fraction of 0.50 and an organic phase of 1.5 g/L asphaltenes in toluene.	68
Figure 5.4 Emulsion layer heights for batch tests (a) and continuous tests (b) over time for W/O emulsions stabilized by OS, CSS, and SAGD asphaltenes at 60°C. Model emulsions were prepared with 50 vol% aqueous phase and 50 vol% organic phase. The organic phase was 1.5 g/L of asphaltenes in toluene.	70
Figure 5.5 Emulsion layer heights for (a) batch experiments and (b) continuous experiments over time for W/O emulsions stabilized by OS/SAGD asphaltene blends at 60°C. Model emulsions were prepared with 50 vol% aqueous phase and 50 vol% organic phase. The organic phase was 1.5 g/L of C7-asphaltenes in toluene.	72

Figure 5.6 Emulsion layer height over time for W/O emulsions stabilized by OS asphaltenes: a) batch experiments at 21°C; b) continuous separations at 60°C. Model emulsions were prepared with 50 vol% aqueous phase and 50 vol% organic phase. The organic phases consisted of 0.5, 1.5, 2.5, 5 and 10 g/L of asphaltenes in toluene.	74
Figure 5.7 Emulsion layer height over time for W/O emulsions stabilized by OS, CSS and SAGD asphaltenes: a) batch experiments; b) continuous separations at 60°C. Model emulsions were prepared with 50 vol% aqueous phase and 50 vol% organic phase. The organic phases consisted of 1.5 g/L of asphaltenes in 50/50 heptol.	76
Figure 5.8 Droplet size distribution of OS asphaltene stabilized water-in-toluene emulsions prepared with an overhead mixer at 1000 rpm or a homogenizer at 10,000 rpm at 60°C.	77
Figure 5.9 Emulsion layer height over time for a) batch experiments W/O emulsions stabilized by OS, CSS and SAGD asphaltenes; b) continuous separations W/O emulsions stabilized by OS asphaltenes prepared at a mixing speed of 10,000 rpm with a homogenizer. Model emulsions were prepared at 60°C with 50 vol% aqueous phase and 50 vol% organic phase. The organic phases consisted of 1.5 g/L of C7-asphaltenes in toluene.	78
Figure 5.10 Batch emulsion layer height over time for W/O emulsions prepared with initial water volume fraction varying from 0.25 to 0.85 at 60°C for emulsions with organic phases consisting of a) 0.5 g/L of OS asphaltenes in toluene; b) 1.5 g/L of OS asphaltenes in toluene.	80
Figure 5.11 Fitted coalescence rate (a) and dimensionless limiting height (b) for batch and continuous tests on W/O emulsions stabilized by OS, CSS, and SAGD asphaltenes. In legend: B=batch, C=continuous; the number indicates the mixing rpm. Note, continuous tests at 10,000 rpm were not performed with the CSS and SAGD asphaltenes due to sample limitations.	81
Figure 5.12 Measured emulsion layer growth rate versus fractional bypass for batch and continuous tests on W/O emulsions stabilized by OS, CSS, and SAGD asphaltenes at 60°C.	82
Figure 5.13 Batch model parameters coalescence rate constant and dimensionless limiting height for W/O emulsions stabilized by OS, CSS, and SAGD asphaltenes.	83
Figure 5.14 Correlation between continuous emulsion model parameters and batch test dimensionless limiting heights for W/O emulsions stabilized by OS, CSS, and SAGD asphaltenes in toluene, 50/50 heptol, at mixing speeds of 1000 and 10,000 rpm at 60°C. The lines are empirical fits to the data.	84
Figure 5.15 Measured contact angles for (a) kaolin and (b) silica solids after treatment with OS asphaltenes in a 50/50 heptol solution.	87
Figure 5.16 Particle size distribution of treated kaolin and silica measured in 50/50 heptol solution.	88

Figure 5.17 Batch separation experiment emulsion layer heights over time for W/O emulsion stabilized by OS asphaltenes with added kaolin with an 80° contact angle at 60°C: a) at low kaolin concentration b) at high kaolin concentration. The emulsions were prepared with 50 vol% aqueous phase and 50 vol% organic phase. The organic phase was 1.5 g/L of OS C7-asphaltene dissolved in toluene plus added kaolin.....	89
Figure 5.18 Batch and continuous (a) dimensionless limiting height and (b) coalescence rate constant and for W/O emulsions stabilized by OS asphaltene and kaolin (80° contact angle) in toluene and mixed at 10,000 rpm at 60°C.	90
Figure 5.19 Batch separation experiment emulsion layer heights over time for W/O emulsion stabilized by OS asphaltene with added kaolin (12 µm) with measured contact angles of 50° (closed symbols) and 125° (open symbols) at (a) low concentrations and (b) high concentrations. Emulsions were prepared with 50 vol% aqueous phase and 50 vol% organic phase with a total volume of 50 mL and 10,800 rpm mixing speed. The organic phase was 1.5 g/L of C7-asphaltene dissolved in toluene plus added kaolin.....	91
Figure 5.20 Batch separation experiment emulsion layer heights over time for W/O emulsion stabilized by silica (32-63 µm) with measured contact angles of 75° (closed symbols) and 115° (open symbols): a) at low silica concentration; b) at high silica concentration. The emulsions were prepared with 50 vol% aqueous phase and 50 vol% organic phase with a total volume of 50 mL and 10,800 rpm mixing speed. The organic phase was 1.5 g/L of OS C7-asphaltene dissolved in toluene plus added silica.	92
Figure 5.21 Batch separation experiment emulsion layer heights over time for W/O emulsion stabilized by OS asphaltene with added silica (18-32 µm) with a 75° contact angle; a) at low concentrations, b) at high concentrations. The emulsions were prepared with 50 vol% aqueous phase and 50 vol% organic phase with a total volume of 50 mL and 10,800 rpm mixing speed. The organic phase was 1.5 g/L of C7-asphaltene dissolved in toluene plus added silica.....	93
Figure 5.22 Batch dimensionless limiting height for W/O emulsions stabilized by OS asphaltene and solids in toluene and mixed at 10,000 rpm at 60°C: a) kaolin (K) with contact angles of 50, 80, and 125°; b) 18 µm silica (S18) with a contact angles of 75° and 32 µm silica (S32) with contact angles of 75 and 115°.	94
Figure 5.23 Continuous experiment emulsion layer height over time for OS asphaltene stabilized W/O emulsions with added kaolin (80° contact angle) at 60°C. The emulsions were prepared with 50 vol% aqueous phase and 50 vol% organic phase with a 10,000 rpm mixing speed. The organic phase was 1.5 g/L of OS asphaltene dissolved in toluene plus added kaolin.	96
Figure 5.24 Continuous experiment emulsion layer height over time for OS asphaltene stabilized W/O emulsions with added silica (32 µm, 75° contact angle) at 60°C. The emulsions were prepared with 50 vol% aqueous phase and 50 vol% organic phase with a 10,000 rpm mixing speed. The organic phase was 1.5 g/L of OS asphaltene dissolved in toluene plus added silica.	96

Figure 5.25 Effect of solids content on continuous experiment emulsion layer growth rate for OS asphaltene stabilized W/O emulsions with added kaolin (80° contact angle) and silica (75° contact angle) at 60°C. The emulsions were prepared with 50 vol% aqueous phase and 50 vol% organic phase with a 10,000 rpm mixing speed. The organic phase was 1.5 g/L of OS asphaltenes dissolved in toluene plus added solids.....	98
Figure 5.26 Effect of solids on correlation between continuous emulsion model parameters and batch test dimensionless limiting heights for W/O emulsions stabilized by asphaltenes in toluene at 60°C.....	100
Figure A.1 Batch separation emulsified water volume fractions over time for W/O emulsions stabilized by OS, CSS, and SAGD asphaltenes at 60°C. Model emulsions were prepared with 50 vol% aqueous phase and 50 vol% organic phase. The organic phase was 1.5 g/L of asphaltenes in toluene.	117
Figure A.2 Batch water volume fractions over time for W/O emulsions stabilized by OS/SAGD asphaltene blends at 60°C. Model emulsions were prepared with 50 vol% aqueous phase and 50 vol% organic phase. The organic phase was 1.5 g/L of C7-asphaltenes in toluene.	118
Figure A.3 Batch water volume fractions over time for W/O emulsions stabilized by OS asphaltenes at 21°C and a total volume of 50 mL. Model emulsions were prepared with 50 vol% aqueous phase and 50 vol% organic phase. The organic phases consisted of 0.5, 1.5, 2.5, 5 and 10 g/L of asphaltenes in toluene.....	118
Figure A.4 Batch water volume fractions over time for water-in-50/50 heptol emulsions stabilized by OS, CSS and SAGD asphaltenes at 60°C. Model emulsions were prepared with 50 vol% aqueous phase and 50 vol% organic phase. The organic phases consisted of 1.5 g/L of C7-asphaltenes in 50/50 heptol.	119
Figure A.5 Batch water volume fractions over time for W/O emulsions stabilized by OS, CSS and SAGD asphaltenes prepared at a mixing speed of 10,000 rpm with a homogenizer. Model emulsions were prepared at 60°C with 50 vol% aqueous phase and 50 vol% organic phase. The organic phase consisted of 1.5 g/L of C7-asphaltenes in toluene.....	119
Figure A.6 Batch water volume fractions over time for W/O emulsions stabilized by OS asphaltenes prepared with initial water volume fractions from 0.25 to 0.85. Model emulsions were prepared at 60°C with 50 vol% aqueous phase and 50 vol% organic phase. The organic phases consisted of a) 0.5 g/L; b) 1.5 g/L of C7-asphaltenes in toluene.	120
Figure A.7 Batch water volume fractions over time for W/O emulsion stabilized by OS asphaltenes with added kaolin with an 80° contact angle (a) low kaolin concentrations and (b) high kaolin concentrations. The emulsions were prepared with 50 vol% aqueous phase and 50 vol% organic phase. The organic phase was 1.5 g/L of OS C7-asphaltenes dissolved in toluene plus added kaolin.	120
Figure A.8 Batch water volume fractions over time for W/O emulsion stabilized by OS asphaltenes with added kaolin (12 µm) with a measured contact angle of 50° at (a) low	

concentrations and (b) high concentrations. Emulsions were prepared with 50 vol% aqueous phase and 50 vol% organic phase with a total volume of 50 mL and 10,800 rpm mixing speed. The organic phase was 1.5 g/L of C7-asphaltenes dissolved in toluene plus added kaolin. 121

Figure A.9 Batch water volume fractions over time for W/O emulsion stabilized by OS asphaltenes with added kaolin (12 μm) with a measured contact angle of 125° at (a) low concentrations and (b) high concentrations. Emulsions were prepared with 50 vol% aqueous phase and 50 vol% organic phase with a total volume of 50 mL and 10,800 rpm mixing speed. The organic phase was 1.5 g/L of C7-asphaltenes dissolved in toluene plus added kaolin. 121

Figure A.10 Batch water volume fractions over time for W/O emulsion stabilized by silica (32-63 μm) with a measured contact angles of 75° : a) at low silica concentration b) at high silica concentration. The emulsions were prepared with 50 vol% aqueous phase and 50 vol% organic phase with a total volume of 50 mL and 10,800 rpm mixing speed. The organic phase was 1.5 g/L of OS C7-asphaltene dissolved in toluene plus added silica.... 122

Figure A.11 Batch water volume fractions over time for W/O emulsion stabilized by silica (32-63 μm) with a measured contact angles of 115° : a) at low silica concentration b) at high silica concentration. The emulsions were prepared with 50 vol% aqueous phase and 50 vol% organic phase with a total volume of 50 mL and 10,800 rpm mixing speed. The organic phase was 1.5 g/L of OS C7-asphaltenes dissolved in toluene plus added silica. . 122

Figure A.12 Batch water volume fractions over time for W/O emulsion stabilized by OS asphaltenes with added silica (18-32 μm) with a 75° contact angle. The emulsions were prepared with 50 vol% aqueous phase and 50 vol% organic phase with a total volume of 50 mL and 10,800 rpm mixing speed. The organic phase was 1.5 g/L of C7-asphaltenes dissolved in toluene plus added silica. 123

Figure B.1 Emulsion layer height over time for W/O emulsions stabilized a) CSS and b) SAGD asphaltenes for batch experiments at 60°C . Model emulsions were prepared with 50 vol% aqueous phase and 50 vol% organic phase with a total volume of 1600 mL and were mixed a 1000 rpm. The organic phases consisted of 0.5, 1.5, 2.5, and 5 g/L of C7-asphaltenes in toluene. 124

Figure B.2 Batch water volume fractions over time for W/O emulsions stabilized by (a) CSS and (b) SAGD asphaltenes at 60°C . Model emulsions were prepared with 50 vol% aqueous phase and 50 vol% organic phase. The organic phase was 0.5, 1.5, 2.5, and 5 g/L of C7-asphaltenes in toluene. 125

List of Symbols, Abbreviations and Nomenclature

English Letters

A	cross-sectional area (m^2)
C	concentration (g/L)
c	constant
d	distribution midpoint
dh/dt	growth rate (cm/min)
f_N	number frequency
h	height (m)
k	coalescence rate constant (min^{-1})
m	mass (g)
M	total mass (g)
n	number of measurements
N	total number of values
s	standard deviation
t	time (s), t -distribution
v	degrees of freedom
V	volume (L)
w	weighted calibration factor
x	position of sedimenting interface
y	position of coalescing interface

Greek Letters

α	confidence interval
γ	calibration exponent
ε	fractional bypass
θ	contact angle ($^\circ$)
μ	population mean
ρ	density (g/m^3)
ψ	droplet coalescence rate
Φ	volume fraction

Superscripts

o	initial measurement
-----	---------------------

Subscripts

<i>d</i>	dispersed phase
<i>e</i>	emulsion
<i>exp</i>	experimental measurement
<i>fit</i>	predicted measurement
<i>fw</i>	free water
<i>i</i>	i^{th} component in the system
<i>in</i>	influx stream
<i>lim</i>	limiting value
<i>o</i>	oil
<i>out</i>	extant stream
<i>p</i>	dense packed zone
<i>s</i>	sedimentation zone
<i>solids</i>	solids content
<i>t</i>	total quantity
<i>w</i>	water
∞	initial experimental value

Abbreviations

OS	oil sands
CSS	cyclic steam stimulation
SAGD	steam assisted gravity drainage
W/O	water-in-oil
O/W	oil-in-water
AARD	average absolute relative deviation
CMC	critical micelle concentration
FBRM	focus beam reflectance measurement
RO	reverse osmosis
TI	toluene insoluble

CHAPTER 1: INTRODUCTION

Alberta contains large unconventional fuel deposits in the form of mineable oil sands and *in situ* heavy oil and bitumen. These oil reserves contain an estimated 168 billion barrels of recoverable oil and in 2016 total oil sands production reached 2.4 million barrels per day (Canadian Association of Petroleum Producers, 2017). One major challenge is the separation of crude oil and co-produced water and solids during oil sand processing or at the oilfield battery for *in situ* processes. This oil-water separation usually requires heat and/or chemical treatment. In some cases, even after treatment, poor separation occurs when a viscous layer of emulsified water droplets stabilized by asphaltenes and fine solids, known as a rag layer, develops at the oil-water interface. The formation and growth of rag layers can be challenging to predict and costly to deal with.

The recovery of bitumen from oil sands deposits consists of two major stages: extraction and froth treatment. Bitumen is extracted from shallow, minable oil sands deposits using the Clark Hot Water Extraction process, an air assisted floatation process, developed by Karl Clark in 1920 and commercialized in the late 1960s. The mined ore is crushed and then mixed with warm water and/or steam, naturally entrained air, and chemical additives (*e.g.*, NaOH) to prepare a 40-55°C slurry. The slurry is conditioned as it is transported in a hydro-transport pipeline to a primary separator, often a large gravity-separation vessel. During transport in the pipeline, turbulence liberates bitumen droplets from solids particles and the droplets attach to entrained air bubbles, becoming aerated. In the separation vessel, the aerated bitumen floats to the top and is skimmed off as a bitumen rich froth. Coarse sand, fine solids, clays and a fraction of the bitumen sink to the bottom and are sent to tailings ponds. The middle layer is often re-aerated to recover additional bitumen.

The bitumen froth from oil sand extraction processes is typically composed of 60% bitumen, 30% water, and 10% solids by mass (Kupai *et al.*, 2013) and must be further treated to meet downstream process specifications. Any remaining air bubbles and free water are easily removed by heating or gravity drainage, but emulsified water (droplets 2-10 μm in diameter) and suspended solids (fine

clays <1-2 μm in diameter) are more difficult to remove. In addition, bitumen and water have similar densities; therefore, there is little driving force for the two liquids to separate by gravity settling or creaming. Methods to separate water droplets from bitumen froths aim to reduce the viscosity and density of the bitumen and flocculate water droplets to promote settling. The separation is typically achieved through the addition of a diluent and settling techniques that include separators, inclined plate settlers, and centrifuges.

Deeper bitumen deposits require the injection of steam in cyclic steam stimulation (CSS) or steam assisted gravity drainage (SAGD) extraction processes. In CSS, steam is injected into a vertical well and left for a period of time to heat the oil sands to approximately 250°C. The heat reduces bitumen viscosity by orders of magnitude so that it can be pumped to the surface out the same well. The cycle of steam injection followed by oil production is then repeated. SAGD uses two parallel horizontal wells, with their horizontal segments drilled one above the other in the lower part of the reservoir, for simultaneous steam injection and bitumen production. Steam is injected into the upper well and the heated bitumen and condensed steam flow to the lower well, where they are pumped to the surface. The product from the well is a mixture of heavy oil or bitumen and water and is sent to a heater-treater separator to separate the oil from the water.

In bitumen/water separation vessels, the accumulation of a persistent, viscous layer of intermediate density at the oil-water interface is commonly observed. This layer, known as a rag layer, is a complex fluid comprised of emulsified water and/or oil, interfacially active organic matter from the bitumen, and produced solids. (Saadatmand *et al.*, 2008; Czarnecki *et al.*, 2007; Kupai *et al.*, 2013). Rag layers grow when the coalescence rate of the emulsified droplets leaving the emulsion is slower than the settling/creaming rate of droplets entering the emulsion layer (Frising *et al.*, 2006). When coalescence rates are significantly reduced, rag layers can grow large enough to reduce separation efficiencies and cause process upset (Saadatmand *et al.*, 2008). Gravity settling alone will not result in timely separation of oil and water and even heating and chemical demulsifying techniques are not always sufficient.

For oil sands bitumen and heavy oil processing, water-in-oil (W/O) emulsions stabilized by asphaltenes and inorganic solids are often the most problematic to treat and are likely contributors to rag layer formation. The presence of asphaltenes and solids in oil sands froths attribute to the stability of these W/O emulsions by absorbing at the oil-water interface and resisting droplet coalescence by hindering collisions and contact between droplets. Solids packing between adjacent droplets further decreases coalescence because the trapped solids prevent dispersed droplets from aggregating, creaming or sedimenting, and coalescing (Yan *et al.*, 2001; Yan and Masliyah, 1993). The ability of solids to stabilize emulsions depends on the solids size, concentration and wettability, and the strong stability and formation of rag layers can be attributed to the presence of high concentrations of fine, oil-wet solids (Sztukowski and Yarranton, 2004).

Rag layer treatment can be costly and therefore, it is desirable to develop less expensive techniques for rag layer destabilization. Most studies have been done as batch bench-top laboratory experiments. These studies can provide insight into characterizing rag materials and understanding the effects of rag components, such as asphaltenes and solids, on emulsion stability in batch separations. However, the mechanisms that trigger rag layer growth in continuous separations have not been investigated. Continuous systems are more complex and it is difficult to stop rag layer accumulation and subsequent flooding in the separator under poor operating conditions. The purpose of this thesis is to investigate rag layer stability and growth in asphaltene stabilized water-in-oil emulsions in the presence of solid particles in both batch and continuous separations.

1.1 Thesis Objectives

In this thesis, the effect of coarse inorganic solids on emulsion stability and rag layer growth and accumulation is investigated using batch and continuous separations performed on model water-in-oil emulsions stabilized by asphaltenes. Solids properties, such as size, concentration and wettability, and asphaltene concentration and source are considered and related to trends in model emulsion stability. The emulsions are then modeled with a material balance to evaluate the use of batch stability experiments as a screening test for rag layer growth and stability. The specific objectives are to:

- Measure rag layer growth in batch and continuous water-oil separations for water-oil emulsions with different asphaltenes, asphaltene concentrations, solvent types, drop size distributions, solids contents, particle size distributions, and solids wettability.
- Model batch and continuous rag layer growth based on the coalescence rate.
- Assess the ability to predict rag layer growth in continuous separations from batch tests and batch model parameters.
- Relate emulsion stability and rag layer growth to solid properties and accumulation.

Model emulsions were used to simplify the systems and to isolate the effects of solids. The first set of water-in-oil emulsions were prepared from an aqueous phase consisting only of water and an organic phase consisting of asphaltenes dissolved in toluene and heptane. These asphaltene stabilized emulsions were intended as baselines for solids addition. The second set of emulsions were prepared in the same way, but kaolin and silica were added to the organic phase with the asphaltenes. These emulsions were used to assess the effect of the solids on rag layer growth.

Emulsion stability was measured in batch experiments and a previously developed laboratory scale continuous separation experiment (Khatri *et al.*, 2011) was used to measure emulsion layer growth. Material balances based on the rate at which the dispersed phase in the emulsions layer exits the settled emulsion were adapted and used to model the experimental results and determine the coalescence rates, emulsion layer growth rates and other parameters.

1.2 Thesis Structure

This thesis is organized into the following chapters:

Chapter 2 reviews the background concepts on emulsions: emulsion stabilization and destabilization and surfactants are reviewed. Previous research on the mechanisms of solid stabilization of emulsions and the characterization of oil sands solids is presented and the rag layer is defined for oil sands and *in situ* process separations.

Chapter 3 outlines the method used to prepare the model emulsions and the procedures for the

batch, decay, and continuous experiments. The experiments performed to determine the wettability and particle size, and drop size distributions of the solids used in this thesis are also presented.

Chapter 4 develops the model equations for batch, decay, and continuous experiments. The models are based on a material balance performed on the dispersed phase within the emulsion layer and are fit to the experimentally measured emulsion layer heights.

Chapter 5 presents the experimental and modeling results. The effects of asphaltene source, asphaltene concentration, solvent type, water content, and drop size distribution are evaluated from both batch and continuous experiments. The predictive capability of the batch model parameters for determining emulsion stability in continuous separations is evaluated. A base case system is defined to evaluate the effect of adding solids. Kaolin and silica solids of different size distributions and surface properties are then added to the emulsions to determine the effect of solids type, size and concentration on emulsion stability in batch and continuous experiments. The predictive capability of the batch model parameters for determining emulsion stability in continuous separations is then re-evaluated.

Chapter 6 summarizes the thesis conclusions and presents recommendations for future work.

CHAPTER 2: LITERATURE REVIEW

Rag layers are an accumulation of emulsions and solids that can form during water/oil separation processes. In this chapter, the fundamentals of emulsions are reviewed with a focus on emulsion stabilization and destabilization mechanisms. The main emulsion stabilizers in heavy oils, asphaltenes and inorganic solids, are discussed. Demulsification processes and the modeling of the accumulation of emulsion layers in these water-oil separations are also discussed. The focus is on water-in-oil emulsions since they are usually the most problematic emulsions encountered in oil sands mining and heavy oil *in situ* operations and are likely contributors to rag layer formation. Finally, rag layer formation in these processes is reviewed.

2.1 Emulsions

An emulsion is a mixture of two immiscible liquids in which droplets of one liquid (the dispersed or internal phase) are dispersed in a second liquid (the continuous or external phase). There are two main types of emulsions: water-in-oil emulsions (W/O), where water droplets are suspended in an oil matrix, or oil-in-water emulsions (O/W) with oil droplets dispersed in a continuous water phase. W/O and O/W emulsions are also referred to as “regular” and “reverse” emulsions, respectively. Multiple emulsions such as oil-in-water-in-oil or water-in-oil-in-water can also occur. The type of emulsion formed depends on several factors such as the water-oil ratio, type and concentration of surfactants and electrolytes, and temperature. The type of emulsion can be determined with a dilution test because the emulsion can be dispersed in the same phase as the continuous phase (Kupai *et al.*, 2013). If the emulsion is diluted with water, water is the dispersion medium and the emulsion is O/W type. If the added water forms a separate layer, the emulsion is W/O type.

Emulsions can also be categorized based on the size of the dispersed droplets. Micro-emulsions have small droplets with diameters on the order of 1 to 100 nm. These isotropic emulsions can be thermodynamically stable and have very low interfacial tension. Most emulsions are macro-

emulsions and are thermodynamically unstable. These emulsions have larger droplets with non-zero interfacial tension. Energy, typically in the form of agitation, is required for their formation.

Macro-emulsions have large interfacial areas where oil and water molecules are forced into contact with each other. The unlike particles at the interface have a greater interaction energy than when surrounded by like molecules in their respective bulk phases. In addition, the hydrogen bonding networks in the water phase are disrupted at the interface. Hence, the formation of an emulsion leads to an increase in excess energy in the form of interfacial tension (also known as surface energy). Droplets tend to be spherical and coalesce in order to reduce the surface area and so minimize the surface energy. Therefore, once formed, emulsions tend to separate back into their constituent bulk phases over time.

2.1.1 Emulsion Destabilization

Emulsions tend to destabilize over time through various breakdown processes such as flocculation, sedimentation or creaming, coalescence, Ostwald ripening, and phase inversion (Figure 2.1). These kinetic processes may take place simultaneously or consecutively and can result in complete separation of the phases. Flocculation and sedimentation/creaming result in a change in the location of the drops. Coalescence and Ostwald ripening result in a change in the drop-size distribution and number of drops.

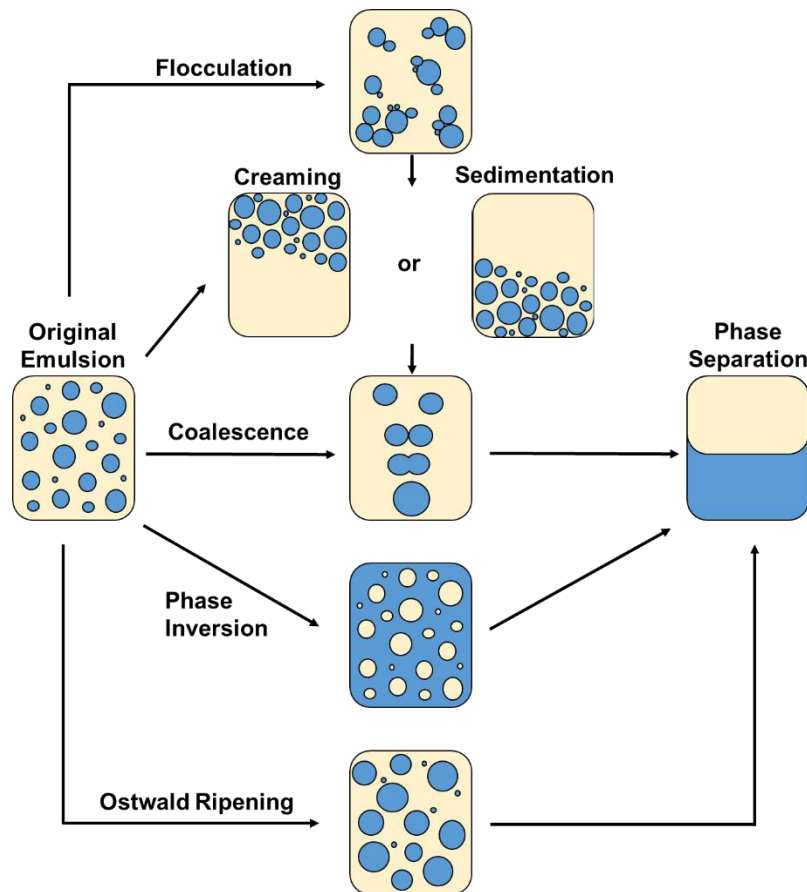


Figure 2.1 Schematic representation of emulsion breakdown processes.

Flocculation

Flocculation is the aggregation of droplets (Tadros, 2009) and occurs when two or more droplets are attracted close to each other without rupturing the droplet interfacial films or changing the original size of the droplet. The overall process is partially reversible (Singh, 1994). Flocculation rates depend on the interaction energy between droplets, which are the sum of van der Waals attraction forces and electrostatic or steric repulsion forces (Natarajan *et al.*, 2011). In order for droplets to remain as an aggregate, the attraction between the droplets must be large enough to overcome the thermal agitation or repulsive forces (Binks and Horozov, 2006). Flocculation can then enhance settling and lead to emulsion destabilization because larger droplets settle faster and the probability of coalescence increases when the droplets are closer together.

Sedimentation/Creaming

Sedimentation and creaming are gravity driven processes where differences in density between the dispersed and continuous phases result in the respective fall and rise of the dispersed droplets. Sedimentation occurs in a W/O emulsion where the denser water droplets sediment downwards. For an O/W emulsion, the less dense oil droplets cream upwards (Tadros, 2009). Both settling and creaming processes occur independently of droplet-droplet interactions and do not change the droplet size distribution of the emulsion (Binks and Horozov, 2006), but bring the droplets closer together. Settling and/or creaming rates can be increased by reducing the viscosity of the continuous phase, increasing the density difference between the two liquids or increasing the droplet size (Farn, 2006). High viscosities are a problem in destabilizing water-in-oil emulsions encountered in the petroleum industry.

Coalescence

Coalescence is an irreversible process where two droplets collide and merge to form one larger droplet. The droplets grow in size and eventually form free water and oil layers, leading to complete separation of the emulsion into two distinct phases. Emulsion destabilization by coalescence results in a decrease in the number of droplets (Singh, 1994) and a reduction of the total droplet surface area. The coalescence rate depends on the droplet encounter rate and interfacial properties (Binks and Horozov, 2006) and is more favourable for larger droplets where the contact area between droplets is greater.

Coalescence takes place in three steps (Frising *et al.*, 2006; Lobo *et al.*, 1996; Sztukowski and Yarranton, 2005), as shown in Figure 2.2:

1. Approach of two or more droplets to within the near molecular dimensions as result of attractive forces, fluid motion, creaming and/or flocculation.
2. Deformation and dimpling of the droplet surface to create a planar interface between droplets. This is followed by the drainage of the continuous phase from the planar region, which thins the film and creates gaps with less interfacial material. The time taken for film drainage contributes significantly to coalescence rates.

3. Bridging between the droplets and the rupture of films, resulting in irreversible fusion of two droplets into a single larger droplet.

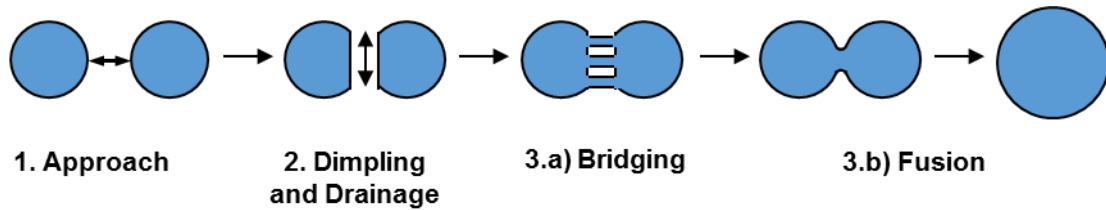


Figure 2.2 Schematic representation of the three step coalescence process.

Ostwald Ripening

Ostwald ripening is a mass transfer process where larger droplets grow at the expense of smaller droplets by diffusion (Tadros, 2009). The process is driven by a concentration gradient which develops from differences in the solubility of the dispersed phase in the continuous phase at the curved surface of the droplets. Solubility increases with increasing interface curvature; therefore, the solubility is greater at the interface of smaller droplets and lower for larger droplets. Eventually, the smaller droplets disappear unless an irreversible film is present at the interface that prevents further shrinkage. Ostwald ripening results in a decreased number of droplets and an increased average drop diameter. This leads to an overall reduction of the interfacial energy due to the lower surface area to volume ratio of larger droplets (Binks and Horozov, 2006).

Note, in asphaltene stabilized emulsions, like the ones considered in this thesis, the irreversibly adsorbed interfacial film retards the ripening process in small droplets so that although the drop size distribution changes, the total number of droplets does not change (Yarranton and Masliyah, 1996). Since ripening is a diffusion controlled process, it usually occurs over longer time scales than encountered in commercial oilfield separation processes or in the experiments performed in this thesis.

Phase Inversion

Phase inversion is a change in emulsion type where the dispersed phase becomes the continuous phase and *vice versa*. Factors such as temperature, surfactant concentration, time, or a change in the dispersed phase volume fraction can result in an exchange between the continuous and dispersed phases (Tadros, 2009). Phase inversion is not a factor in oil sand related emulsions.

2.1.2 Emulsion Stabilization

Emulsions are considered stable when there is no significant change in the number, size distribution, and spatial arrangement of the droplets within the given time scale. In separation processes, they are considered stable as long as there is no significant change in the number of droplets; that is, no phase separation occurs. Most emulsions are thermodynamically unstable, but can be kinetically stable over long periods of time if a surface active component (see Sections 2.1.3 and 2.1.4) adsorbs at the interface. There are three main mechanisms by which a surface active component can stabilize the emulsion: electrostatic, steric, and mechanical stabilization.

Electrostatic stabilization occurs when dissociated ionic groups in the molecules adsorbed at the water/oil interface create a surface charge. The surface charge attracts counter-ions from the bulk phase and repels co-ions, forming an electrostatic double layer with charge separation. If the counter-ion layer is diffuse, the droplets act as similarly charged spheres and repel each other, stabilizing the emulsion. Electrostatic stabilization is significant only for oil-in-water emulsions where water is the continuous phase because the electric double-layer thickness is much greater in water than in oil.

Steric stabilization prevents the close approach between droplets when high molecular weight materials or solids adsorb at the oil-water interface and form a thick interfacial film. The films provide a physical barrier to droplet contact. Mechanical stabilization occurs if the interfacial films are irreversibly adsorbed. Irreversible adsorption can occur if the surfactants at the interface rearrange to form a cross-linked network in the film. Since coalescence reduces the interfacial area and the surfactant molecules are trapped at the interface, these films become compressed during

coalescence. The increasing film thickness and viscosity resists further compression and coalescence. The thickened film may also form a steric barrier to coalescence.

2.1.3 Emulsion Stabilizers: Surfactants

Surfactants, or surface active agents are molecules which, even at low concentrations, adsorb at a surface or interface and significantly lower the interfacial free energy. Note, an interface is defined as the boundary between two immiscible liquids and a surface is an interface where one phase is a gas or a solid. Surfactant structure is amphipathic and consists of two groups: a polar hydrophilic head which is orientated towards the aqueous phase and a nonpolar hydrophobic tail orientated towards the oil phase. The hydrophobic tail generally includes a long chain hydrocarbon. Surfactants are classified based on the charge of the hydrophilic head group as follows:

1. Anionic: The surface active or hydrophilic portion of the molecule carries a negative charge (*e.g.*, carboxyl ($\text{RCOO}^- \text{M}^+$), sulfonate ($\text{RSO}_3^- \text{M}^+$) or sulfate ($\text{ROSO}_3^- \text{M}^+$)).
2. Cationic: The hydrophilic group carries a positive charge (*e.g.*, quaternary ammonium halides ($\text{R}_4\text{N}^+\text{Cl}^-$)).
3. Zwitterionic (or amphoteric): The hydrophile may contain both positive and negative charges (*e.g.*, sulfobetaines ($\text{RN}^+(\text{CH}_3)\text{CH}_2\text{CH}_2\text{SO}_3^-$)).
4. Non-ionic: The hydrophile carries no apparent ionic charge, but may contain polar groups. (*e.g.*, polyoxyethylene ($-\text{OCH}_2\text{CH}_2\text{O}-$), or polyol ($-\text{RX}(\text{C}_3\text{H}_5\text{OH})_n\text{OH}-$) groups).

Surfactant molecules tend to orientate themselves at the oil-water interface so that their hydrophilic heads are towards the polar water phase and the hydrophobic tails are towards the oil phase, as shown in Figure 2.3a, forming a film around the droplets. These films reduce the interfacial energy because the interactions between the surfactant molecules and the individual phases (polar-polar interactions and nonpolar-nonpolar interactions) are more favorable than the polar-nonpolar interactions between the dispersed and continuous phases. The lower interfacial energy decreases the driving force for coalescence. The films can also provide a steric barrier to coalescence by preventing close approach and contact between droplets and increasing film thickness and viscosity.

At sufficiently high surfactant concentrations, the surfactant monomers in the bulk phase will self-arrange to form aggregate structures with the lowest possible free energy, Figure 2.3b. The simplest aggregates are micelles, where the lyophilic groups form a sphere to protect the lyophobic groups from contacting the solvent and reduce the interactions between unlike polar and nonpolar molecules. Surfactant monomers may form other structures in the bulk phase, including vesicles, liquid crystals, and reverse micelles. The surfactant concentration at which micelles begin to form is known as the critical micelle concentration (CMC) and is dependent on surfactant structure and temperature. For pure surfactants, the CMC is marked by a sharp break in the slope of an interfacial tension versus concentration plot where the apparent molar mass of the solute changes. Above the CMC, there are no significant changes in surface properties because the concentration of surfactant monomers is nearly constant.

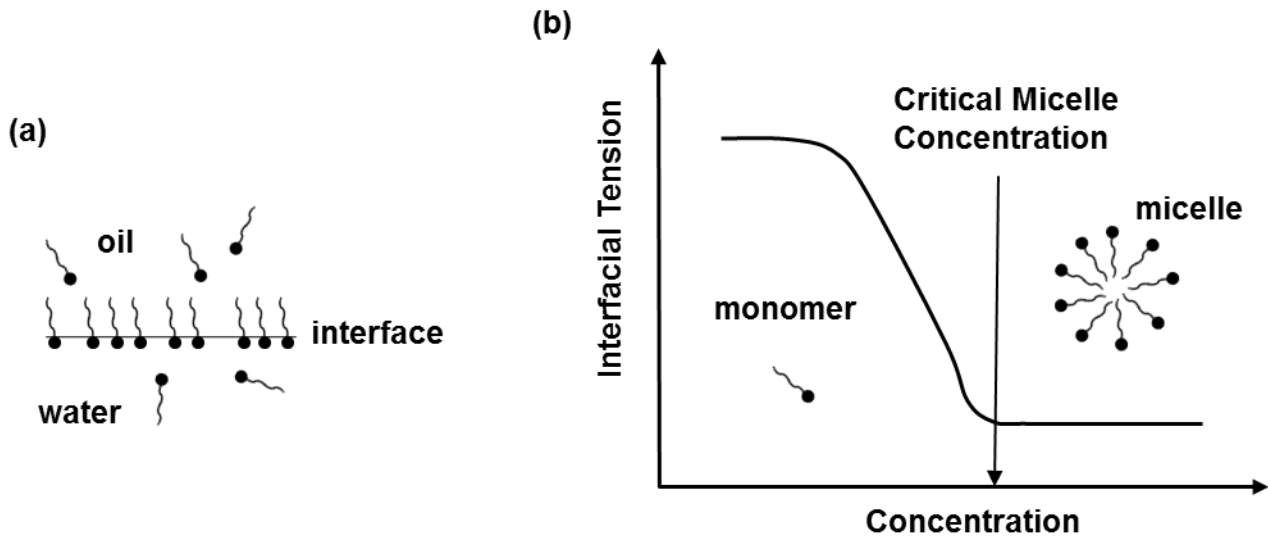


Figure 2.3 Surfactant structures for water continuous phases below CMC adsorb as monomers at interface or above CMC as micelles. Adapted from Sztukowski (2005).

2.1.4 Emulsion Stabilizers: Solids

Particles adsorbed at the water-oil interface can create a steric barrier between adjacent water drops which hinders droplet contact and collisions, film drainage and coalescence (Horozov and Binks, 2006; Sztukowski *et al.*, 2003; Tadros and Vincent, 1983). The nature of the barrier and the degree to which solids enhance emulsion stability depends on several factors such as particle size and distribution, shape and morphology, density, concentration, surface properties and coverage, wettability and interactions with surface active molecules (Sparks *et al.*, 2003; Sullivan and Kilpatrick, 2002; Menon and Wasan, 1988). The strong stability and formation of rag layers has been attributed to the presence of high concentrations of fine, oil-wet solids (Sztukowski and Yarranton, 2004).

Effect of Solids Wettability

Solids stabilized emulsions were first discovered by Pickering (1907). He found that the stabilization potential of solids depends on their wettability. Wettability is a measure of the relative affinity of a solid surface to two different liquids (often oil and water) or a liquid and a gas. It influences the type of emulsion stabilized, the partitioning of the particles between the bulk phases (concentration in each phase), and the surface coverage of particles adsorbed on the dispersed phase droplets (Perino *et al.*, 2013; Hannisdal *et al.*, 2006; Aveyard *et al.*, 2003; Bensebaa *et al.*, 2000; Binks and Lumsdon, 2000; Tambe and Sharma, 1993; Schulman and Leja, 1954). It is quantified by measuring the three phase contact angle formed between a solid and two liquids (or a liquid and vapor). Wettability can also be measured indirectly by critical surface tension in the film floatation method (Fuerstenau *et al.*, 1991). This method can be used to quantify the relative hydrophilicity and hydrophobicity of solids and the standard deviation can determine the surface heterogeneity of the solids (Wang *et al.*, 2015; Dang–Vu *et al.*, 2009).

A water-wet or hydrophilic solid refers to one preferentially wetted by water (contact angle less than 90° when measured through water) whereas an oil-wet or hydrophobic solid is more easily wetted by oil (contact angle greater than 90°), Figure 2.4. Solids particles are best able to stabilize emulsions when they position themselves at the oil-water interface. The solids that collect at the interface are bi-wetted, which means that the solids have both hydrophilic and hydrophobic areas

and have contact angles that do not largely deviate from 90° . Bi-wettable solids are in their lowest free energy state when adsorbed at the interface and therefore are expected to adsorb more strongly and produce more stable emulsions than solids with other wettabilities. Strongly hydrophilic solids tend to reside in the water phase instead of adsorbing at the interface and have a low attachment efficiency. Similarly, strongly hydrophobic particles can be readily detached from the interface. Such interfaces are not sufficient to provide a barrier to prevent droplet coalescence and therefore may not stabilize emulsions.

The wettability of the solids can indicate if the solid will stabilize W/O or O/W emulsions with solids stabilizing emulsions of the type where the solids preferentially disperse in the continuous phase. Moderately hydrophobic solids stabilize water-in-oil emulsions and moderately hydrophilic solids tend to promote oil-in-water emulsions. Factors such as particle partitioning, surface coverage, and the phase in which the particle is originally dispersed must be considered in addition to contact angle.

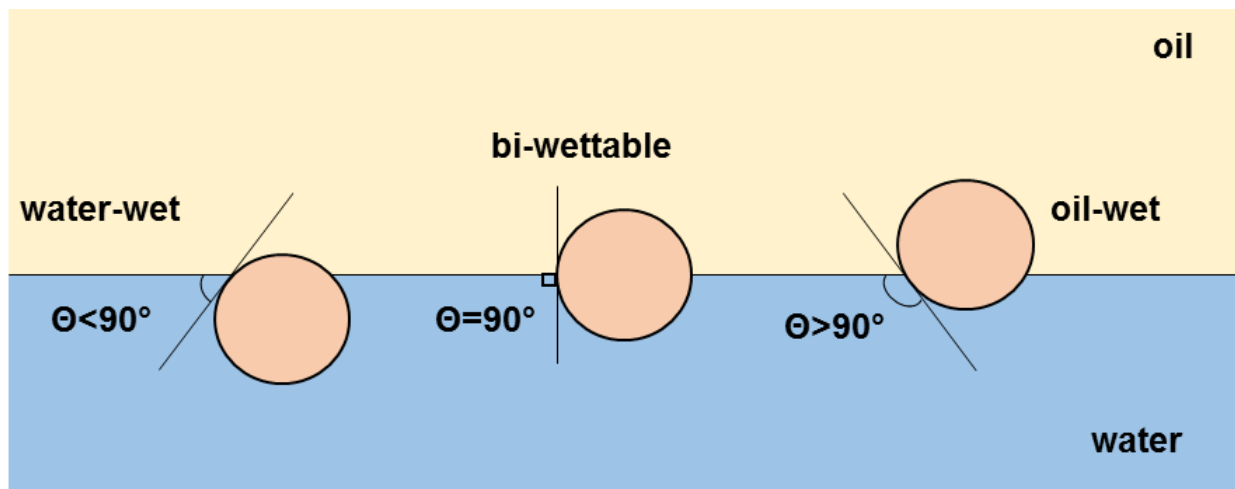


Figure 2.4 Position of spherical water-wet, bi-wettable and oil-wet solids at the oil water interface.

Effect of Initial Particle Location

Some studies suggest that the phase in which the solids are dispersed prior to emulsification determines the type of emulsion formed (Sullivan and Kilpatrick, 2002; Binks and Lumsdon, 2000; Tambe and Sharma, 1993). In these studies, with the oil-water volume ratio set to one, silica nanoparticles of intermediate wettability originally dispersed in water yield O/W emulsions, whereas those initially dispersed in oil produce W/O emulsions. However, Gavrielatos *et al.* (2017) found that W/O emulsions were formed in all cases regardless of initial particle location. All studies agree that the initial dispersion medium has a significant impact on emulsion stability. W/O emulsions were less stable when the particles were initially dispersed in oil as opposed to water. In a W/O emulsion, it is easier for water-wet particles to stabilize water droplets when they do not first have to redistribute in the continuous phase before covering the droplets. Gavrielatos *et al.* (2017) found that the difference in emulsion stability decreases with an increase in the initial water volume fraction and the difference was insignificant at high solids concentrations. Sufficient mixing times also greatly diminish the difference in emulsion stability due to initial particle location.

Effect of Solids Size, Shape, and Concentration

Generally, emulsion stability increases with decreasing particle size and density and increasing particle concentration. (Gavrielatos *et al.*, 2017; Aveyard *et al.*, 2003; Sullivan and Kilpatrick, 2002; Binks and Lumsdon, 2000; Yan *et al.*, 1999; Tambe and Sharma, 1993; Gelot *et al.*, 1984). Solid particles must be at least ten times smaller than the water droplets to effectively stabilize an emulsion (Binks and Kirkland, 2002; Tadros and Vincent, 1983; Schulman and Leja, 1954).

The effect of solids concentration on emulsion stability depends on the size and positioning of the solids in the emulsion. The positioning of solids in an emulsion based on particle size is shown in Figure 2.5. Fine solids, with diameters typically less than 1 μm (Sztukowski and Yarranton, 2005; Yan *et al.*, 2001; Levine and Sanford, 1985) and high surface area to volume ratios, are expected to stabilize emulsions at all concentrations by adsorbing at the droplet interface, with stability increasing with increasing solids concentration. However, maximums in emulsion stability with solids concentration have been found (Sztukowski and Yarranton, 2005) and partial surface

coverage by solids at the interface can be sufficient to stabilize emulsions (Binks and Kirkland, 2002; Vignati *et al.*, 2003). At very low solids concentrations, there may insufficient surface coverage to provide stability, whereas at very high concentrations (total surface coverage by solids), interfaces may not be rigid enough to maintain stability (because there is too little surfactant remaining on the interface).

Sztukowski and Yarranton (2004) found that coarse solids, with diameters greater than 1 μm , destabilize water-in-oil emulsions at low concentrations, likely by acting as bridges between the droplets, promoting coalescence. Bridging occurs when a single layer of particle adsorbs simultaneously at the film interface of two droplets. Complete separation of water and oil phases occurred for solids concentrations below 1 kg/m^3 . However, as the solids concentration increased above a 5 kg/m^3 threshold, emulsion stability began to increase. As concentration increases, coarse particles can form a multilayer around the droplet interface or become trapped in the continuous phase between adjacent water drops. Solids packed between droplets form a thick steric barrier to prevent aggregation among water droplets and direct bridging of solids between interfaces, thus reducing coalescence and increasing emulsion stability. For solids concentrations exceeding 10 kg/m^3 , stable emulsions were formed. Hence, in high enough concentrations, coarse solids alone are sufficient to impart long term stability to an emulsion.

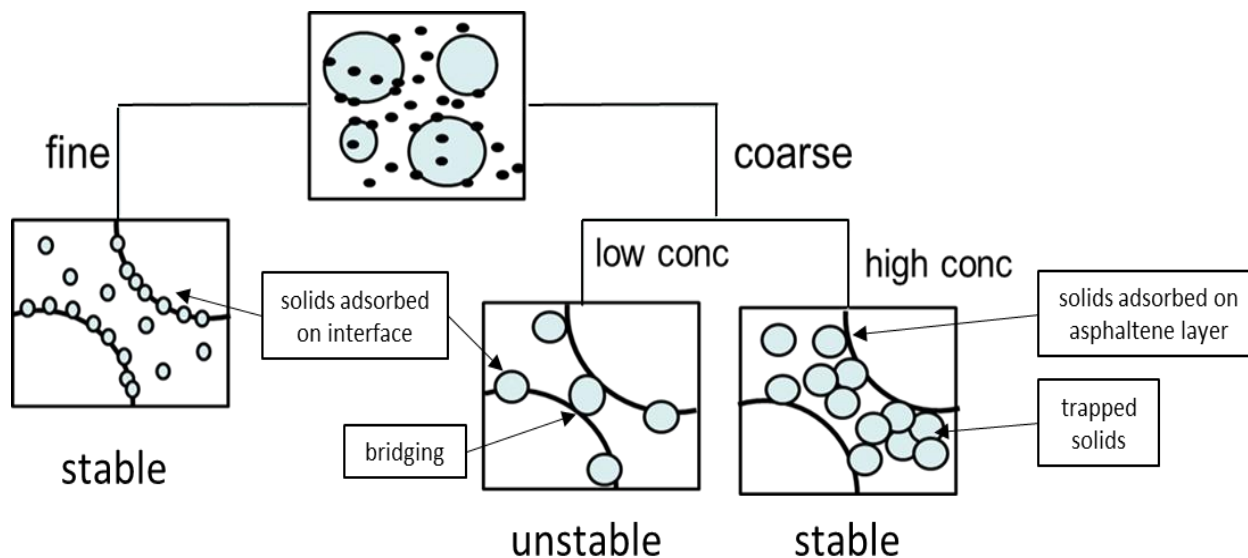


Figure 2.5 Positioning of fine and coarse solids in an emulsion. Adapted from Sztukowski and Yarranton (2004).

Emulsion stability can also be affected by particle density and shape. An increase in particle density tends to result in a decrease in emulsion stability (Gelot *et al.*, 1984; Schulman and Leja, 1954). Morphology can affect the wettability of the particles, with smooth particles often being more hydrophobic (Yekeler *et al.*, 2004). In addition, asymmetric particles such as bentonite clays can more effectively stabilize an emulsion than spherical particles, such as silica (Tadros and Vincent, 1983).

2.1.5 Emulsion Stabilizers in Crude Oils

Both surface active molecules and solid stabilizers are found in crude oils. Molecular surface active components include naphthenic acids, resins, and asphaltenes. Only asphaltenes are considered in this thesis. Solid stabilizers include sand, clay, and corrosion products. Only sand and clay are considered here.

2.1.5.1 Asphaltenes

Asphaltenes are often identified as being responsible for stabilizing water-in-crude oil emulsions (Tchoukov *et al.*, 2014; Sztukowski *et al.*, 2003; Gu *et al.*, 2002; Yarranton *et al.*, 2000, 2007; McLean and Kilpatrick, 1997b). Asphaltenes are the solubility class of a crude oil which is soluble in toluene (an aromatic solvent), but insoluble in *n*-heptane (an aliphatic solvent). They are the most heavy, polar, and surface-active fraction of the crude oil.

Asphaltenes are a mixture of hundreds of thousands of species (Podgorski *et al.*, 2013). They are polyaromatic hydrocarbons made up of condensed aromatic rings, aliphatic side and bridging chains, and various heteroatom functional groups that include nitrogen, oxygen, and sulfur atoms (Varadaraj and Brons, 2007; Strausz *et al.*, 1992). A hypothetical “average” asphaltene molecule proposed by Strausz *et al.* (1992) is shown in Figure 2.6. These asphaltene molecules have monomer molar masses of approximately 1000 g/mol (Yarranton *et al.*, 2000; Powers, 2014). The hydrocarbon structure interspersed with polar groups means that asphaltenes are amphiphilic.

Asphaltenes self-associate into nano-aggregates with average molecular weights of 4000 to 10,000 g/mol depending on the asphaltene concentration, solvent, temperature, and source crude oil (Yarranton *et al.*, 2000). The aggregation increases step-wise with increasing asphaltene concentration and decreases with increasing temperature (Agrawala and Yarranton, 2001; Merino-Garcia *et al.*, 2004). Asphaltenes appear to aggregate more as their solubility in decreases; that is, in a poorer solvent (Spiecker *et al.*, 2003). A variety of aggregation mechanisms have been proposed including π - π stacking of the aromatic regions in the asphaltene structure (Yen *et al.*, 1961; Mullins, 2010), hydrogen bonding, and acid-base interactions (Gray *et al.*, 2011).

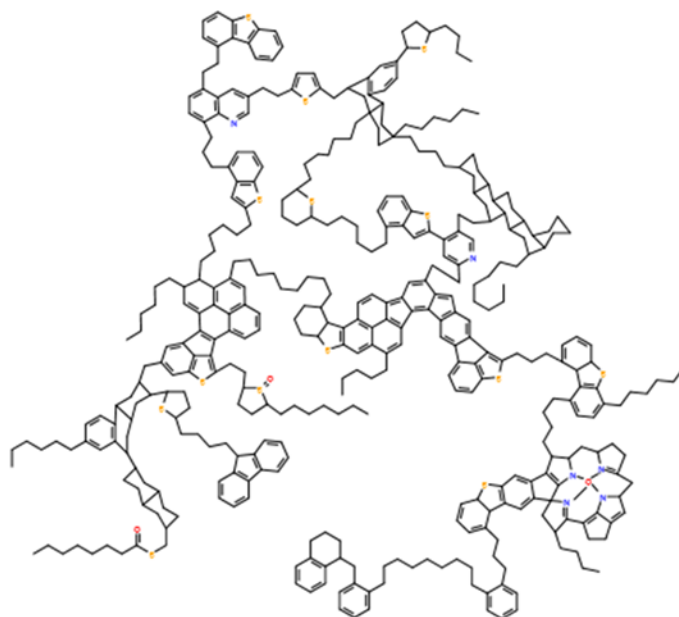


Figure 2.6 Proposed archipelago structure of an asphaltene molecule with an elemental formula of $C_{420}H_{496}N_6S_{14}O_4V$, an H/C ratio of 1.18 and a molecular weight of 6191 g/mol (Spiecker *et al.*, 2003).

Asphaltene monomers and nano-aggregates are surface active and reduce the interfacial tension of crude oils or hydrocarbons versus water (Zhang *et al.*, 2016). They adsorb irreversibly at the water-oil interface as an insoluble monolayer film (Shi *et al.*, 2017; Liu *et al.*, 2015; Rane *et al.*, 2012; Spiecker and Kilpatrick, 2004; Sztukowski *et al.*, 2003; Czarnecki *et al.*, 2013; Zhang *et al.*, 2005; Yan *et al.*, 1999; Siffert *et al.*, 1984). Asphaltene film properties (*e.g.*, compressibility, crumpling, elasticity, interfacial tension) are governed by several factors such as solvent chemistry, asphaltene concentration, temperature, aging time, and interactions with other surface active components in the crude oil. In general, the films become more rigid and more strongly adsorbed in poorer solvents, higher concentrations, lower temperatures, and greater aging times (Liu *et al.*, 2017).

The irreversibly adsorbed asphaltene film mechanically, and possibly sterically, stabilize water-in-oil emulsions. Yarranton *et al.* (2007) found that emulsions become more stable when the heptane fraction in heptol increases, the asphaltene concentration decreases, the interface aging time increases, and when the asphaltenes have a higher molar mass.

2.1.5.2 Inorganic Solids

W/O emulsions are more stable when both asphaltenes and fine solids are present than asphaltenes or solids alone (Gu *et al.*, 2002; Yan *et al.*, 1999). The solids stabilize emulsions by competing with asphaltenes to adsorb at the water-oil interface, either directly or on an existing surfactant film, and/or packing between droplets (Sztukowski and Yarranton, 2005; Aveyard *et al.*, 2003; Yan *et al.*, 2001; Tambe and Sharma, 1993; Menon and Wasan, 1988) as shown in Figure 2.7. As noted previously, adsorbed solids form a steric barrier to coalescence. Tightly packed networks of solids trapped between droplets contribute to the mechanical rigidity and viscosity of the film when there are strong particle-particle interactions. (Binks and Kirkland, 2002; Tambe and Sharma, 1994). These networks of solids suspended in the continuous phase may lower the probability of close contact between the droplets, reduce aggregation and creaming/sedimentation (Yan *et al.*, 2001), increase the overall emulsion viscosity (Yaghi *et al.*, 2001) and reduce the chances of coalescence and segregation of water and oil (Yan and Masliyah, 1993). The composition, size, shape and wettability of solids encountered in heavy oil and oil sands operations are discussed below.

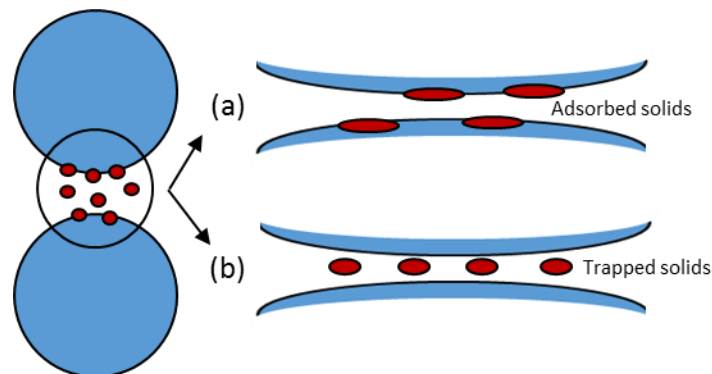


Figure 2.7 Role of solids in the stabilization of water-in-oil emulsions: a) solids adsorbed on the interface, b) solids trapped between droplets.

Crude oils contain natural reservoir solids and in oilfield applications, oils may also contain material introduced during production and processing (Zahabi *et al.*, 2010; Jiang *et al.*, 2011). Solids originating from the reservoir rock may include silicates, clays, quartz, calcite, feldspar and pyrite. Precipitated chemical additives and insoluble corrosion products are examples of solids that

can be introduced after extraction (Sztukowski and Yarranton, 2005). The solids content is an indicator of ore processability and potential bitumen recovery from the froth (Sparks *et al.*, 2003). High concentrations of solids in low quality oil sands can result in the formation of large, stable rag layers. Bensebaa *et al.* (2000) and Kotlyar *et al.* (1998, 1999) have identified the solids most associated with oilfield emulsions as fine (<1-2 μm), bi-wettable aluminosilicate clays, with kaolinite being the most abundant in oil sand froths.

Clays are crystalline in nature and composed of two structural units: an octahedral unit of six oxygen atoms or hydroxyl groups surrounding metal atoms (aluminum, iron or magnesium) and a tetrahedral unit of four oxygen atoms (or hydroxyl groups) surrounding silica atoms. The first unit has an elemental composition of $\text{Al}_2(\text{OH})_6$ or $\text{Mg}_3(\text{OH})_6$ depending on the central atoms present. The second unit forms a repeating hexagonal pattern with a formula of $\text{Si}_4\text{O}_6(\text{OH})_4$. Clay minerals are formed from combined sheets of alternating octahedral and tetrahedral units.

Kaolinite is the most abundant clay in oil sands reservoirs and has been shown to preferentially partition into the froth stream during oil sands processing by Kaminsky (2009). Kaolinite is a layered 1:1 type aluminosilicate clay mineral, with alternating sheets of tetrahedral silica and octahedral alumina structures linked through oxygen atoms. Each layer, consisting of one tetrahedral structure and one octahedral structure, is bound together by hydrogen bonding to form pseudo-hexagonal platy particles (Lebedeva and Fogden, 2011). This forms a rigid structure that does not swell in water. There is a limited capacity for cation exchange within the kaolinite sheets. The replacement of Si^{4+} with Al^{3+} in the tetrahedral sheet or Al^{3+} with Mg^{2+} in the octahedral sheet, results in a negative charge on the clay surface.

Bensebaa *et al.* (2000) developed a conceptual model based on elemental and structural analysis of oilfield aluminosilicate clays where humic and asphaltene-like petroleum matter has absorbed onto the solids surface, Figure 2.8. The solids have a predominantly hexagonal/platelet shape with diameters of less than 200 nm and thicknesses of approximately 10 nm. Chen *et al.* (2017a) analyzed the fine solids in a bitumen froth using adhesion force mapping and were able to clearly identify platy clay particles with layer thickness of 5-6 nm which were consistent with kaolinite

partially covered in organic matter. The organic material was found to be polar, aromatic matter similar to asphaltenes. Solids in oil sand froths are hydrophobic (Kupai *et al.*, 2013).

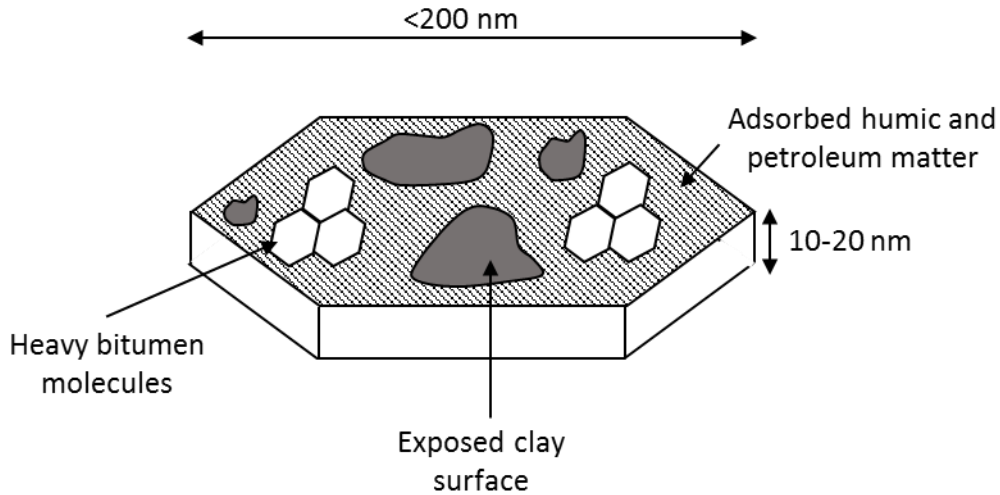


Figure 2.8 Conceptual model of bitumen solids. Adapted from Bensebaa *et al.* (2000).

Kaolin and silica particles are naturally hydrophilic. However, exposure of the solid surface to bitumen in the absence of water can alter the overall surface wettability, surface energy and surface charge of the solids (Chen *et al.*, 2017b; Pourmohammadbagher and Shaw, 2016; Jiang *et al.*, 2011). Organic material, typically multi-ring hydrocarbons found in bitumen such as asphaltenes, can adsorb onto the solid surface or onto humic matter already deposited on the particle surface from the surrounding soil (Wang *et al.*, 2016; Hannisdal *et al.*, 2006; Bensebaa *et al.*, 2000; Standal *et al.*, 1999). The adsorption of hydrophobic organic material changes the surface composition and increases the hydrophobicity of the clay (Wang *et al.*, 2013; Darcovich *et al.*, 1989), leading to oil-wet particles. Organic material only partially covers the clay surface (Pourmohammadbagher and Shaw, 2016; Wang *et al.*, 2013; Sparks *et al.*, 2003; Bensebaa *et al.*, 2000), leaving some hydrophilic surfaces exposed. This results in particles that are overall biwettable or of intermediate hydrophobicity. Generally, the organic coating is thin and does not greatly alter the size or topography of the solid surfaces (Pourmohammadbagher and Shaw, 2016). However adsorbed organic matter has a high adhesion force that can act as a glue, forming aggregates of solids.

2.1.6 Other Factors in Emulsion Stability

Droplet Size Distribution

The size distribution of the emulsified droplets is another factor affecting emulsion stability. As the average drop size decreases, emulsion stability tends to increase. Emulsions with large initial diameters are likely to have a faster coalescence rate than those with smaller diameters because larger droplets more readily sediment and have a higher probability for collision. In addition, larger droplets are more likely to deform and experience film rupture upon collision, resulting in coalescence and reducing emulsion stability. Droplet size can also affect the viscosity of the emulsion: emulsions with smaller droplets and narrower drop size distributions have higher viscosities.

The drop-size distribution is dependent on the mixing process used to prepare the emulsions. Drop size generally decreases with increasing mixing speed. Greater mixing intensities result in more stable emulsions because droplets are smaller and better dispersed. However, high speed shearing above a critical value, from a pump may result in demulsification. The dispersed phase droplet diameter also decreases both with an increasing solids concentration and a decreasing particle size (Aveyard *et al.*, 2003; Tambe and Sharma, 1993; Gelot *et al.*, 1984).

Dispersed Phase Volume Fraction

Generally, if there is a limited supply of surface active material, the stability of a W/O emulsion decreases with an increase in the volume fraction of the dispersed (water) phase while other conditions are held constant. The size of the droplets depends on the mixing conditions and the amount of surface active material. The mixing conditions set an initial drop size. If there is sufficient surface active material, the droplets do not coalesce and their size is mainly set by the mixing conditions. When the supply of surface active material is limited, the droplets coalesce until there is sufficient stabilizing material on their surface to stop the coalescence. In this case, their size is set by the amount of stabilizing material. The larger droplets are more likely to coalesce, hence an increase in the dispersed phase volume leads to less stable emulsions.

Phase inversion can occur when the volume fraction of the dispersed phase exceeds a critical value. For monodisperse spherical droplets, the maximal volume fraction of the dispersed phase is 0.74, which is the closest possible packing of the spherical emulsion droplets. However, the droplets of most emulsions are polydisperse and deformable; thus, emulsions with a dispersed phase volume fraction of >0.74 can be prepared (Wen *et al.*, 2014).

2.1.7 Demulsification

Industrial demulsification processes must achieve rapid separation into water and oil phases and provide a clean product. Hence, the key process variables are the separation rate and the quantity of residual water remaining in the crude oil. Unaided gravity driven separations of emulsions are often ineffective. Most industrial water-oil demulsification processes require chemical, thermal, mechanical, or electrical treatments to increase the demulsification rate, weaken interfacial films, and promote flocculation and coalescence. Oilfield demulsification methods are often field specific due to the large variations in produced crude oils. Refinery emulsions may require more than one type of treatment for effective water resolution. Each treatment method is described below.

Chemical Treatment

In the petroleum industry, the addition of chemical demulsifiers is the most common method for breaking oil-water emulsions stabilized by asphaltene and solids. Demulsifiers are typically surface active agents of complex organic compounds that destabilizes the emulsion by increasing flocculation or by weakening the film, and increasing coalescence (Frising *et al.*, 2006; Singh, 1994). The demulsification efficiency depends on the molecular structure and composition of the demulsifier in addition to the solution conditions. To ensure a good separation, the demulsifier must effectively partition between the oil and aqueous phases and displace the existing material adsorbed on the interfacial film (Ortiz, 2010). The demulsifiers at the interface weaken the protective film without significantly reducing the interfacial tension, thus promoting droplet coalescence and separation of the water and oil phases. Chemical demulsifiers are often used in conjunction with thermal methods.

Thermal Treatment

The temperature at which the emulsion is treated can effect emulsion stability. Generally, emulsion stability decreases with increasing emulsion temperature. Heating lowers the viscosity and density of the bulk emulsion and weakens the interfacial films, which increases sedimentation/creaming and collision rates and facilitates drainage in coalescence (Schramm, 1992; Singh, 1994). The effectiveness of thermal treatments are dependent on crude oil properties and are often not effective alone. The addition of heat may result in the loss of light end hydrocarbons, reducing the total volume of the oil and leaving a more dense and viscous oil upon cooling. In addition, thermal treatments have a high operation cost due to the high cost of fuel required to heat the emulsion.

Mechanical Treatment

Mechanical separation methods use different configurations of grids, baffles, fibrous beds, or membranes to put obstacles in the flow path of the emulsion. The barriers increase droplet collisions and therefore increase coalescence rates (Frising *et al.*, 2006). Ultrasonication can be effective in breaking relatively stable petroleum emulsions at low capacities (Singh, 1995). High speed centrifugation is used in the oil industry for oil-water separations.

Electrical Treatment

Electrical treatments improve flocculation and coalescence in water-in-crude oil emulsions (Frising *et al.*, 2006) by increasing droplet collisions and weakening interfacial films. Electric grids provide a high voltage electrical field that induces a dipole charge on the droplets, causing the droplets to polarize and align themselves along field lines. The rapid movement of droplets increases flocculation which in turn results in faster gravity settling. The rigidity of interfacial film is reduced, enhancing coalescence, because the electric field can rearrange the polar molecules at the interface.

Electric field separations are particularly useful when space is a major concern because the accelerated settling rates allow for the use of small dimension vessels (Schramm, 1992). It should be noted that electrostatic methods are only applicable for water-in-oil emulsions. In order to be effective, the dispersed phase must be conductive and the continuous phase non-conductive. A

conductive dispersed phase is required to induce a dipole in the droplets and a non-conductive continuous phase is necessary to prevent large power losses. The strength and frequency of the field, droplet diameter, composition of crude oil, and the hydrodynamic conditions are other factors that must be considered for the effectiveness of separations by an electric field.

2.2 Emulsion Layers in Water/Oil Separation Processes

Emulsion layers are the accumulation of settling water or rising oil droplets at the water-oil interface in a separation process. Emulsions layers have previously been modeled as liquid-liquid dispersion separations. The systems studied are generally hydrodynamic, are less stable than rag layers in crude oil-water separations and do not contain solids. However, the accumulation of a third layer of intermediate density at the interface between the pure light and dense phases is consistent with rag layers. Emulsion layer formation and models are presented below.

2.2.1 Settling in Liquid-Liquid Dispersions

Three main zones have been identified in the formation of a steady-state settling dispersion. These zones are given in Figure 2.9 and are defined as follows (Lobo *et al.*, 1993; Barnea and Mizrahi, 1975; Hartland and Vohra, 1980; Hartland and Jeelani, 1985; Hartland and Jeelani, 1987, 1988; Jeelani and Hartland, 1986a; Jeelani *et al.*, 2005):

- I. Flocculation Zone: droplets form close aggregates but there is no change in droplet diameter or shape. The flocculation zone does not exist in all liquid-liquid separations.
- II. Sedimentation Zone: droplets, with a dispersed phase volume fraction varying from 0.50 to 0.75, move relative to each other and deform and change size by binary (droplet-droplet) collisions and coalescence. The height of the sedimentation zone is a function of the binary coalescence and sedimentation rates, which in turn depend on droplet size and the dispersed phase volume fraction.
- III. Dense-Packed Zone: droplets, with a dispersed phase volume fraction varying from 0.75 to 1, change size and move only through binary or interfacial coalescence. The height of the dense-packed zone depends on the coalescence rate. The coalescence rate is a function of drop size and varies with the height of the dense-packed zone since the magnitude of gravitational forces transferred between droplets that press down on the draining films increase with zone height.

At any given time, the height of the total dispersion is the sum of the sedimentation and dense-packed zone heights and depends on the difference between the sedimentation and coalescence rates. Rag layers are considered dense-packed layers that form if the sedimentation rate is faster than the interfacial coalescence rate.

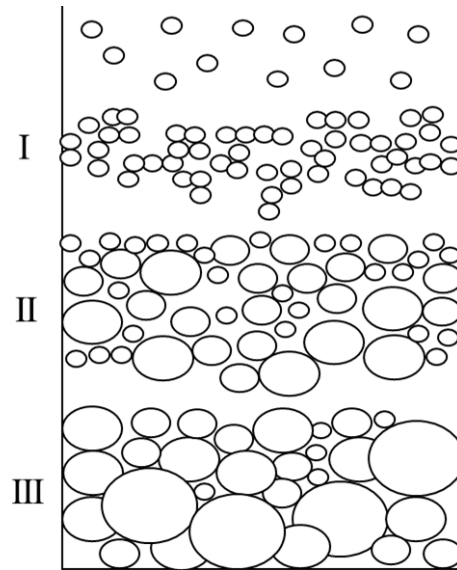


Figure 2.9 Flocculation (I), sedimentation (II) and dense-packed (III) zones in a steady-state closed packed dispersion where the dense phase is the dispersed phase. Adapted from Hartland and Vohra (1980).

Batch Dispersions

In a batch dispersion, droplets enter the dense-packed zone by sedimentation as the droplets simultaneously grow due to binary coalescence. Droplets exit the dense-packed zone by coalescing with their bulk phase at the coalescing interface. Initially, the height of the dense-packed zone increases because the sedimentation rate of droplets entering the dense-packed is faster than the coalescence rate of the droplets exiting the dense-packed zone. Over time, sedimentation is completed and coalescence dominates. At this point, the height of the dense-packed zone decreases with time as droplets merge with the bulk phase. The sedimentation and dense-packed zone heights, shown in Figure 2.10, can be predicted respectively from the profiles of the sedimenting and coalescing interfaces (Hartland and Jeelani, 1987, 1988). When the dispersion is comprised only of a dense-packed zone, coalescence rates are initially rapid but then decrease over time,

sedimentation is controlled by holdup as opposed to drop-size control and the overall decay profile is exponential.

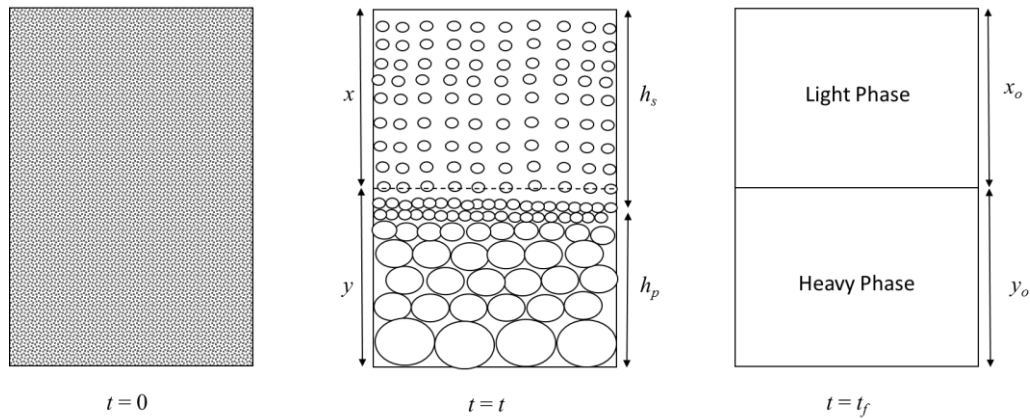


Figure 2.10 Non steady-state batch dispersion containing sedimentation and dense-packed zones over time. Adapted from Hartland and Jeelani (1987).

Continuous Dispersions

A continuous dispersion separation is one where the dispersion is continuously fed into a gravity settler. Similar to batch dispersions, droplets entering a continuous settler first sediment to the oil-water interface while growing in size due to binary coalescence. At the interface, the droplets collect in a dense-packed layer before merging with the free layer by interfacial coalescence.

The height of the dispersion layer increases to a steady state height, where the sedimentation and coalescence rates of the droplets are equal to the specific volumetric flowrate of the dispersed phase entering the settler (Jeelani and Hartland, 1985; Hartland and Jeelani, 1987). For a given flow rate, the time a droplet occupies a given zone is proportional to the height of that zone. The heights of the sedimentation and dense-packed zones depend on the size distribution of the droplets in the dispersion feed as follows:

- I. The dispersed phase droplets in the feed are large and their volume sedimentation rate is greater than the dispersed phase flow rate. In this case, the height of the sedimentation zone is negligible and dispersion is a dense-packed zone. The interfacial coalescence

- rate depends only on the total dispersion height and is equal to the dispersed phase flowrate at steady state.
- II. The droplets are small and sediment at a lower volume rate than the dispersed phase flow rate. The droplets coalesce immediately upon arrival at the water-oil interface and no dense-packed layer forms. A steady state is reached when the droplets have sufficiently grown through coalescence such that their sedimentation rate is equal to the dispersed phase flowrate.
 - III. The droplets are moderately small and both sedimentation and coalescence zones exist, with heights of similar magnitude. The droplets move through the sedimentation zone, growing due to binary coalescence, and enter the dense-packed zone where the droplets ultimately coalesce with their bulk phase over time.

Most liquid-liquid dispersions are described by the third case (Barnea and Mizrahi, 1975a; Jeelani and Hartland 1986ab; Hartland and Jeelani, 1987).

2.2.2 Mathematical Models

Liquid-liquid dispersion separations in gravity settlers have been modeled based on the two major separation mechanisms: sedimentation and coalescence rates (Barnea and Mazrahi, 1975; Golob and Modic, 1977; Hartland and Jeelani, 1986ab, 1987, 1988; Nadiv and Semiat, 1995). These models are mostly purely hydraulic in nature and do not account for chemical composition or intermolecular interactions (Khatri, 2010; Frising *et al.*, 2006).

2.2.2.1 Hindered Settling and Coalescence Model

Hartland and Jeelani (1988) proposed the following model for a batch dispersion based on hindered settling and inter-drop coalescence, where the total height of the dispersion is the sum of the heights of the sedimentation and dense-packed zones for a constant cross-sectional area:

$$h_t = h_s + h_p = x + y \quad \text{Equation 2.1}$$

where h is height with subscripts t , s and p indicating the total dispersion, the sedimentation zone and the dense packed zone respectively. x and y represent the positions of the sedimenting and coalescing interfaces (Figure 2.10) with the free bulk phase respectively in relation to the final undisturbed interface between the two free liquid phases.

Assuming the relative volumes of the continuous and dispersed phases are proportional to x and y respectively, the dispersed phase volume fraction, Φ , is given as:

$$\Phi = \frac{y}{h_t} \quad \text{Equation 2.2}$$

The dispersed phase volume fraction in the sedimentation zone is assumed to be constant at the initial value:

$$\Phi_s = \Phi_s^o = \frac{y^o}{h_t^o} \quad \text{Equation 2.3}$$

The dispersed phase volume fraction in the dense-packed zone varies with time. Initially, while sedimentation occurs, the volume fraction is held constant at Φ_p^* . The volume fraction then varies from Φ_p^* to near unity when there is no sedimentation. A volume fraction equal to one indicates that coalescence is complete. A typical value of Φ_p^* is 0.75 for dense-packed spheres.

The profiles of the sedimenting and coalescing interfaces can then be written as variations of x and y with respect to time, with their instantaneous position written as:

$$y = \Phi_s h_s + \Phi_p h_p \quad \text{Equation 2.4}$$

$$x = (1 - \Phi_s)h_s + (1 - \Phi_p)h_p \quad \text{Equation 2.5}$$

The height of the respective sedimenting and dense-packed zones can then be given as:

$$h_s = \frac{(\Phi_p h_t - y)}{(\Phi_p - \Phi_s)} \quad \text{Equation 2.6}$$

$$h_p = \frac{(y - \Phi_s h_t)}{(\Phi_p - \Phi_s)} \quad \text{Equation 2.7}$$

The heights of the sedimentation and dense-packed zones can be determined by simultaneously the above material balances, if the water volume fractions and the coalescence rates are known over time.

Coalescence Rates in Batch Dispersions

In a batch dispersion, the decrease in the dispersion height over time per unit cross sectional area of the separator is equal to the droplet coalescence rate, ψ :

$$\frac{dh}{dt} = -\psi \quad \text{Equation 2.8}$$

When the sedimentation rate is constant, the coalescence rate is drop-size controlled. Once sedimentation is complete, the coalescence rate is controlled by the height of the dense-packed zone and is independent of drop-size. In a close packed dispersion, the drops are constrained so that a portion of the net force pressing on each drop is transmitted to the drop below. Thus, the force acting on each drop increases with increasing depth and the coalescence rate increases with dispersion depth as:

$$\psi = ch_p^a \quad \text{Equation 2.9}$$

where c and a are constants whose values are determined from a least square fit of experimental data for Eq. 2.8.

Coalescence Rates in Continuous Dispersions

For a continuous separator, the coalescence rate at steady state is equal to the volume flux in the dispersed phase:

$$\psi = \frac{\dot{V}_d}{A} \quad \text{Equation 2.10}$$

where \dot{V}_d is the volumetric flow rate of the dispersed phase and A is the cross sectional area of the separator. The height of dense-packed zone in a continuous separator is then determined as:

$$h_p = c \left(\frac{\dot{V}_d}{A} \right)^a \quad \text{Equation 2.11}$$

where c and a are experimentally defined constants that depend on the dispersion characteristics. Constants used in the batch and continuous systems are not necessarily the same for a given dispersion. Differences in the batch and continuous coalescence constants may be due to the dense packed zone being continuously replenished with fresh dispersion in the continuous separator.

2.2.2.2 Material Balance Model

More recently, a material balance based model was proposed by Khatri *et al.* (2011) for surfactant stabilized oil-in-water emulsion layer decay and growth. In all cases, the emulsion layer was assumed to be a dense packed zone where the volume changes only through coalescence and compaction of the dispersed phase and not through free settling. The model is based on a mass balance performed on the dispersed phase (oil in this case) in the emulsion layer. The coalescence rate was assumed to be proportional to the volume of the dispersed phase. The model is fit to

experimental data by adjusting the coalescence rate constants. The model was applied to both batch and continuous separations. This model was adapted for use in this thesis and is presented in detail in Chapter 4.

2.3 Rag Layers in Heavy Oil and Oil Sands Processes

Rag layers are similar to the emulsion layers described in Section 2.2, but in addition to water and/or oil droplets they also contain solid particles. The droplets are stabilized by natural surfactants in the crude oil, typically found in the asphaltene fraction of the oil. The solids likely enhance the stability of the emulsion. The high stability of rag layers makes their formation problematic for process operators because they cannot be readily separated by conventional treatment and can persist over long periods of time. Rag layers can reduce separation efficiency, reduce bitumen recovery with unrecovered bitumen lost to the tailings stream, lead to corrosion and fouling in upgrading equipment through contamination of the product stream and process upset.

Rag layers can form in separators and heater-treaters used in *in situ* operations and often occur in the processing of bitumen froth. Most research has focussed on the rag layers from oil sand operations. Bitumen is extracted from minable oil sands using a water-based, air-assisted floatation process where the mined ore is mixed with air and hot water to form a slurry. The aerated bitumen floats to the top and is collected as a bitumen froth. The bitumen froth has an average composition of 60% bitumen, 30% water, and 10% fine solids by mass and must be further treated to remove water and solids. Free water remaining in the bitumen froth can be removed by heating or gravity drainage, but emulsified water (droplets 2-10 μm in diameter) is difficult to separate. The emulsified water droplets are stabilized by bitumen components such as asphaltenes and solids (clay solids with diameters $<1\text{-}2\ \mu\text{m}$) that accumulate at the droplet interface and form a skin that prevents the droplets from coalescing.

In froth treatment and some heavy oil processes, a hydrocarbon solvent or a paraffinic solvent is added to the bitumen to reduce its viscosity and density. The added diluent also contributes to the separation of water droplets and fine solids (McLean and Kilpatrick, 1997ab; Gafonova and

Yarranton, 2001). The addition of a strongly aromatic solvent reduces emulsion stability. In aromatic solvents (hydrocarbon solvents), the asphaltenes are in their mostly soluble state (Yang *et al.*, 2004) and are more mobile; therefore, the asphaltenes will form weaker more elastic films and coalescence is more rapid. The addition of a paraffinic solvent promotes rapid settling. In paraffinic solvents, the asphaltenes are in their insoluble range and will precipitate. The precipitated asphaltenes flocculate and collect the water droplets and solids into relatively large structures that settle rapidly.

There are currently two commercialized froth treatment processes in Alberta: the Syncrude process and Shell's Albian process. The Syncrude process, in addition to dilution with naphtha (a hydrocarbon solvent that does not precipitate asphaltenes), utilizes cyclones, centrifugation or inclined-plate settlers to further accelerate settling. Inclined-plate settlers confine the suspension on an incline that establishes a circulation pattern, called the Boycott effect, where the downward motion of the settling water droplets and solids particles at the bottom of the plate is unimpeded by the upward motion of the free liquid along the top of the plate. The combination of chemical and mechanical treatment methods typically results in a bitumen with 1-2 wt% residual water in the form of small droplets with diameters of 1-2 μm and approximately 1 wt% solids remaining.

The Albian froth treatment process uses a paraffinic solvent, such as pentane and hexane mixtures, to precipitate a fraction of the asphaltenes in the bitumen. As already noted, asphaltene precipitation promotes the flocculation of water droplets and solids and forms aggregates that trap water and solids, which enhances settling. Treatment with a paraffinic solvent and gravity separation results in a bitumen product with less than 100 ppm water and almost no solids or precipitated asphaltenes (Romanova *et al.*, 2004). Although the Albian froth treatment process produces a higher quality bitumen, the high solvent to bitumen ratio increases operation costs and some of the bitumen is rejected as asphaltenes. Many operations use the naphtha-based froth treatment. In both froth treatment processes, the cleaned diluted bitumen is then sent to refineries for solvent removal and further upgrading to produce crude oil.

In the separation vessels of both froth treatment processes, material often accumulates at the oil-water interface, forming a viscous third layer of intermediate density between the two bulk phases. This layer, known as a rag layer as shown in Figure 2.11, is a complex fluid comprised of emulsified water and/or oil, interfacially active organic material from the bitumen such as asphaltenes, and produced solids (Czarnecki *et al.*, 2007; Vandaraj and Brons, 2007) that resists complete separation of oil and water. Saadatmand *et al.* (2008) described the rag layer as a close packed layer of water droplets stabilized by asphaltene films and oil-wet solids suspended in a continuous oil phase. Asphaltenes isolated from the rag layer contain twice as many heteroatoms (N, S, and O) and more volatiles and residues than the asphaltenes obtained from the bulk bitumen (Gu *et al.*, 2007). Solids contained in rag layers are predominantly fine (<1-2 μm) oil-wet heavy minerals, such as kaolinite, that are highly contaminated with hydrophobic organic material in the bitumen (Kupai *et al.*, 2013). Siderite, illite and pyrite (iron-bearing clays) have also been found to preferentially partition to the rag layer along with quartz sands. Rag layers accumulate over time, do not easily separate and can persist for long periods of time. Rag layer formation is known to be problematic in oil-sand crude oils processes, but can also occur in conventional and heavy oil separation processes.

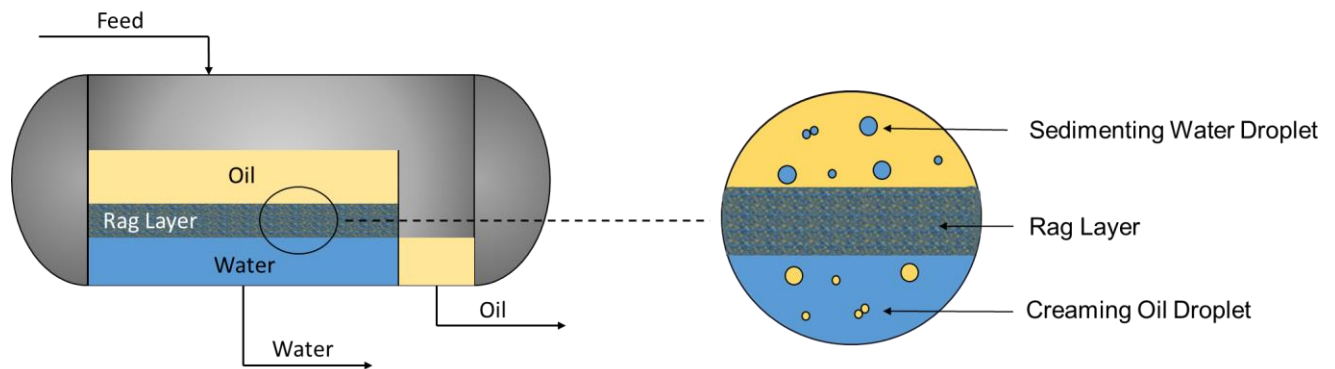


Figure 2.11 Rag layer formation in oil sand separation vessels.

The growth of a rag layer depends on the settling rate of the droplets dispersed in the continuous phases and the coalescence rate of the concentrated emulsion. Rag layers diminish in height when the dispersed water droplets coalesce at the free water phase interface (interfacial coalescence), exiting the rag layer. If the coalescence rate of the dispersed phase droplets is slow compared to the accumulation (settling/creaming) rate of droplets entering the rag layer or there is hindered settling, the rag layer will grow (Saadatmand *et al.*, 2008; Frising, 2006). The coalescence rate depends on the interfacial properties of the droplets but may also depend on dynamic factors such as the accumulation of fine, oil-wet solid particles at the oil-water interface that form a mechanical barrier to coalescence and prevent droplets from crossing the interface (Hirasaki *et al.*, 2008; Saadatmand *et al.*, 2008). When coalescence is significantly reduced, the settling droplets become trapped in a stable network and rag layers can grow large enough to upset the process (Saadatmand *et al.*, 2008) as large rag layers must be removed mechanically.

In the oil sands industry, water-in-oil emulsions stabilized by natural organic constituents in the bitumen, such as asphaltenes and fine oil-wet solids, are the most problematic to treat and have been identified as contributing to rag layer formation (Sztukowski *et al.*, 2003; Gu *et al.*, 2002; Yarranton *et al.*, 2000, 2007; McLean and Kilpatrick, 1997). Efforts to reduce rag layer volume involve the addition of chemical diluents and demulsifiers and agitation. Dilution of the bitumen prevents rag layer formation by removing fine solids and asphaltenes that act as emulsion stabilizers and weakening stabilizing films. Agitation and mixing can also be used to break rag layers (Ng *et al.*, 2015).

Sodium metasilicate (NaSiO_3) has been used at the bench-scale as a demulsifier to alter the association of solids and organics and make the solids less oil-wet. Jiang *et al.* (2011, 2010) determined that adsorption of bitumen components onto kaolinite is dependent on the surface charge. Kaolinite in oil sands fort treatments (pH of approximately 8.5) has a heterogeneous surface charge: the basal surface of kaolinite is negatively charged, while the edges are positively charged. Anionic carboxylate material adsorbs onto the positively charged surfaces of the kaolinite, making the solids more oil-wet and stabilizing water-in-oil emulsions. The addition of the silicates makes the ζ -potential of the kaolinite more negative by increasing the pH of the

system. The more negatively charged solids are more water-wet, which enhances emulsion separation and minimizes rag layer formation. By adjusting the pH in the system, the surface wettability, dispersion and flocculation of the clay can be controlled. Chemical demulsifiers, oil soluble, low molecular weight compounds with high surface activity, can also be used to improve separation by increasing the coalescence efficiency between colliding droplets (Czarnecki *et al.*, 2007).

2.4 Chapter Summary

During crude oil production, the oil and co-produced water are often emulsified into water-in-oil emulsions. Most of the water is separated from the oil prior to transportation and upgrading at the oilfield battery and the remainder at a refinery. This oil-water separation usually requires heat and/or chemical treatment. In some cases, even after treatment, poor separation occurs when a viscous layer, known as a rag layer, develops at the oil-water interface. The formation and growth of rag layers can be challenging to predict and costly to deal with.

Rag layers have been characterized as a complex fluid of intermediate density comprised of emulsified water and/or oil, organic matter such as asphaltenes, and produced solids. These rag layers grow when the coalescence rate of the emulsified phase is slower than the settling rate. In bitumen and heavy oil processing, water-in-oil emulsions stabilized by asphaltenes and inorganic solids are often the most problematic to treat and are likely contributors to rag layer formation.

Asphaltenes are surface-active, amphiphilic molecules that tend to adsorb irreversibly at the interface to form rigid cross-linked networks that provide steric and mechanical resistance to coalescence. The solids most associated with oilfield emulsions are bi-wettable aluminosilicate clays, with kaolinite being the most abundant in the oil sands. Although kaolin and silica particles are naturally hydrophilic, exposure of the solid surface to bitumen in the absence of water can alter the wettability of the solids. Organic material, typically asphaltenes or multi-ring hydrocarbons found in bitumen, can adsorb onto the solid surface making the particles bi-wettable or even hydrophobic. The bi-wettable solids then accumulate at the oil-water interface and stabilize emulsified droplets.

Solid particles can stabilize emulsions by adsorbing at the water-oil interface and/or packing between droplets. A steric barrier to coalescence between water drops is created when the solids adsorb directly on the droplet interface or adsorb on top of an existing asphaltene film. The film barrier reduces coalescence by hindering collisions and contact between droplets. Mechanical stabilization by solids can also occur if the solids form a strong network structure. Packing between adjacent droplets further decreases coalescence because the trapped solids prevent dispersed droplets from aggregating, creaming or sedimenting, and coalescing. Solids can also destabilize emulsions by acting as bridges between droplets and promoting coalescence.

The main factors controlling the stabilizing effect of solids are their size, concentration, and wettability. Smaller particles and higher particle concentrations tend to produce smaller emulsion droplets and therefore more stable emulsions because collisions between droplets are less frequent. Bi-wettable solids (contact angles of approximately 90°) are in their lowest free energy state when adsorbed at the interface and therefore are expected to adsorb more strongly and produce more stable emulsions than solids with other wettabilities. The strong stability and formation of rag layers can be attributed to the presence of high concentrations of fine, oil-wet solids.

CHAPTER 3: EXPERIMENTAL METHODS

This chapter presents the experimental methods used to study the effect of inorganic solids on water-in-oil emulsions. The methods include: preparation of the asphaltenes and solids used to make emulsions; preparation of model emulsions at 60°C from reverse osmosis water and an organic phase consisting of asphaltenes, solids, heptane, and toluene; measurement of emulsion stability and emulsion layer growth in batch and continuous separation experiments. The measurement of particle size, solids wettability, and drop size distribution are also discussed.

3.1 Materials

The emulsions were prepared with toluene, *n*-heptane, reverse osmosis water, asphaltenes and solids. ACS grade toluene of 99.5%+ purity and technical grade *n*-heptane of 99.9% purity were purchased from VWR International. Reverse osmosis (RO) water was supplied by the University of Calgary.

3.1.1 Asphaltenes

The asphaltenes used in this study were recovered from bitumen samples from three different processes: oil sand (OS) extraction, cyclic steam stimulation (CSS), and steam assisted gravity drainage (SAGD). The OS and SAGD bitumen samples were provided by Suncor Energy Inc. and the CSS sample was provided by Shell Canada Ltd. The OS bitumen had been blended with naphtha and centrifuged to facilitate water separation at the plant site. The added naphtha was removed from the final product bitumen by distillation at Maxxam Analytics, Inc. The SAGD bitumen had been treated in the field without chemical addition to remove most of the water. The CSS bitumen had no chemicals added prior to recovery from the field. Water was separated from this bitumen in the lab by sonicating the sample at room temperature for a minimum of 7 days and then settling in a separatory funnel for 5 days at 50°C. The separated water was decanted. The residual water content was less than 3.5 wt% in all three bitumen samples (Rocha *et al.*, 2016). The asphaltene and toluene-insoluble (TI) contents of the bitumen samples are provided in Table 3.1.

Table 3.1 Solids free C7-asphaltene and toluene-insoluble (TI) contents of OS, CSS, and SAGD bitumen.

Sample	C7-Asphaltene Content (wt%)	TI Content (wt%)
OS bitumen	16.2	3.55
CSS bitumen	15.1	1.76
SAGD bitumen	18.7	0.40

Asphaltenes were extracted from bitumen by precipitation in *n*-heptane (Yarranton and Masliyah, 1996). Heptane was added to 40 g of bitumen at a 40:1 (mL/g) ratio in a 2000 mL beaker. The beaker was covered with plastic wrap and aluminum foil to prevent evaporation, sonicated for one hour, and then let stand for 23 hours for a total contact time of 24 hours. The supernatant was then decanted and filtered through VWR Grade 413 (5 μ m pore size) filter paper until approximately 400 mL of solution remained. An additional 4 mL of *n*-heptane per gram of original bitumen was added to the beaker, sonicated for 45 minutes, and then let stand for 18 hours. The whole solution was filtered through the same filter paper. The beaker was washed with a small amount of *n*-heptane and the washings poured through the same filter. The filter cake was washed with 25 mL of *n*-heptane three times daily for 5 days or until the filtrate was colorless. The filter cake was then left to dry until the weight was constant (4-5 days). The filter cake consisted of asphaltenes and TI solids such as fine clays that precipitated along with the asphaltenes.

To remove toluene-insoluble inorganic solids from the filter cake, 10 g/L of the filter cake material (asphaltenes and TI) was added to toluene and sonicated for 30 minutes. The asphaltenes are dissolved and the TI dispersed in the solution. The solution was then transferred into 50 mL Nalgene centrifuge tubes and centrifuged at 3600 rpm for 6 minutes to settle out the dispersed TI. The supernatant, consisting of asphaltenes and toluene, was decanted into a beaker. The same centrifuge tubes were reused to sequentially centrifuge the entire solution. The TI at the bottom of the tube were dried in a fume hood and weighed. The TI content of the bitumen is the mass of TI divided by the mass of bitumen used to obtain the filter cake. The TI were not used further in this study. The supernatant was dried in a fume hood to recover the solids-free asphaltenes. The asphaltene content of the bitumen is the mass of asphaltenes divided by the mass of bitumen used

to obtain the filter cake. These asphaltenes were used to prepare the model water-in-oil emulsions and are termed C7-asphaltenes.

3.1.2 Solids

The solids used in this study were silica and kaolin. Amorphous silica was selected in two particle size distributions: 18-32 μm and 32-63 μm supplied by MP Biomedical and purchased from Fisher Scientific. Kaolin (Hydrite® UF 90) was purchased from Imerys Kaolin with an average particle diameter of $<0.2 \mu\text{m}$.

The solids were treated by asphaltene adsorption to vary the wettability of the solids (Menon and Wasan, 1986 and Yan and Masliyah, 1994). To treat the solids, 10 g/L of solids was added to a solution of OS asphaltenes in 50 vol% *n*-heptane and 50 vol% toluene (50/50 heptol). The wettability alteration depended on the asphaltene concentration which was set between 0 and 1 g/L. The mixture was shaken for 24 hours in a mechanical shaker to ensure contact between the asphaltenes and the solid particles. The solution was then filtered through VWR Grade 413 filter paper and the solids were air-dried before use. The wettability of the treated solids was measured in terms of contact angle and critical surface tension, as described in Section 3.3.2. Note that the size distribution of the solids can be altered by this treatment and therefore was measured after treatment, as discussed in Section 3.3.1.

3.2 Emulsion Separation Experiments

Emulsion layer stability and growth were examined with three types of experiments (batch, continuous and decay) as described by Khatri *et al.* (2011). In batch separation experiments, the coalescence rate was determined from the change in height of the free water and oil layers in a beaker over time as an emulsion was left to coalesce. In continuous separation experiments, emulsion layer growth was measured as a prepared emulsion was continuously fed into a vertical separator. In decay experiments, the decrease in the emulsion layer height was measured after the feed into the separator was stopped. The data collected from all three separation experiments were the water, oil, and emulsion layer heights over time.

3.2.1 Apparatus

The emulsions were prepared in a 2 L glass beaker (dimensions 125 mm diameter by 160 mm high, Figure 3.1d). A Teflon lid (Figure 3.1a) was fitted to the beaker and Teflon baffles (dimensions 11 mm wide by 160 mm high, Figure 3.1b) were positioned along the beaker periphery to ensure uniform mixing. The apparatus was configured with either: 1) an IKA-RW20 digital variable speed overhead mixer with a 4-blade impeller (dimensions 10 mm wide by 8 mm high by 50 mm diameter, Figure 3.1c), or 2) a PRO250 homogenizer. Both mixers were positioned just below the oil-water interface. The beaker was immersed in a 20 L water bath fitted with a water circulator and temperature controller to maintain constant temperature of 60°C. The water bath was capable of maintaining temperatures from 20 to 80°C.

The batch separation experiments were carried out in the beaker only. For continuous separation experiments, the apparatus used is shown in Figure 3.2. A graduated glass separator equipped with a glass jacket for temperature control was added. The separator had an internal volume of 250 mL and a cross sectional area of 10.5 cm². The separator components and dimensions are given respectively in Figure 3.3 and Figure 3.4. Flow of the emulsion from the beaker to the separator was controlled through Viton tubing (#24, 130 cm long) with a Masterflex L/S peristaltic pump. The pump consisted of an economy digital drive and a Masterflex pump head (L/S Easy-Load II) and was capable of flow rates between 5 and 280 cm³/min. The tubing was positioned at the oil-water interface inside the beaker, passed through the pump and then connected to the glass feed tube inside the separator. Recycled free water and oil were returned to the emulsion beaker from the separator through Masterflex tubing (Viton #36) with respective lengths of approximately 26 cm and 62 cm. A thermostatted water circulator was used to feed the water jacket through Tygon tubing (8 mm diameter). Water exiting the top of the jacket was returned to the water bath with the same Tygon tubing.

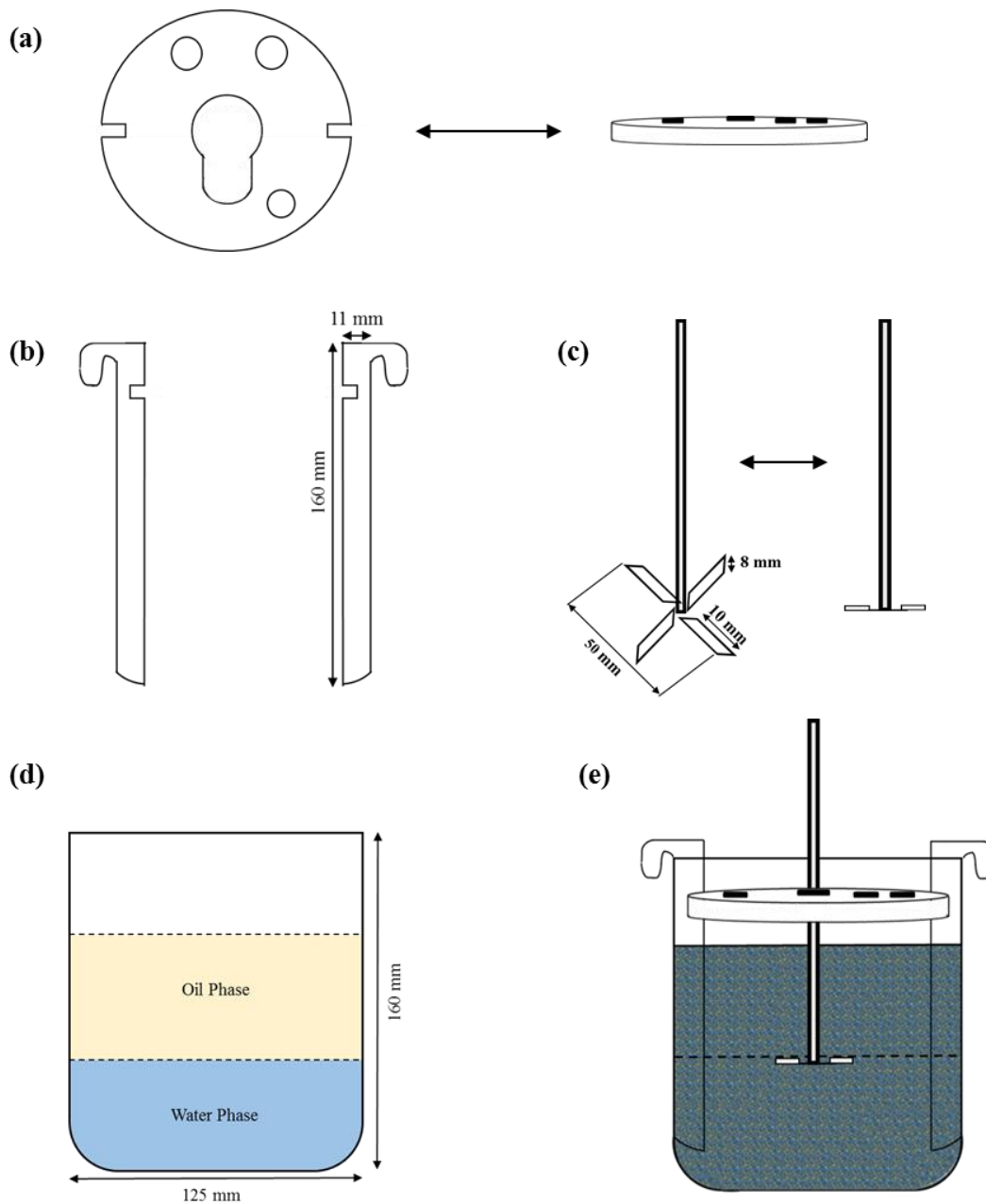


Figure 3.1 Emulsion preparation apparatus: a) Teflon disc (lid); b) Teflon baffles; c) overhead mixer; d) beaker; e) beaker setup assembled with all parts from (a) to (d).

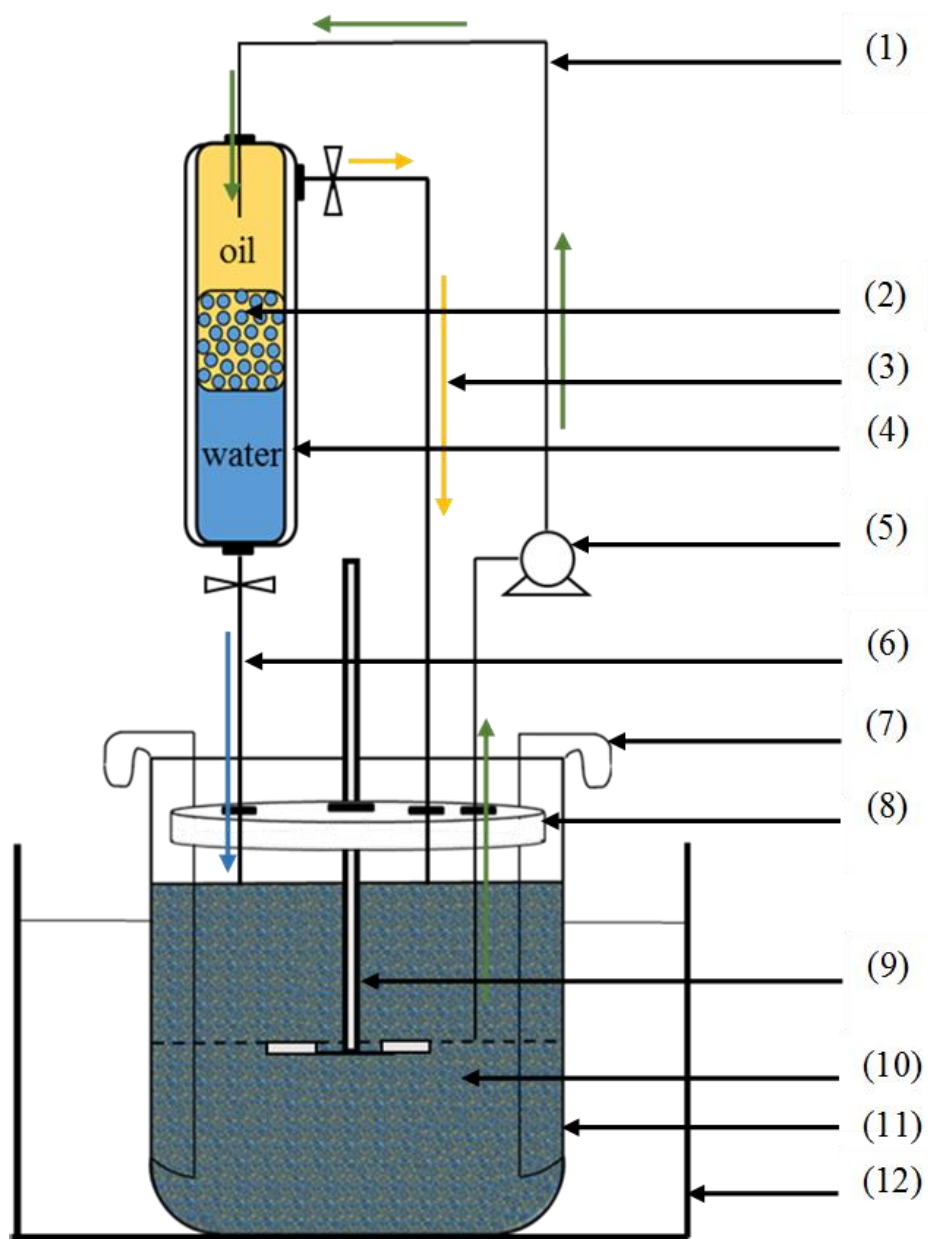


Figure 3.2 Schematic diagram of the continuous apparatus setup: 1) feed emulsion tubing; 2) emulsion layer; 3) oil recycle tubing; 4) separator with water jacket; 5) pump; 6) water recycle tubing; 7) Teflon baffle; 8) Teflon disc (lid); 9) impeller; 10) water-in-oil emulsion; 11) beaker; 12) water bath. Adapted from Khatri, 2010.

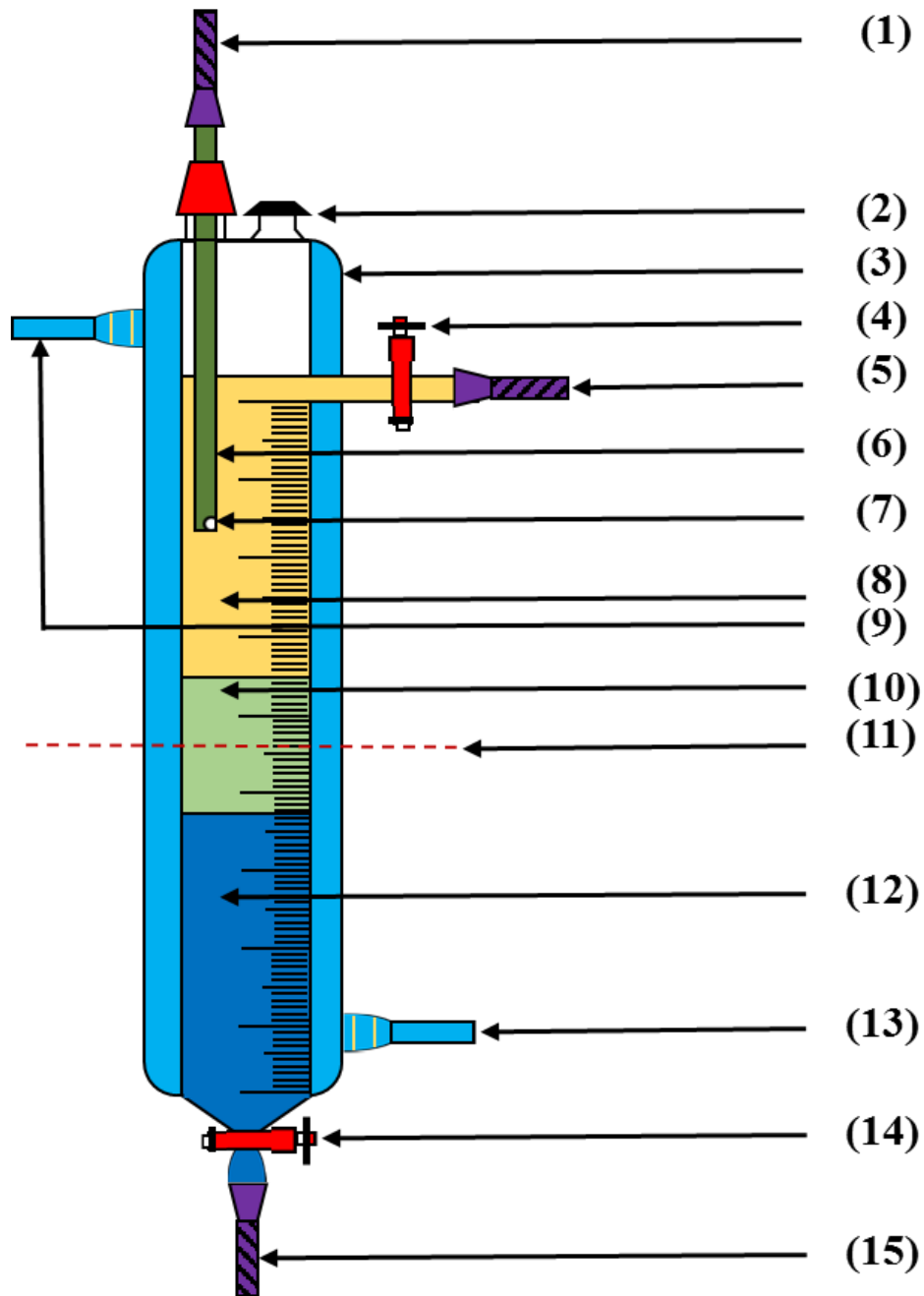


Figure 3.3 Schematic diagram of the separator used in continuous experiments: 1) feed port; 2) separator overflow exit; 3) water jacket; 4) oil exit valve; 5) oil exit; 6) glass emulsion feed tube; 7) feed outlet; 8) free oil phase; 9) water jacket outlet; 10) emulsion layer; 11) centerline; 12) free water phase; 13) water jacket inlet; 14) water exit valve; 15) water exit.

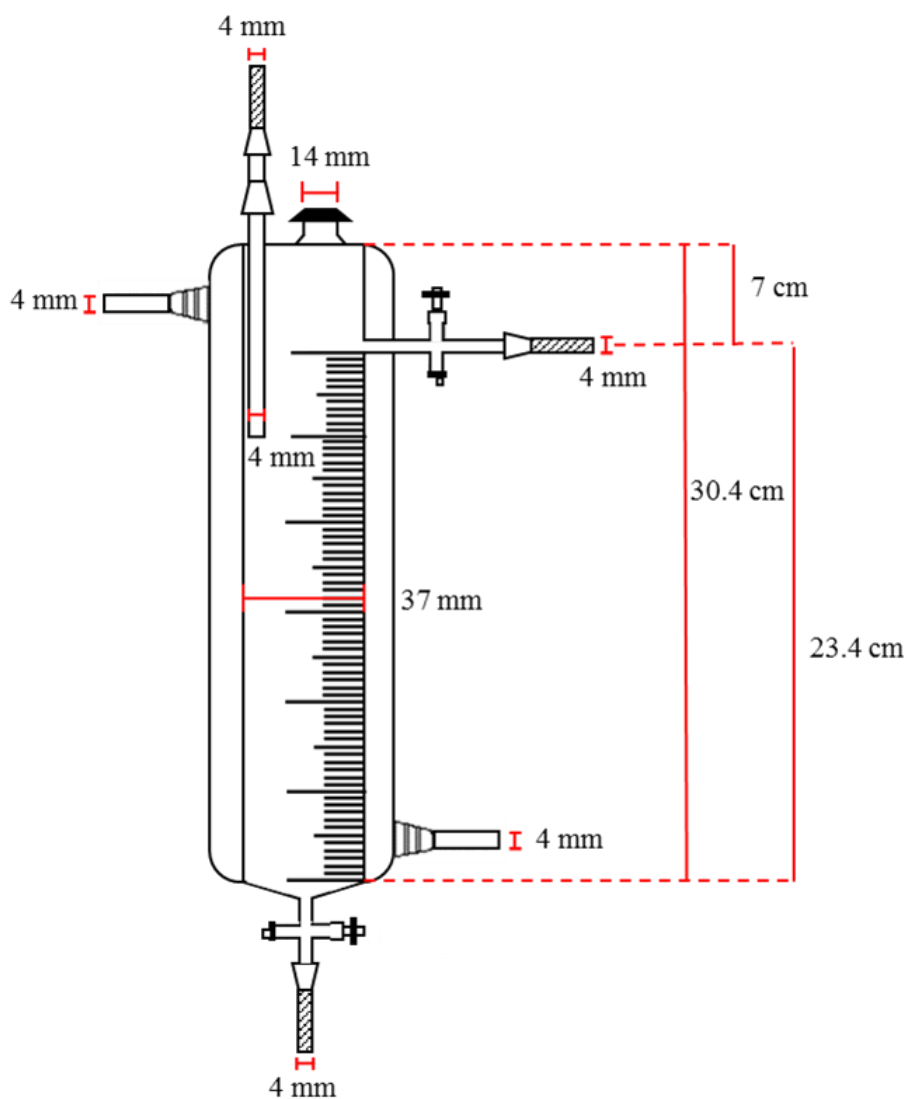


Figure 3.4 Dimensions of the 250 mL glass separator used in continuous experiments.

3.2.1.1 Apparatus Cleaning

In order to take accurate and repeatable measurements and to ensure there were no impurities in the apparatus, the following steps were taken to clean the apparatus:

- After each experiment, the beaker and separator were rinsed with toluene, air-dried completely, rinsed with RO water and then air-dried again.
- The separator was soaked with 2% Hellmanex III solution for 2 hours and then flushed with RO water for approximately 30 minutes and left to dry overnight after each run.

- After several runs, the beaker was scrubbed with Comet cleanser, rinsed with RO water and then sonicated/flushed repeatedly to remove any traces of the cleanser. It was found that three cycles of flushing with RO water for 5 minutes and sonicating for 20 minutes was sufficient to remove all surface active material from the glass beaker.
- The tubing was rinsed with toluene, continuously flushed with RO water for 5-10 minutes, and dried after every use. The tubing was replaced after approximately 20 uses.
- The Teflon baffles and lid were rinsed with toluene after every use and stored in RO water.

3.2.2 Preparation of Bulk Phases

Model water-in-oil emulsions of 1600 mL were prepared with 50 vol% aqueous phase and 50 vol% organic phase unless otherwise stated. The aqueous phase consisted of reverse osmosis (RO) water. Unless otherwise stated, the organic phase was 1.5 g/L of solids-free C7-asphaltenes in a solution of 50 vol% *n*-heptane and 50 vol% toluene (50/50 heptol). The asphaltenes were first dissolved in toluene and sonicated for 30 minutes to ensure complete dissolution. Then *n*-heptane was added and the mixture was sonicated for an additional 10 minutes to ensure homogeneity. The solids, if required, were added with the asphaltenes and dispersed in the organic phase. Prior to emulsification, the aqueous and oil phases were heated separately in a water bath for 20-25 minutes at 60°C.

3.2.3 Batch Experiment

The emulsions in the batch experiment were prepared in two ways: 1) using the overhead mixer described in the apparatus section at a speed of 1000 rpm for 10 minutes; 2) using a homogenizer mixing at 10,000 rpm for 10 minutes. In both cases, the impeller was placed just below the oil-water interface and the aqueous phase was added dropwise to the top of the oil phase during mixing. The beaker was covered with aluminum foil to prevent solvent evaporation during heating and mixing.

After mixing for 10 minutes, the lid and baffles were removed from the beaker and the initial height of the emulsion layer was recorded. Over time, the emulsified oil and water coalesced and separated from the emulsion layer as free oil and water. The height of the emulsion layer was

measured periodically until the emulsion had fully separated or there was no further change in emulsion layer height with time. The water volume fraction was determined at each time step directly from the measured layer heights as follows:

$$\Phi_w = \frac{h_w^o - h_w}{h_e} \quad \text{Equation 3.1}$$

where h_w^o is the initial height of water in the beaker before mixing, and h_w and h_e are the height of the free water layer and the emulsion layer, respectively, at any given time. The height of the emulsion layer over time in the batch experiment was repeatable to ± 0.2 cm based on a 95% confidence interval. A schematic of emulsion heights over time in the batch experiments is shown in Figure 3.5.

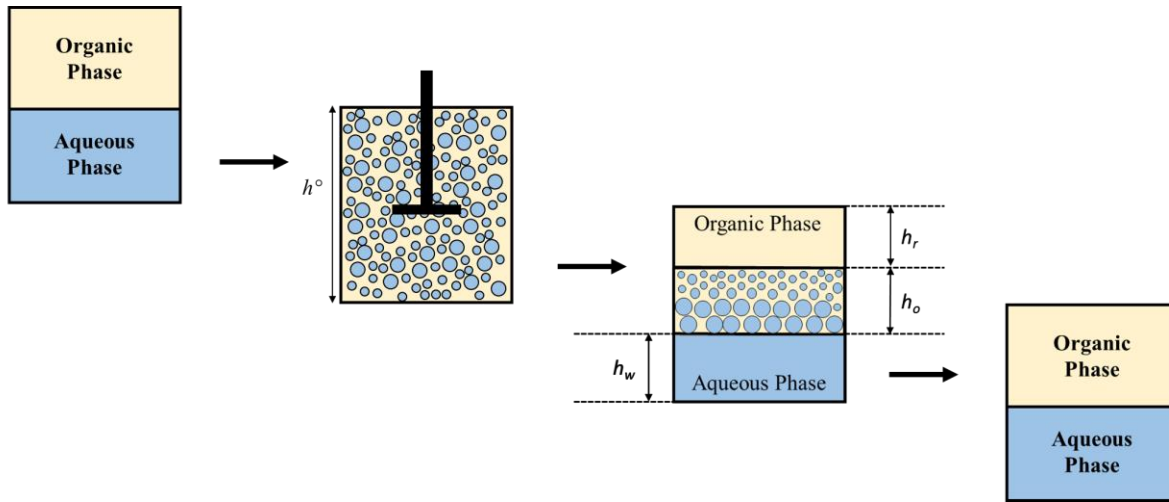


Figure 3.5 Batch experiment schematic of the emulsion beaker at different time steps. Adapted from Khatri, 2010.

3.2.4 Continuous Experiment

The emulsion was prepared as described in Section 3.2.2 for the batch experiment. However, after mixing for 10 minutes, the mixer was left on at a constant speed and the emulsion was pumped with a peristaltic pump at a flowrate of 20 mL/min into the vertical glass separator. The separator initially contained 250 mL of fluid: 50 vol% organic phase and 50 vol% aqueous phase of the same composition as the original emulsion mixture preheated to 60°C. As the emulsion was pumped into the top of the separator, material accumulated at the oil-water interface after passing through

the oil phase and an emulsion layer began to grow. Separated free water and oil were recycled into the original emulsion beaker by gravity. The emulsion layer was maintained in the middle of the separator by adjusting the flowrate of exiting water stream. The oil exit valve was open throughout the continuous experiment to allow excess free oil to return to the emulsion beaker. The height of the emulsion layer was measured (repeatable to ± 0.2 cm) periodically until either the layer filled the separator or the height did not change with time and a steady state condition was achieved.

3.2.5 Decay Experiment

Each decay experiment was started upon completion of a continuous experiment. The pump was turned off, the oil and water exit valves closed, and the emulsion was left to coalesce undisturbed in the separator. As with the batch experiment, the decrease in emulsion layer height was measured periodically until it remained constant with time and there was no further coalescence. The height of the emulsion layer over time in the decay experiment was repeatable to ± 0.2 cm. The variation in the emulsion layer height over time during the continuous and decay experiments is shown schematically in Figure 3.6.

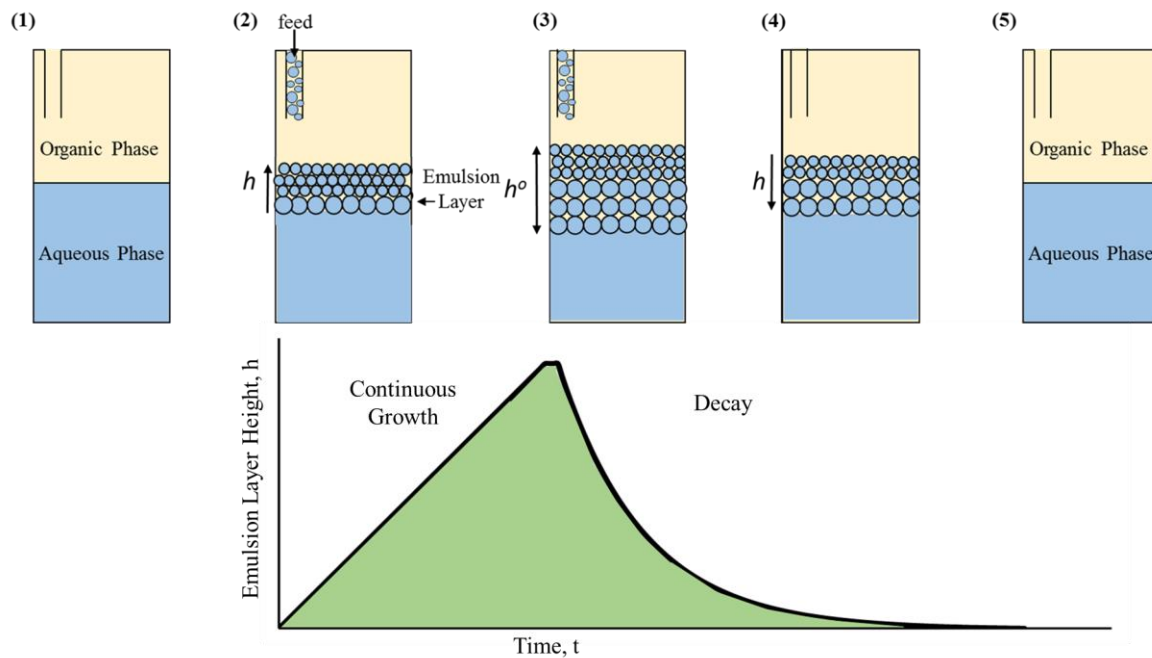


Figure 3.6 Schematic representation of the emulsion layer height over time during the continuous and the decay experiment: 1) original separator; 2) continuous experiment begins with pump turned on and emulsion feed into separator; 3) emulsion layer growth in separator; 4) pump turned off at beginning of decay experiment; 5) emulsion layer coalesces into free water and oil layers. Adapted from Khatri, 2010.

3.2.6 Determination of Emulsion Layer Water Volume Fraction in Continuous Separation

The volume fraction of emulsified water in the emulsion layer was required to model emulsion layer growth and was measured for several emulsions using the method described by Khatri *et al.* (2011). To measure the water fraction in the emulsion layer, a series of continuous experiments at the same conditions were performed with the exit valves open, stopping the feed (and outlet flows) at a different time (3, 5 and 10 minutes) in each case. At each time, the emulsion was left to decay and the volume of resolved water was determined from the change in the height of the water column. The water volume fraction is simply the volume of water resolved divided by the initial volume of the emulsion layer. The water volume fraction determined from each decay experiment was the water fraction in the continuous experiment emulsion layer at the time the continuous experiment was stopped.

3.2.7 Determination of Solids Content in Emulsion Layer from Continuous Separations

For solids stabilized emulsions in the continuous experiment, the solids content of the emulsion layer was measured by collecting the emulsion layer and drying it to recover the solids. The collected solids were then washed with toluene until the filtrate was colourless to remove any asphaltenes that were not absorbed onto the solids surface. The solids concentration in the continuous phase within the emulsion layer, C_{solids} , was then calculated as:

$$C_{solids} = \frac{m_{solids}}{V_e(1-\Phi_w)} \quad \text{Equation 3.2}$$

where m_{solids} is the mass of the collected solids, V_e is the volume of the collected emulsion and Φ_w is the water volume fraction in the emulsion layer.

3.3 Property Measurements

3.3.1 Particle Size Distribution

Particle size distributions for kaolin and silica solids were measured with a Lasentec Model D600 Particle Size Analyzer using the Focus Beam Reflectance Measurement (FBRM) method. The particle size analyzer provides an *in-situ* particle chord length distribution for particles, where chord length is defined as a straight line between any two points on the edge of an individual particle.

The main component of the apparatus is a probe that rotates a 780 nm laser beam at a fixed speed of 4500 rpm through the suspension. As the beam scans across a particle, a portion of the light backscatters to the photodetector in the probe, which uses the duration of the light pulse and the scan speed (approximately 2 ms^{-1}) to calculate the chord length of each particle (Heath *et al.*, 2002). The particle size analyzer is capable of measuring thousands of chords, which produces a robust chord length distribution and represents the particle population of the system (Sathe *et al.*, 2010). The particle number count per second was also collected. However, since the particle size analyzer can only measure one particle at a time and the reflection time must return to zero between measurements, the count does not correlate well with the actual particle concentration in the system.

The particle size analyzer calculates the number mean diameter every 30 seconds using fine discrimination electronics in the FBRM Control Interface (Version 6) software. The fine electronics provides sharper resolution and higher sensitivity on fine chords when interpreting the backscattered signals to detect smaller particles travelling closely together. The 30 second interval between data collection and updating of the current statistics and chord length distribution provides a trade-off between measurement precision and time resolution. The software categorizes diameter distributions using 90 log normal intervals over a channel range of 1 to 1080 μm .

The chord length distribution is calibrated to better match the real particle diameter distribution. Since the chord length is measured as a random distance between two edges on the particle, a distribution of sizes is produced even for perfectly monodispersed solids. To calibrate the distribution for the irregular particles, a weight factor is introduced to the number frequency equation as follows:

$$f_N = w \frac{n}{n_t} \quad \text{Equation 3.3}$$

where f_N is the calibrated number frequency, n is the number of primary chord measurements at that diameter interval, n_t is the total number of chord measurements and w is the weighted calibration factor. The calibration factor is weighted to give greater importance to larger particles to compensate for chord length measurements which are generally shorter than the actual diameter and is given as follows:

$$w = \frac{d^\gamma}{\sum d_i^\gamma} N \quad \text{Equation 3.4}$$

where d is the midpoint of the distribution interval, γ is the calibration exponent, and N is the total number of channels. The exponent can range from -1 to 3 according to the nature of the system, with a value of 0 indicating that the true diameter distribution of the particles is the measured chord length distribution. The selection of exponent is validated by comparison with micrographic distributions.

The repeatability of the number mean diameter measured by the particle size analyzer was determined to be 8.1% at a 90% confidence interval based on three repeated measurements of flocculated asphaltenes in a bitumen-*n*-heptane mixture (Casas, personal communication, 2017).

The measured chord lengths were found to be reproducible, with no significant difference in the mean values measured for a suspension of 8.33 wt% polyvinyl chloride in water and the reference value at a 90% confidence interval (Casas, personal communication, 2017).

To measure the particle size distribution, a solution was prepared with 10 g/L of particles in 50 vol% toluene and 50 vol% *n*-heptane. The solution was sonicated for 30 minutes and then placed in a beaker equipped with a four-angle blade impeller situated 3 mm below the sapphire window of the probe. During the measurements, the solution was mixed at 275 rpm to suspend the particles and provide a flow of particles across the window. The size distribution was measured every 30 seconds for a total of 10 minutes. In this work, a cubic calibration factor was used to give greater importance to larger particle diameters. The FBRM method appears to skew towards smaller diameters for irregular particles when compared to diameter distributions determined from micrographs. This underestimation of the particle size distribution may be due to the greater probability of measuring shorter chord lengths than longer ones.

3.3.2 Wettability of Solids

3.3.2.1 Contact Angle Measurement

Contact angles were measured using the sessile drop technique on a flat surface prepared from the solid particles. The flat surface was formed by compacting particles into a disc using a manual hydraulic press (Carver Model 4350) with a 1.3 cm die at ambient conditions. Approximately 0.2 g of solids were added to the die and a force of 24.2 kN was applied for 2 minutes under light vacuum. The disc was then immersed in organic solvent and a water drop was placed on the flat surface. The three phase contact angle through the water phase (Figure 3.7) was measured directly by an IT Concept (now Teclis) Tracker Drop Shape Analyzer equipped with a camera.

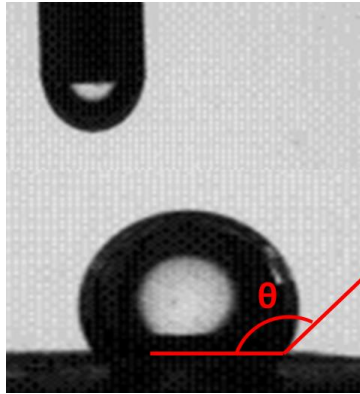


Figure 3.7 Drop shape analyzer equipped with camera measures the solid-water-heptol contact angle of compressed solids through the water phase. Lines are for visual reference.

3.3.2.2 Film Flotation Method

The critical surface tension of the solids was assessed with the film flotation method to validate the compressed disc contact angle measurements. In the film floatation method (Fuerstenau *et al.*, 1991), solids were placed on a water/methanol surface in air (Figure 3.8) and the fraction of solids that remains floating was determined. The experiment was repeated at different water/methanol ratios and therefore different surface tensions to find the point at which half the particles settled. The surface tension at this point, the critical surface tension, is defined as the highest surface tension of a liquid that completely wets the solids, causing the solids to sink. To determine the mass fraction of floating solids, the surface material was collected by decanting the top layer after 1 minute of contact, dried, and weighed. The fraction that remained floating is the mass of floating solids divided by the initial mass of solids. Note, the film flotation method does not provide a quantitative contact angle, but is used to assess the relative wettability of different particles.

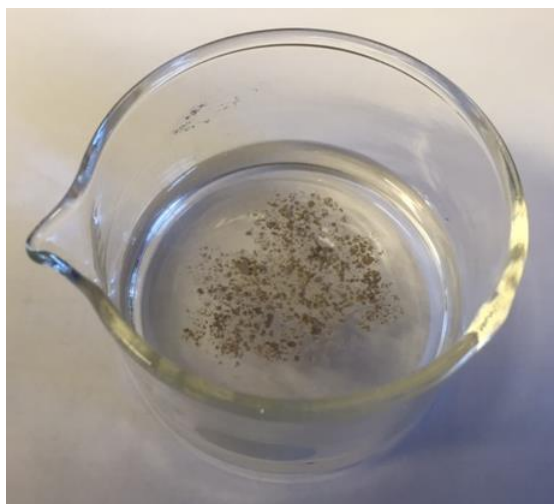


Figure 3.8 Film floatation method to measure relative wettability of coarse solids through critical surface tension.

3.3.3 Drop Size Distribution

Drop size distributions for the emulsions were determined using a Carl Zeiss Axiovert S100 inverted microscope equipped with video camera and AxioVision software. A plastic pipette was used to place a sample of the emulsion on a hanging-drop glass slide for observation under the microscope. The continuous phase (50/50 heptol) was added to the sample to separate the droplets for easier viewing. A slip cover was placed over the slide cavity to prevent solvent evaporation. For each sample a minimum of 500 droplets were analyzed to obtain drop size distributions, giving an expected error of 5-10% (Dixon and Massey, 1969).

CHAPTER 4: MODELING

This chapter discusses the methodology used to model the experimental data for the batch, continuous and decay experiments. The models were adapted for W/O emulsions stabilized by asphaltenes and solids from those developed by Khatri *et al.* (2011) for the growth of surfactant stabilized O/W emulsion layers. These models are based on a material balance of the dispersed phase in the emulsion layer. It was assumed that the emulsion layer is a dense packed zone whose volume changes with coalescence and compaction of the dispersed phase, but not through free settling. In each case, the models were developed for water-in-oil emulsions and the material balances were performed on the water phase in the emulsion layer. In this thesis, a constant coalescence rate and limiting height and fractional bypass terms have been introduced into the model. The model development and adaptations made in this thesis are presented below.

4.1 Batch Model

The batch experiment involves a water-in-oil emulsion created in a beaker and left to coalesce into free water and oil layers. The height of the water and oil layers were measured over time. The experimental heights were modeled by performing a material balance on the dispersed water phase in the emulsions layer, as shown in Figure 4.1, to determine emulsion stability and coalescence rates. Initially, all of the water phase was emulsified and was dispersed in the emulsion layer. Hence, the accumulation of water in the emulsion layer is given by:

$$\frac{dM_w}{dt} = -\dot{m}_{w,out} \quad \text{Equation 4.1}$$

where M_w is the mass of water in the emulsion layer at time t and $\dot{m}_{w,out}$ is mass flow rate of free (coalesced) water exiting the emulsion layer. The mass of water in the emulsion layer is given by:

$$M_w = Ah\Phi_w(t)\rho_w \quad \text{Equation 4.2}$$

where A is the cross sectional area of the emulsion layer, h is the height of the emulsion layer, Φ_w is the volume fraction of dispersed water in the emulsion layer at time t , and ρ_w is the density of water. In this case, the cross sectional area of the emulsion layer is the cross sectional area of the beaker. Note that the water volume fraction can vary with time if the emulsion layer compacts.

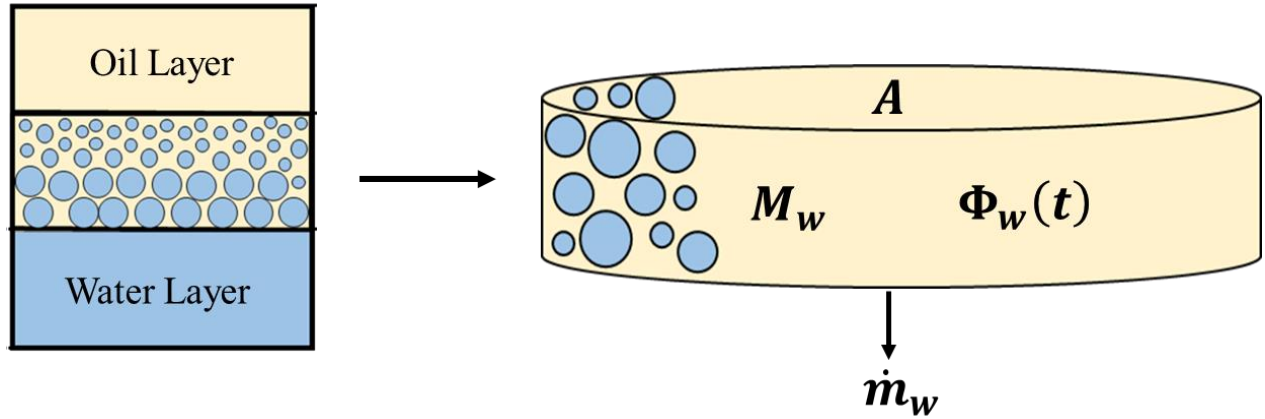


Figure 4.1 Material balance on the dispersed water in the emulsion layer over time in the batch experiment. Adapted from Khatri, 2010.

It was assumed that the mass flow rate of water exiting the emulsion layer is equal to the bulk coalescence rate of water droplets within the emulsion layer. Direct coalescence between droplets and the free liquid phase was neglected. In this case, the coalescence rate is proportional to the number of droplet-droplet contacts. If the droplet size distribution is assumed to be invariant, the coalescence rate is also proportional to the volume of water in the emulsion layer. Hence, the flow rate of coalesced water exiting the emulsion layer can be expressed as follows:

$$\dot{m}_{w,out} = kAh\Phi_w(t)\rho_w \quad \text{Equation 4.3}$$

where k is the bulk coalescence rate and is assumed to be constant. In this study, it was observed experimentally that the asphaltene-stabilized emulsions did not completely coalesce into free water and oil layers and therefore Eq. 4.3 was modified as follows:

$$\dot{m}_{w,out} = kA(h - h_{lim})\Phi_w(t)\rho_w \quad \text{Equation 4.4}$$

where h_{lim} is the limiting height representing the portion of the emulsion which does not fully coalesce. The limiting height can be varied from 0 to 1, with a value of 0 indicating that the emulsion fully coalesces and a value of 1 indicating no coalescence. Note, a variable time dependent coalescence rate modeled by an exponential decay was previously used in this model to account for the observed decrease in coalescence over time. The use of the limiting height model with a constant coalescence rate was found to be simpler and required fewer additional tuning parameters.

Eqs. 4.2 and 4.4 were substituted into Eq. 4.1 to obtain:

$$\frac{d(Ah\Phi_w(t)\rho_w)}{dt} = -kA(h - h_{lim})\Phi_w(t)\rho_w \quad \text{Equation 4.5}$$

The beaker cross sectional area and the water density are constant. Eq. 4.5 can therefore be simplified to obtain the following equation for the change in emulsion layer height with time:

$$\frac{dh}{dt} = -k(h - h_{lim}) - \frac{h}{\Phi_w(t)} \frac{d\Phi_w(t)}{dt} \quad \text{Equation 4.6}$$

The dimensionless form of Eq. 4.6, with the emulsion layer height at a given time divided by the initial height of the emulsion layer immediately after mixing, is given as follows:

$$\frac{d\left(\frac{h}{h^o}\right)}{dt} = -k\left(\frac{h}{h^o} - \frac{h_{lim}}{h^o}\right) - \frac{1}{\Phi_w(t)} \frac{h}{h^o} \frac{d\Phi_w(t)}{dt} \quad \text{Equation 4.7}$$

All of the terms in Eq. 4.7 were directly measured except for the water volume fraction, the coalescence rate, and the limiting height. The water volume fraction was determined at each time step from the measured layer heights as follows:

$$\Phi_w = \frac{h_w^o - h_w}{h_e} \quad \text{Equation 4.8}$$

where h_w^o is the initial height of water in the beaker before mixing, and h_w and h_e are the height of the free water layer and the emulsion layer, respectively, at any given time. Eq. 4.7 was then fit to the experimental batch data to determine the coalescence rate constant and limiting height.

A material balance on the water in the emulsion layer can also be used to model the height of the free water layer as shown in Figure 4.2. The instantaneous water balance across the water layer where coalesced water in the emulsion layer enters the free water layer, is given by:

$$\frac{dM_{fw}}{dt} = \dot{m}_{w,out} \quad \text{Equation 4.9}$$

where M_{fw} is the mass of water in the free water layer and \dot{m}_w is the rate of water exiting the emulsion layer by coalescence as before. The mass of free water at a given time is then:

$$M_{fw} = Ah_w\rho_w \quad \text{Equation 4.10}$$

where h_w is the height of the water layer and A is the cross sectional area of the water layer and is equal to the cross sectional area of the beaker.

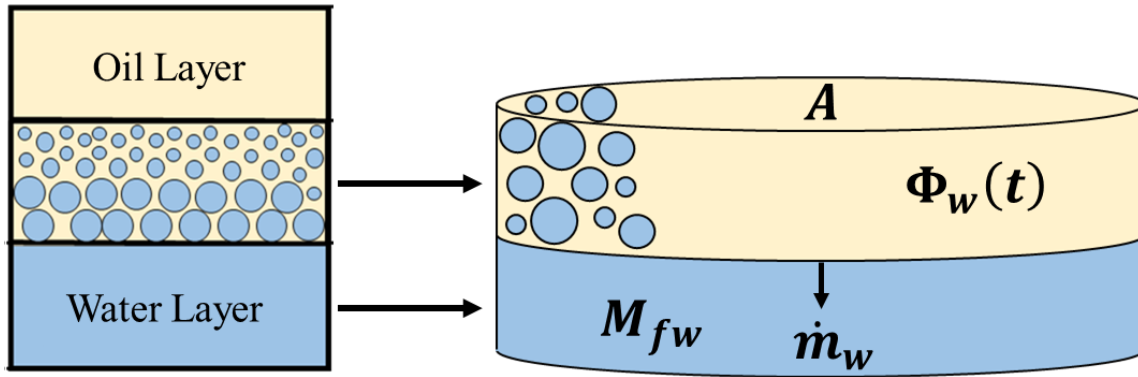


Figure 4.2 Material balance on the free water in the batch experiment. Adapted from Khatri, 2010.

Eqs. 4.4 and 4.10 were substituted into Eq. 4.9 and simplified with constant cross sectional area and water density to obtain the following equation for the change in the free water layer height with time:

$$\frac{d(h_w)}{dt} = k \left(\frac{h}{h^o} - \frac{h_{lim}}{h^o} \right) \Phi_w(t) \quad \text{Equation 4.11}$$

Eq. 4.11 was made dimensionless by dividing by the total height of the initial emulsion layer, h^o :

$$\frac{d\left(\frac{h_w}{h^o}\right)}{dt} = k \left(\frac{h}{h^o} - \frac{h_{lim}}{h^o} \right) \Phi_w(t) \quad \text{Equation 4.12}$$

Eq. 4.12 was used to model the free water layer height in the batch experiments. Similar to the batch model for the emulsion layer height, the water volume fraction was determined at each time step using Eq. 4.8 and the model was fit to the experimental data by adjusting the coalescence rate constant and the limiting height.

4.2 Continuous Growth and Decay Model

To model the continuous experiment, models of both the growth of the emulsion layer and its decay are required. Each model is developed below and then combined into a single numerical model. The use of a single numerical model for the continuous experiment is a unique development of the model for this thesis.

4.2.1 Decay Model

The decay experiments are essentially the same as the batch experiments except that, in the decay experiment, the emulsion layer accumulated over time in the separator instead of forming

instantaneously after emulsification in the beaker. It was observed experimentally that the volume fraction of the dispersed phase was approximately constant in the decay experiments even though it varied with time in the batch experiments. Therefore, a constant volume fraction was introduced into Eq. 4.7 to obtain the following expression for the change in dimensionless emulsion layer height over time in a decay experiment:

$$\frac{d\left(\frac{h}{h^o}\right)}{dt} = -k \left(\frac{h}{h^o} - \frac{h_{lim}}{h^o} \right) \quad \text{Equation 4.13}$$

where h^o is the initial height of the emulsion layer at the beginning of the decay experiment.

4.2.2 Continuous Model

The continuous experiment measures emulsion layer growth with time while an emulsion was continuously fed into a separator, as shown in Figure 4.3. In this case, the material balance performed on the dispersed phase becomes:

$$\frac{dM_w}{dt} = \dot{m}_{w,in} - \dot{m}_{w,out} \quad \text{Equation 4.14}$$

where $\dot{m}_{w,in}$ is the rate at which emulsified water is entering the separator from the feed. This influx of emulsified water to the emulsion layer in the separator is given by:

$$\dot{m}_{w,in} = \rho_w \Phi_w^o \dot{V}_{in} (1 - \varepsilon) \quad \text{Equation 4.15}$$

where Φ_w^o is the volume fraction of emulsified water in the feed, \dot{V}_{in} is the flow rate of the pump, and ε is the fractional bypass (the portion of the emulsified water that breaks into free water as the feed emulsion passes through the pump). This free water was assumed to rapidly reach the free water phase in the separator and to have negligible effect on the volume of the emulsion layer. The water accumulation and mass of water leaving the emulsion layer are given by Eqs. 4.2 and 4.4, respectively, as for the batch experiments.

Eqs. 4.2, 4.4 and 4.15 are substituted into Eq. 4.14 to obtain the following expression for emulsion layer growth in the separator:

$$\frac{dh}{dt} = \frac{\Phi_w^o \dot{V}_{in}}{\Phi_w A} (1 - \varepsilon) - kh \quad \text{Equation 4.16}$$

All of the terms in Eq. 4.16 were measured directly except for the fractional bypass, the coalescence rate, and the limiting height. Note, the water volume fraction in the emulsion layer, Φ_w , was measured for a small set of emulsion layers as described in Section 3.2.6 and was found

to be nearly constant. The water volume fraction in the feed, Φ_w^o , is held constant at 0.50, the initial water volume fraction in the original emulsion beaker. Eq. 4.16 is fit to the experimental data by adjusting the fractional bypass, the coalescence rate constant, and the limiting height.

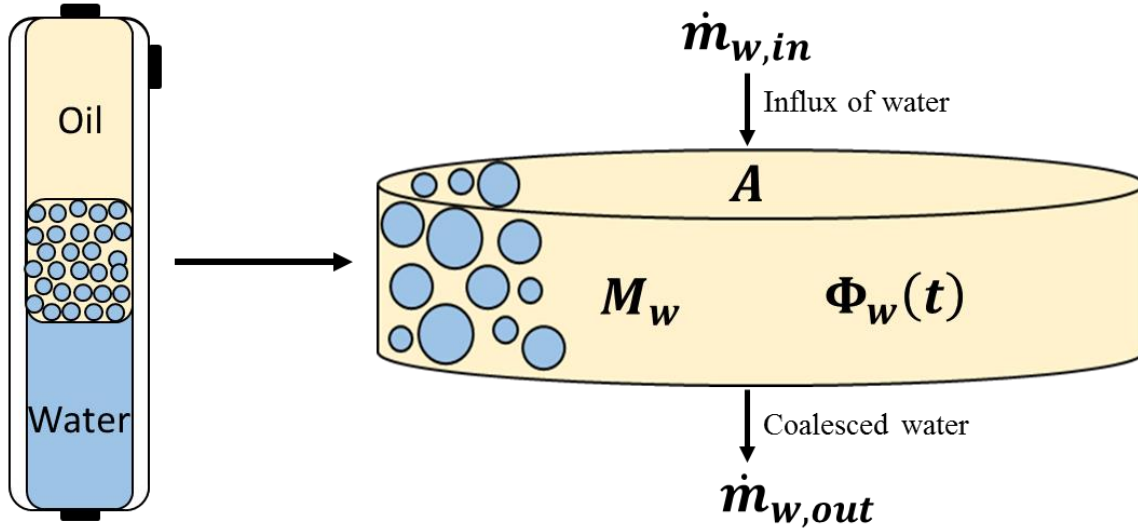


Figure 4.3 Material balance on the dispersed water in the emulsion layer in the continuous experiment. Adapted from Khatri, 2010.

4.2.3 Combined Continuous and Decay Model

To model emulsion layer growth and decay together, the continuous and decay separation experiments were numerically modeled explicitly as a column of layers accumulating and decaying over 1 minute time steps as shown in Figure 4.4. The emulsion entering the separator each minute constitutes one layer and a new layer is added for each minute emulsion is pumped into the separator. The height of each new layer after 1 minute is calculated using Eq. 4.16 for emulsion layer growth. The height of that layer at each subsequent time step is determined using Eq. 4.13 for emulsion decay. The height of all layers are then summed to obtain the total height. A flowchart for the numerical model is shown in Figure 4.5. The model was fit to the combined data by adjusting the fractional bypass, the coalescence rate, and the limiting height.

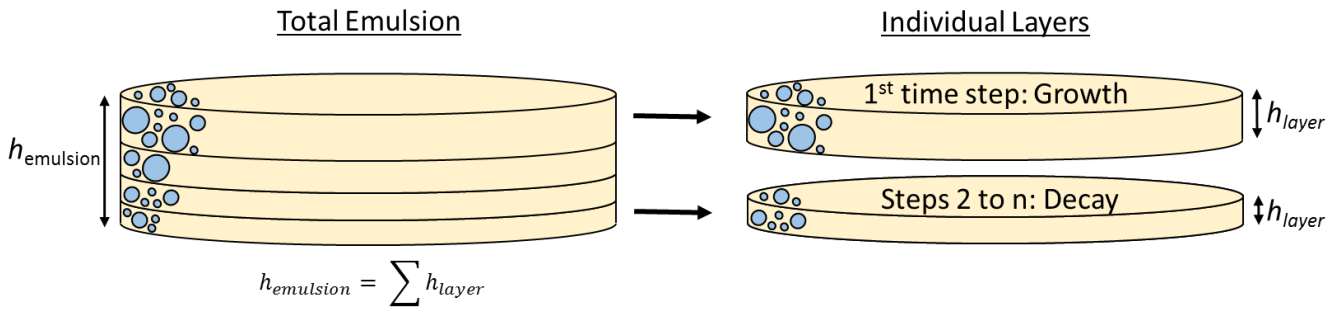


Figure 4.4 Division of emulsion into individual layers in combined continuous and decay model. The newly added layer models emulsion layer growth for the first time step and emulsion layer decay is modeled for all subsequent time steps in each layer. The total emulsion height is the sum of all layer heights.

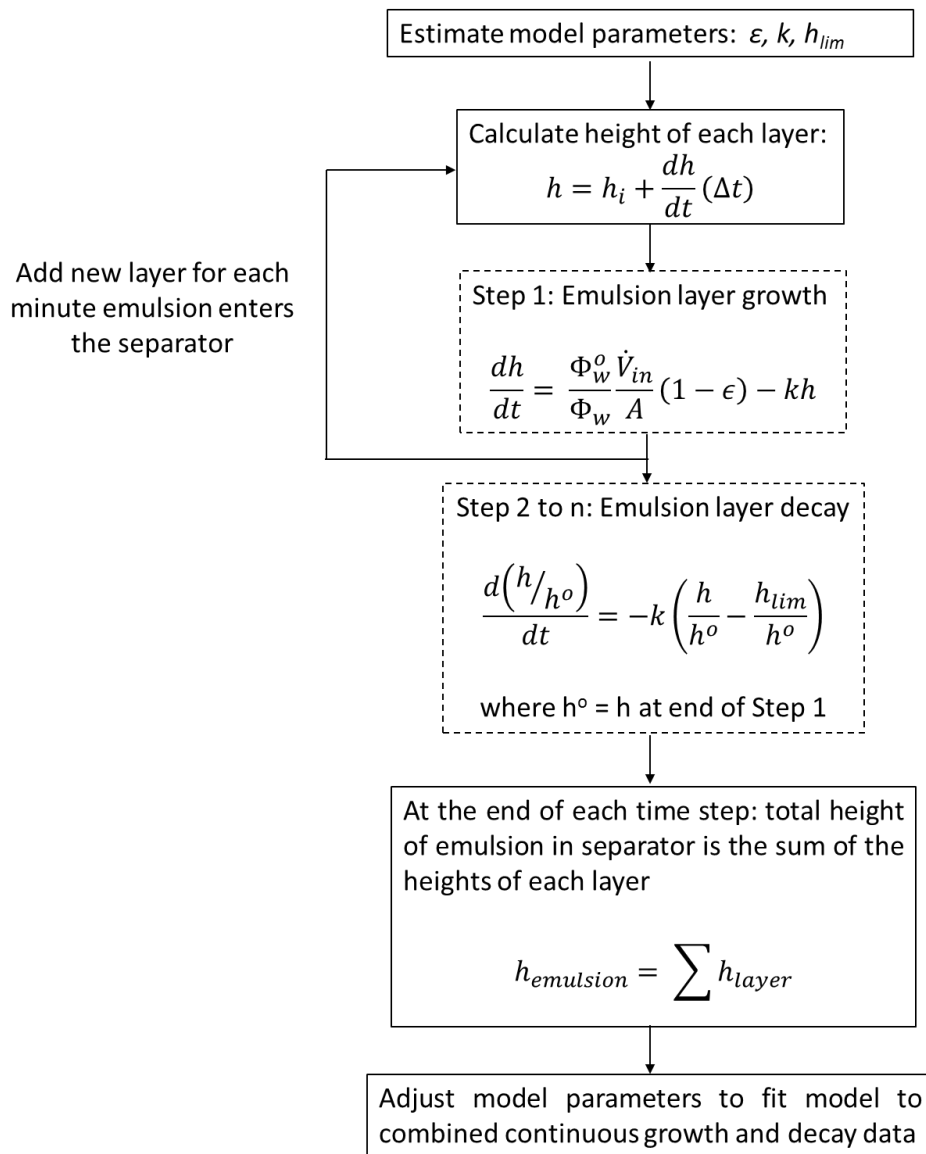


Figure 4.5 Block flow diagram of the algorithm for the numerical model.

CHAPTER 5: RESULTS AND DISCUSSION¹

This chapter discusses the experimental results and modeling of the emulsion stability and growth experiments. Batch experiments and continuous experiments were performed on asphaltene stabilized emulsions with and without added solids. The objectives of the experiments without solids were: 1) to investigate the potential to predict rag layer growth from batch tests; 2) to establish a base case emulsion for the experiments with solids. Data were collected for asphaltenes from different sources (OS, CSS, and SAGD), with different solvents (toluene and 50/50 heptol), and with different drop size distributions (mean diameters of 8 and 20 μm). The objectives of the experiments with solids were: 1) to investigate the effect of solids on coalescence rates and rag layer growth; 2) to assess the potential to predict rag layer growth from batch tests when solids are present. The batch and continuous experiments were repeated for the base case emulsion, but with added solids. The effect of the type (kaolin and silica), size (mean diameters of 12, 18, and 32 μm), and wettability (contact angles of 50 to 125°) of the solids were considered.

5.1 Asphaltene-Stabilized Emulsions

Batch and continuous separation experiments were first run on solids-free model emulsion systems stabilized by asphaltenes to examine the effects of asphaltene source and concentration, solvent characteristics, and drop size distributions on emulsion layer stability and growth. The data were used to determine a base case emulsion for solids addition. The model was fit to the experimental data to determine if batch experimental parameters can be used to predict the behaviour of emulsion layers in continuous separations. Before examining the data, the approach used to fit the model to the data is described.

5.1.1 Modeling the Experimental Data

The collected experimental data of batch and continuous emulsion layer heights over time was modeled with the mass balance based model presented in Chapter 4. Model parameters of

¹ The contents of this chapter have been accepted for publication in the Canadian Journal of Chemical Engineering.

coalescence rates, limiting heights, and fractional bypass values were determined by tuning the model to fit the data. These model parameters captured the trends in emulsion stability and were useful for comparing emulsion stability and growth rates at different conditions.

Batch Separation Experiments

Figure 5.1 shows the change in the dimensionless height of the emulsion and free water layers over time in the batch experiment where the emulsion stabilized by OS asphaltenes (no solids) was left undisturbed to coalesce into free oil and water phases. The emulsion was prepared with the overhead mixer at 1000 rpm at 60°C in toluene solvent. Both the emulsion and free water layer experimental heights were made dimensionless by dividing by in the initial height of the emulsion layer measured immediately after mixing. In this case, there was a rapid decrease in the emulsion layer height and increase in the free water height as the droplets settle. This period was followed by a slow change in the emulsion height over time and no change in the free water height as the settled emulsion compacts over time.

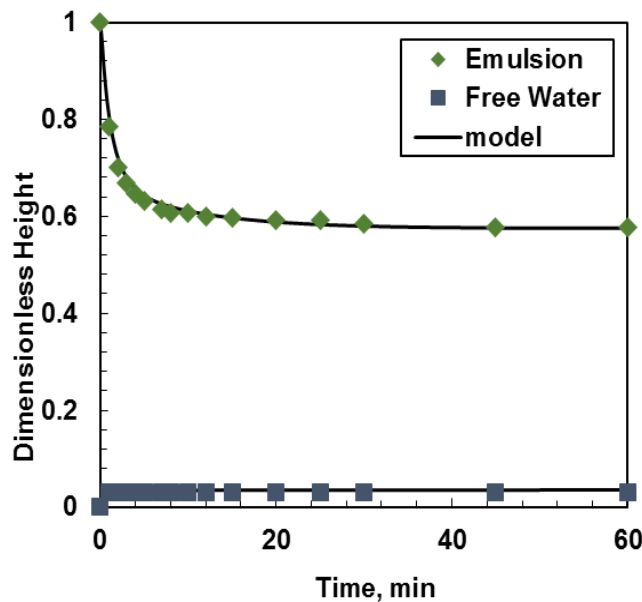


Figure 5.1 Emulsion and the water layer heights over time for a batch experiment performed at 60°C and 1000 rpm with an overhead mixer. The emulsion was prepared with an initial water volume of 0.50. The organic phase consisted of 1.5 g/L OS asphaltenes in toluene.

The dimensionless heights of the emulsion and water layers were modeled according to the methodology presented in Chapter 4, using Eqs. 4.7 and 4.12, respectively. First, the water volume fraction and its derivative were required as inputs to the model. The water volume fraction in the emulsion layer was calculated directly from experimental data at each time step using Eq. 4.8. The data were then fitted with an equation of the form:

$$\Phi_w(t) = \Phi_\infty + c_1(1 - \exp(-c_2t)) + c_3(1 - \exp(-c_4t)) \quad \text{Equation 5.1}$$

where $\Phi_w(t)$ is the fitted water volume fraction at time t , Φ_∞ is the initial experimental volume fraction at time $t = 0$, and c_1 , c_2 , c_3 , and c_4 are constants used to fit the experimental water volume fractions determined using Eq. 4.8 with Eq. 5.1. The derivative of Eq. 5.1 is given by:

$$\frac{d\Phi_w(t)}{dt} = c_1c_2\exp(-c_2t) + c_3c_4\exp(-c_4t) \quad \text{Equation 5.2}$$

The fitted water volume fractions for the data in Figure 5.1 are shown in Figure 5.2. The volume fraction of the dispersed phase increased over time. The initial rapid increase in water volume fraction corresponds to the droplet settling period. The following slow increase corresponds to the compaction period. The water volume fraction is required for modeling, but is not useful in assessing emulsion stability. Water volume fraction plots for all remaining emulsions presented in this chapter can be found in Appendix A.

The coalescence rates and dimensionless limiting heights were then determined by fitting the model to the experimental height data, as shown in Figure 5.1. The limiting height was fit to the measured final height of the emulsion layer and is the asymptote of the model. It provides an indication of emulsion stability because it represents the portion of the emulsion which does not coalesce. The limiting height can be varied from 0 to 1, with a value of 0 indicating that the emulsion fully coalesces and a value of 1 indicating no coalescence. The coalescence rate dictates how fast the emulsion will reach the limiting height. Overall as emulsion stability increases, the limiting height tends to increase and the coalescence rate constant decreases. The same model parameters were used to fit both the emulsion and free water layer data for each emulsion and are presented in Table 5.1. The model fit the data with an average absolute relative deviation (AARD) of 0.02.

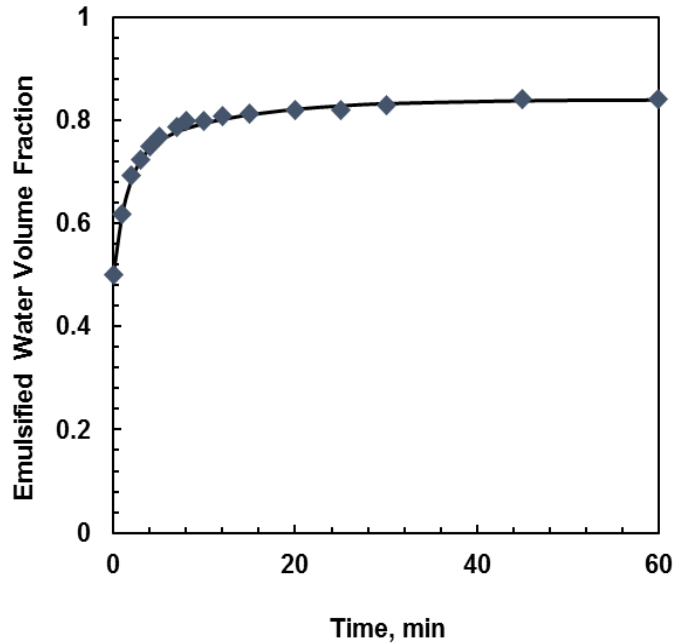


Figure 5.2 Water volume fractions over time for a batch experiment performed at 60°C and 1000 rpm with an overhead mixer. The emulsion was prepared with an initial water volume of 0.50. The organic phase consisted of 1.5 g/L OS asphaltenes in toluene.

Table 5.1 Model parameters used for batch and continuous experiments for water-in-toluene emulsions stabilized by asphaltene extracted from OS bitumen. The measured emulsion layer growth rate, dh/dt , for the continuous experiment is also tabulated.

Parameter	Batch	Continuous
dh/dt , cm/min	-	1.23
ε	-	0.09
h_{lim}/h^o	0.60	0.65
k , min^{-1}	0.02	0.04

Continuous Separation Experiments

Figure 5.3 shows emulsion layer growth and decay during the continuous separation experiment for the OS asphaltene stabilized emulsions without solids. The initial rise in the emulsion layer height is the growth period. When the feed is shut-off, the rag layer no longer grows and the decay period begins. The decay period is equivalent to a batch experiment.

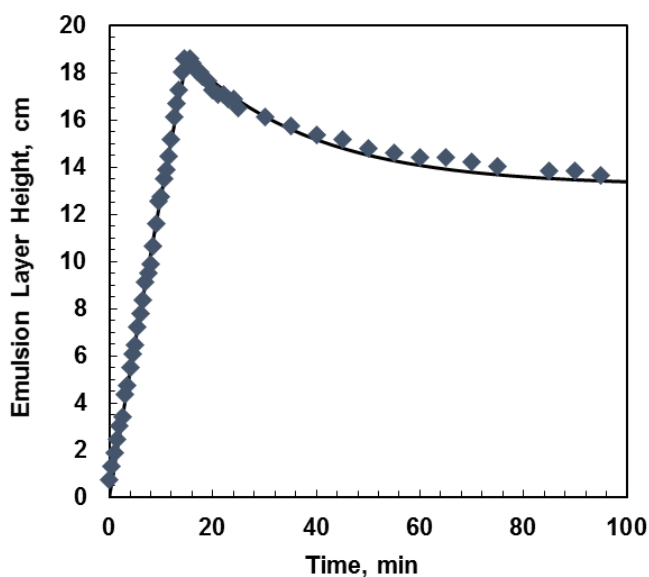


Figure 5.3 Continuous experiment emulsion layer heights over time for a W/O emulsion stabilized by OS asphaltenes at 60°C. The emulsion was prepared with an initial water volume fraction of 0.50 and an organic phase of 1.5 g/L asphaltenes in toluene.

The required inputs to the model are the water volume fraction in the feed and in the emulsion layer. The water volume fraction in the feed was set to the initial water volume fraction in the prepared emulsion beaker, 0.5 in all cases. Note, the water volume fraction in the prepared emulsion beaker may vary with time if unequal volumes of free water and oil are returned to the emulsion beaker from the separator. In these experiments, only water was held up in the emulsion layer. The maximum water volume fraction that could occur in the beaker in these experiments was calculated from a material balance performed on the beaker assuming no water return over the entire run. This maximum water volume fraction was 0.54. The change in water volume fraction is relatively small because the volume in the separator is relatively small compared to the total volume of the emulsion beaker. The actual variation is much smaller for most of each experimental run until the rag layer height fills a significant fraction of the separator. This variation was minimized by maintaining the emulsion layer in the centre of the separator by adjusting the exit water flowrate. Hence, the error introduced by assuming a constant water volume fraction in the beaker is small.

The water volume fraction in the emulsion layer was measured for two solids free emulsions: one stabilized by OS asphaltenes and the other with CSS asphaltenes. Both were prepared at 60°C and 1000 rpm with an overhead mixer with an initial water volume fraction of 0.50 and an organic phase consisting of 1.5 g/L C7-asphaltenes in toluene. The emulsion layer water volume fraction was found to be the same in both test cases although it varied randomly over time with an average value of 0.68 ± 0.11 based on a 95% confidence interval. Therefore, the water volume fraction in the emulsion layer was assumed to be 0.68 for all runs. Note that this value is approximately equal to the close random packing volume fraction for monodispersed spheres.

The model was then fit to the data using Eqs. 4.16 and 4.13 for respective emulsion layer growth and decay using the coalescence rate constant, dimensionless limiting emulsion layer height, and fractional bypass as fitting parameters. The limiting height and coalescence rate constant match the final height of the emulsion layer as the amount of emulsion that will not destabilize and slope of the decay curve, respectively, as in the batch experiment. The fractional bypass is specific to the apparatus but, is required to match the rag layer growth rate. The rag layer growth rate is defined as the emulsion layer growth in the continuous experiment divided by time and is the slope of the emulsion layer growth curve. A lower fractional bypass indicates a faster growth rate. The rag layer growth rate is not a model input, but is convenient for comparing the behaviour of different emulsions and is therefore included in Table 5.1. Overall, a more stable emulsion will have a higher limiting height, lower coalescence rate, and lower fractional bypass (faster growth rate).

The fitted model parameters are presented in Table 5.1. The model fit the data with an AARD of 0.03. Note that the decay parameters are not the same as the batch experiment parameters. The difference between batch and continuous coalescence rates may be due to the shear force applied by the pump during the continuous experiment. In addition, the continuous emulsion layer accumulated over time while the batch emulsion layer was formed immediately. Hence, the structure of the layers in each type of experiment may differ.

5.1.2 Effect of Experimental Variables on Emulsion Stability

5.1.2.1 Effect of Asphaltene Source on Emulsion Stability

Emulsions stabilized by asphaltenes extracted from three different source bitumen: OS, CSS and SAGD, were prepared at 60°C with a mixing speed of 1000 rpm using the overhead mixer and a asphaltene concentration of 1.5 g/L in toluene solvent. Figure 5.4 compares the height of the emulsion layers from batch and continuous experiments for OS, CSS, and SAGD asphaltene stabilized emulsions in the absence of solids. The fitted model parameter values are provided in Table 5.2.

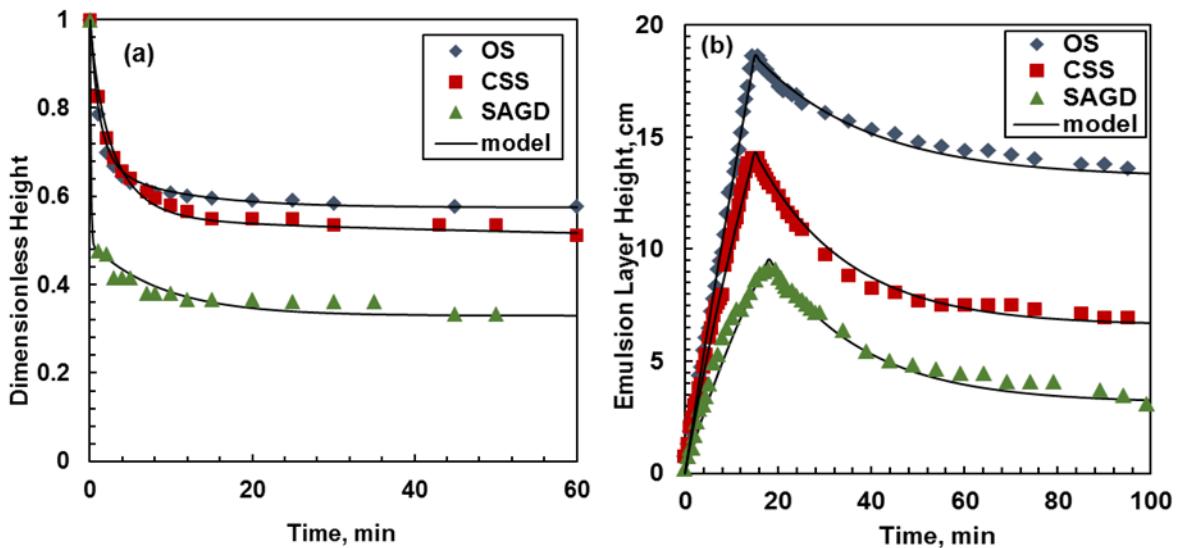


Figure 5.4 Emulsion layer heights for batch tests (a) and continuous tests (b) over time for W/O emulsions stabilized by OS, CSS, and SAGD asphaltenes at 60°C. Model emulsions were prepared with 50 vol% aqueous phase and 50 vol% organic phase. The organic phase was 1.5 g/L of asphaltenes in toluene.

Table 5.2 Model parameters used for batch and continuous experiments for water-in-toluene emulsions stabilized by asphaltene extracted from OS, CSS, and SAGD bitumen.

Parameter	Batch			Continuous		
	OS	CSS	SAGD	OS	CSS	SAGD
dh/dt , cm/min	-	-	-	1.23	0.94	0.51
ε	-	-	-	0.09	0.23	0.54
h_{lim}/h^o	0.60	0.54	0.33	0.65	0.38	0.27
k , min ⁻¹	0.02	0.04	0.11	0.04	0.05	0.06

The emulsion stabilized by asphaltenes extracted from the OS bitumen was the most stable and SAGD the least stable in both batch and continuous experiments. The CSS asphaltene stabilized emulsions had an intermediate stability. These results were consistent with those from Rocha *et al.* (2016) who found that the differences in emulsion stability correlated to the mass surface coverage and apparent molecular weight at the interface. The higher emulsion stability of the OS and CSS asphaltenes was attributed to the presence of a larger number of self-associating aggregates with high molecular weight that adsorb on the water-oil interface and form a thicker film. The SAGD asphaltenes may be deficient in more polar material or large nanoaggregates, possibly as a result of extended exposure to high steam temperatures or adsorption of these components on the reservoir rock.

Asphaltene Blends

Emulsions with a range of stabilities can be obtained by blending asphaltenes from different sources. By combining asphaltenes from the most stable OS bitumen and the least stable SAGD bitumen at different ratios (with the total asphaltene concentration held constant at 1.5 g/L), the emulsion stability can be controlled in batch and continuous experiments as shown in Figure 5.5. Fitted model parameters for the emulsions stabilized by asphaltene blends are provided in Table 5.3. Emulsions containing any amount of SAGD asphaltenes were significantly less stable (lower limiting height parameters and higher coalescence rate constants) than the emulsion stabilized only by OS asphaltenes in both batch and continuous experiments. Even small amounts of SAGD asphaltenes added to the system tended to destabilize the emulsion. This observation suggests that there may be competitive adsorption at the interface with SAGD asphaltenes, which are less effective emulsion stabilizers, arriving first to the interface or preferentially adsorbing. The range of emulsion stabilizing capabilities provides a wider range of conditions over which to compare the batch and continuous experiments.

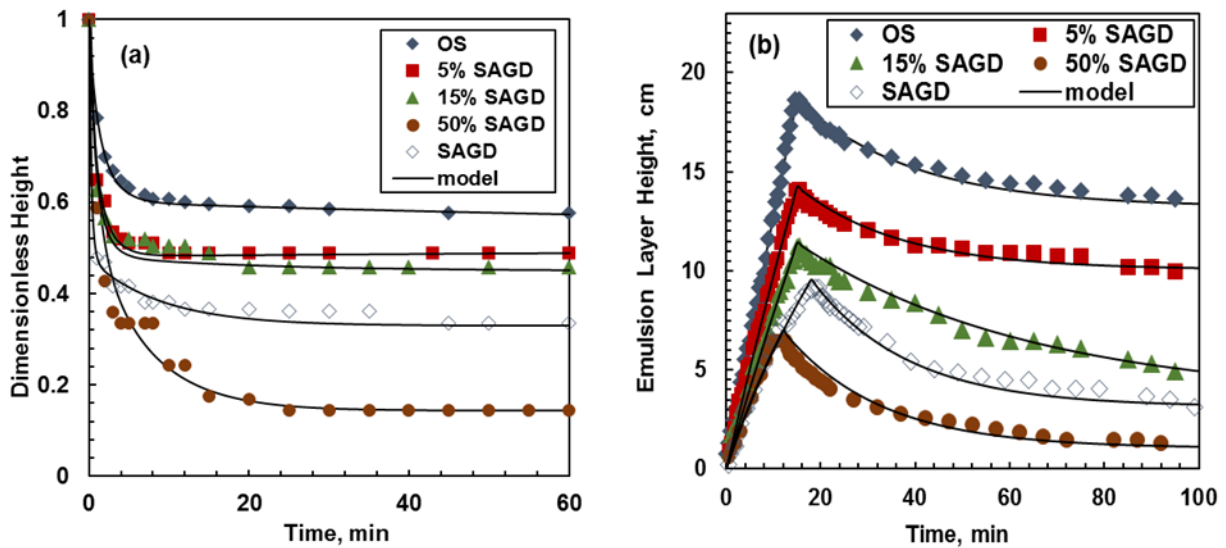


Figure 5.5 Emulsion layer heights for (a) batch experiments and (b) continuous experiments over time for W/O emulsions stabilized by OS/SAGD asphaltene blends at 60°C. Model emulsions were prepared with 50 vol% aqueous phase and 50 vol% organic phase. The organic phase was 1.5 g/L of C7-asphaltenes in toluene.

Table 5.3 Model parameters used for batch and continuous experiments for water-in-toluene emulsions stabilized by OS/SAGD asphaltene blends.

Parameter	Batch			Continuous		
	95/5	85/15	50/50	95/5	85/15	50/50
dh/dt , cm/min	-	-	-	0.90	0.69	0.56
ε	-	-	-	0.25	0.28	0.46
h_{lim}/h^o	0.48	0.42	0.15	0.42	0.30	0.12
k , min ⁻¹	0.04	0.05	0.06	0.03	0.03	0.05

5.1.2.2 Effect of Asphaltene Concentration

Gafonova and Yarranton (2001) found that emulsion stability increased as the asphaltene concentration increased significantly up to approximately 5 g/L in 50/50 heptol and then decreased slightly at higher asphaltene concentrations. At low asphaltene concentrations, there were insufficient asphaltenes to stabilize the emulsions. Relatively large droplets were formed which coalesced more readily than the smaller droplets formed at higher asphaltene concentrations.

To evaluate the effect of asphaltene concentration, batch and continuous experiments were performed for emulsions stabilized by OS asphaltenes prepared with asphaltene concentrations of 0.5 g/L to 10 g/L in toluene. To minimize the mass of asphaltenes used, the batch emulsions at different asphaltene concentrations were prepared with a total volume of only 50 cm³. The emulsions were mixed at 10,800 rpm with a CAT 520D homogenizer at 21°C. These screening experiments were run at room temperature instead of 60°C for convenience; a few experiments were repeated at 60°C and similar results were obtained. Continuous emulsions were prepared in the usual fashion as described in Section 3.2.4.

Figure 5.6a shows the effect of asphaltene concentration on the batch emulsions stabilized by OS asphaltenes. The fitted model parameters are given in Table 5.4. The stability of the batch emulsions increased as the concentration increased to 5 g/L and there was little change in stability from 5 to 10 g/L. These results are consistent with the results from Gafonova and Yarranton (2001). Similar results were obtained for CSS and SAGD asphaltenes (see Appendix B). The emulsions with OS asphaltene concentrations of 0.5, 1.5, and 2.5 g/L were run in the continuous separator to evaluate the rag layer growth rates. Figure 5.6b shows that, in agreement with the batch results, the less stable emulsion at 0.5 g/L grew more slowly, but there was little difference between the growth rate at 1.5 and 2.5 g/L.

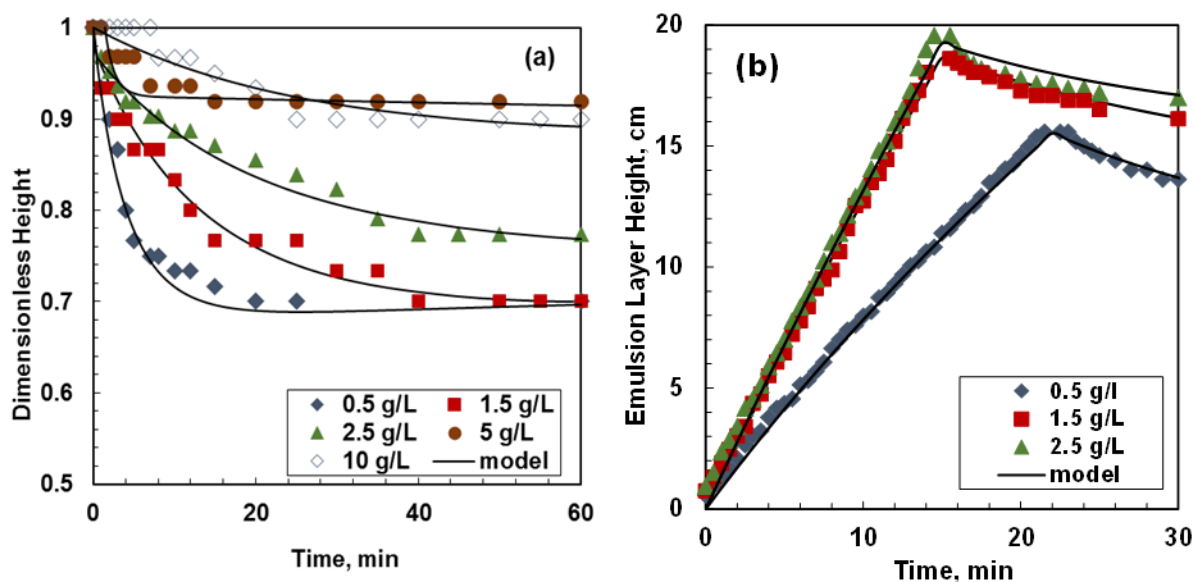


Figure 5.6 Emulsion layer height over time for W/O emulsions stabilized by OS asphaltenes: a) batch experiments at 21°C; b) continuous separations at 60°C. Model emulsions were prepared with 50 vol% aqueous phase and 50 vol% organic phase. The organic phases consisted of 0.5, 1.5, 2.5, 5 and 10 g/L of asphaltenes in toluene.

Table 5.4 Model parameters used for batch and continuous experiments for water-in-toluene emulsions stabilized by OS asphaltene at concentrations between 0.5 and 10 g/L.

Parameter	Batch					Continuous		
	0.5	1.5	2.5	5	10	0.5	1.5	2.5
Asphaltene Concentration (g/L)	0.5	1.5	2.5	5	10	0.5	1.5	2.5
dh/dt , cm/min	-	-	-	-	-	0.70	1.23	1.27
ε	-	-	-	-	-	0.42	0.03	0.01
h_{lim}/h^o	0.70	0.76	0.78	0.86	0.90	0.55	0.65	0.75
k , min^{-1}	0.01	0.008	0.004	0.003	0.002	0.04	0.04	0.06

5.1.2.3 Effect of Solvent Type

The degree of surface activity of asphaltenes varies according to their solubility (Kiran, 2011). Asphaltene-stabilized emulsions tend to be more stable when the solubility of the asphaltenes in the continuous phase decreases, as long as there is no precipitation (Spiecker and Kilpatrick, 2004). As the heptane fraction in the heptol solvent increases, the asphaltenes are less soluble and the interactions between asphaltenes become stronger. The increase in adhesion strength and greater

asphaltene stacking in poor solvents (Shi *et al.*, 2017) leads to the formation of aggregates of asphaltene monomers. These asphaltene aggregates have a higher affinity for the oil-water interface and are attributed to a more strongly adsorbed, crosslinked asphaltene film at the interface (Sztukowski and Yarranton, 2004). Therefore, emulsions prepared from mixtures of heptane and toluene are expected to be more stable than emulsions prepared from toluene alone.

Emulsions were prepared in toluene (good solvent) and 50/50 heptol (poor solvent) to investigate the effect of the asphaltene solubility in the continuous phase on emulsion stability and emulsion layer growth. The results in toluene were presented previously in Figure 5.4 and Table 5.2. Figure 5.7 shows the batch and continuous emulsion layer heights for the water-in-50/50 heptol emulsions stabilized by OS, CSS, and SAGD asphaltenes. The fitted model parameters for the water-in-50/50 heptol emulsions are provided in Table 5.5. As observed in toluene, the emulsions stabilized by asphaltenes extracted from the OS bitumen and SAGD bitumen were the most and least stable, respectively. A comparison of Figures 5.7a and 5.4a shows that all of the batch water-in-50/50 heptol emulsions were more stable than the water-in-toluene emulsions. The limiting height batch model parameter is higher in 50/50 heptol than in toluene and the coalescence rate constant is lower. The change in emulsion stability was greatest for the SAGD asphaltene stabilized emulsions. If OS and CSS asphaltenes are already capable of forming strongly crosslinked films in toluene, then the increased rigidity of the interfacial film due to solvent effects may be less significant than for an unstable film like that formed with SAGD asphaltenes.

Figure 7.b shows that, consistent with the batch experiments, the continuous OS emulsions prepared in 50/50 heptol are the most stable and the SAGD emulsions are the least stable. The water-in-toluene (Figure 5.4b) emulsions were again consistently more stable than the water-in-50/50 heptol (Figure 5.7b) emulsions. Overall, as expected, the emulsions in 50/50 heptol were somewhat more stable than in toluene with similar albeit scattered coalescence rates and consistently higher dimensionless limiting heights. The emulsion layer growth rate also increased (fractional bypass decreased) with increasing heptane content in the organic solvent.

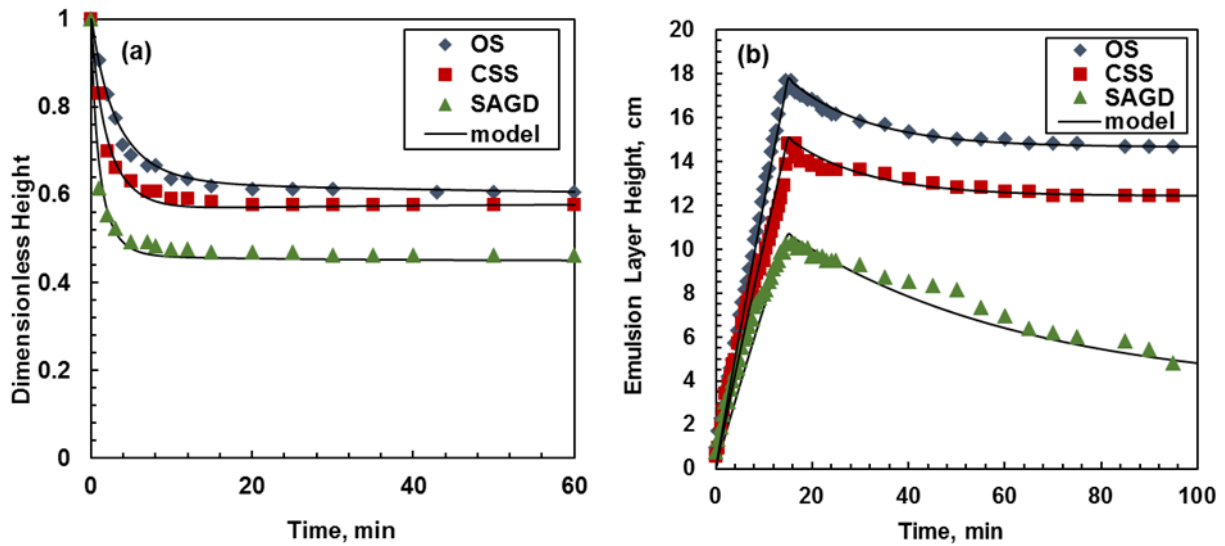


Figure 5.7 Emulsion layer height over time for W/O emulsions stabilized by OS, CSS and SAGD asphaltenes: a) batch experiments; b) continuous separations at 60°C. Model emulsions were prepared with 50 vol% aqueous phase and 50 vol% organic phase. The organic phases consisted of 1.5 g/L of asphaltenes in 50/50 heptol.

Table 5.5 Model parameters used for batch and continuous experiments for water-in-50/50 heptol emulsions stabilized by asphaltene extracted from OS, CSS and SAGD bitumen.

Parameter	Batch			Continuous		
	OS	CSS	SAGD	OS	CSS	SAGD
dh/dt , cm/min	-	-	-	1.15	0.84	0.67
ε	-	-	-	0.15	0.28	0.48
h_{lim}/h^o	0.61	0.58	0.45	0.76	0.76	0.30
k , min ⁻¹	0.01	0.03	0.05	0.06	0.06	0.02

5.1.2.4 Effect of Drop Size Distribution/Mixing Conditions

Emulsions with smaller drop sizes are expected to be more stable than emulsions with large droplets because the probabilities of collision and coalescence are greater with larger contact areas between the droplets (Gafonova and Yarranton, 2001). The drop size distribution is partly determined by the mixing speed. Two cases were examined in this study: 1000 rpm with an overhead mixer and 10,000 rpm with a homogenizer. Figure 5.8 shows that the drop-size distributions were narrower when using the homogenizer. The average droplet diameters were $20.0 \pm 2.5 \mu\text{m}$ and $8.0 \pm 0.3 \mu\text{m}$ for 1000 and 10,000 rpm, respectively.

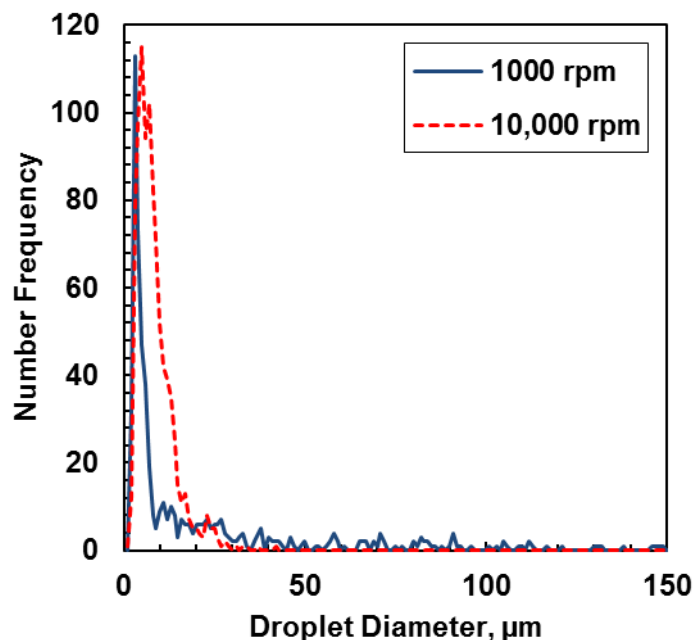


Figure 5.8 Droplet size distribution of OS asphaltene stabilized water-in-toluene emulsions prepared with an overhead mixer at 1000 rpm or a homogenizer at 10,000 rpm at 60°C.

Water-in-toluene emulsions stabilized by OS, CSS, and SAGD asphaltenes were prepared at 10,000 rpm in batch (Figure 5.9a) and continuous (Figure 5.9b) experiments and model parameters are provided in Table 5.6. Note, continuous tests at 10,000 rpm were not performed with the CSS and SAGD asphaltenes due to sample limitations. As expected, the batch emulsions with the smaller droplets (10,000 rpm) were more stable with lower coalescence rates and higher dimensionless limiting heights than at 1000 rpm. The effect of the drop size distribution was less pronounced in the continuous experiments where the growth rate increased as expected, but the dimensionless limiting height decreased slightly. It is likely that some coalescence occurred in the pump before reaching the separator. Hence, the emulsion in the continuous separator may have similar average drop sizes regardless of the drop size distribution in the original emulsion beaker.

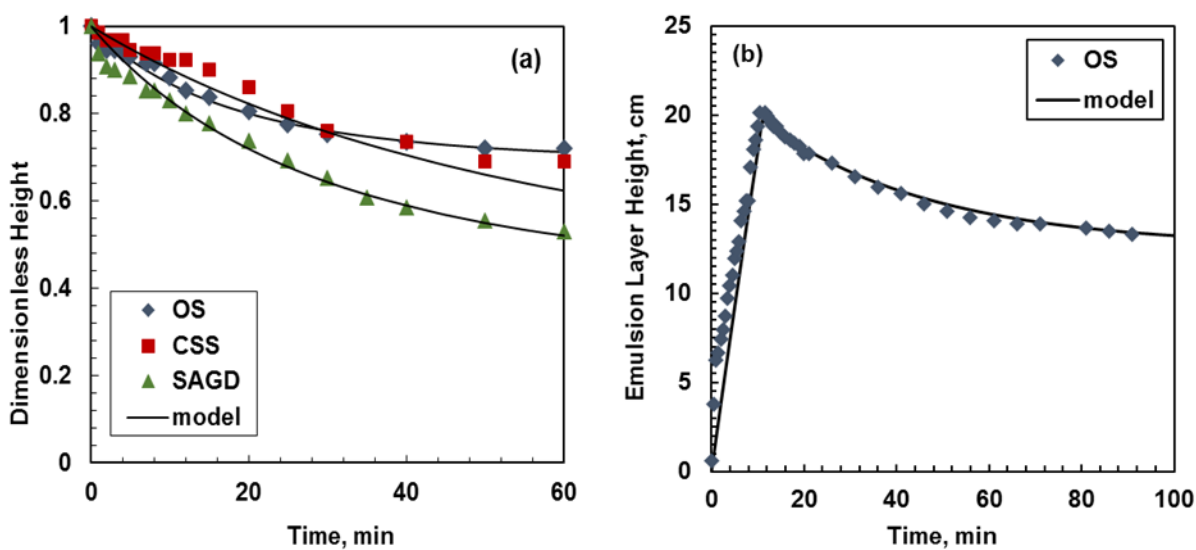


Figure 5.9 Emulsion layer height over time for a) batch experiments W/O emulsions stabilized by OS, CSS and SAGD asphaltenes; b) continuous separations W/O emulsions stabilized by OS asphaltenes prepared at a mixing speed of 10,000 rpm with a homogenizer. Model emulsions were prepared at 60°C with 50 vol% aqueous phase and 50 vol% organic phase. The organic phases consisted of 1.5 g/L of C7-asphaltenes in toluene.

Table 5.6 Model parameters used for batch and continuous experiments for water-in-toluene emulsions stabilized 1.5 g/L OS, CSS, and SAGD asphaltenes at a mixing speed of 10,000 rpm.

Parameter	Batch			Continuous
	OS	CSS	SAGD	OS
dh/dt , cm/min	-	-	-	1.59
ε	-	-	-	0.08
h_{lim}/h^o	0.80	0.60	0.50	0.61
k , min ⁻¹	0.001	0.01	0.01	0.03

5.1.2.5 Effect of Water Volume Fraction

The initial water volume fraction can affect both emulsion stability and the type of emulsion formed. The initial water volume fraction in the batch emulsions was varied from 0.25 to 0.85 for water-in-toluene emulsions stabilized by 0.5 and 1.5 g/L of OS asphaltenes. For emulsions stabilized by 0.5 g/L asphaltenes, oil-in-water emulsions were formed for water volume fractions above 0.60, as determined by a dilution test. In this test, the addition of water created a more dilute

emulsion and a separate layer was formed with the addition of toluene, indicating that the continuous phase was water. Emulsions prepared with initial water volume fractions below the inversion point of 0.60 were water-in-oil emulsions. For emulsions stabilized by 1.5 g/L of asphaltenes, the inversion point increased to 0.75. Only the emulsion formed at a water fraction of 0.85 was an oil-in-water type. All other emulsions at the higher asphaltene concentration, with initial water fractions below 0.75, were water-in-oil emulsions.

At 0.5 g/L asphaltenes in toluene, Figure 5.10a shows a minimum in stability at the inversion point of 60 vol% water. Emulsion stability decreased with increasing water phase fraction until the inversion point was reached and then increased with increasing water phase content above the inversion point. In both cases, emulsion stability decreased with increasing dispersed phase (or decreasing continuous phase) volume fraction. The decrease in stability with increasing dispersed phase volume may result from the formation of larger droplets when the supply of stabilizing asphaltenes are limited in the continuous phase. As the dispersed phase volume increases, larger droplets are in closer contact, which increases the chance of collision and coalescence. Phase inversion likely occurs when there are insufficient asphaltenes to stabilize the large dispersed phase surface area.

The opposite affect was observed for emulsions stabilized by 1.5 g/L asphaltenes, where in Figure 5.10b shows an increase in emulsion stability with increasing dispersed phase content until an inversion point is reached at a water volume fraction of 0.75. Emulsion stability drastically decreased above this point and phase inversion occurs. It appears that at 1.5 g/L of asphaltenes, there is an excess of stabilizing material so that the drop size and emulsion stability do not change at difference water volume fractions. In this case, the drop size is dictated by the mixing conditions rather than the amount of asphaltenes. The dimensionless limiting emulsion layer height increases with increasing water volume fraction simply because there is a higher proportion of dispersed water in the beaker.

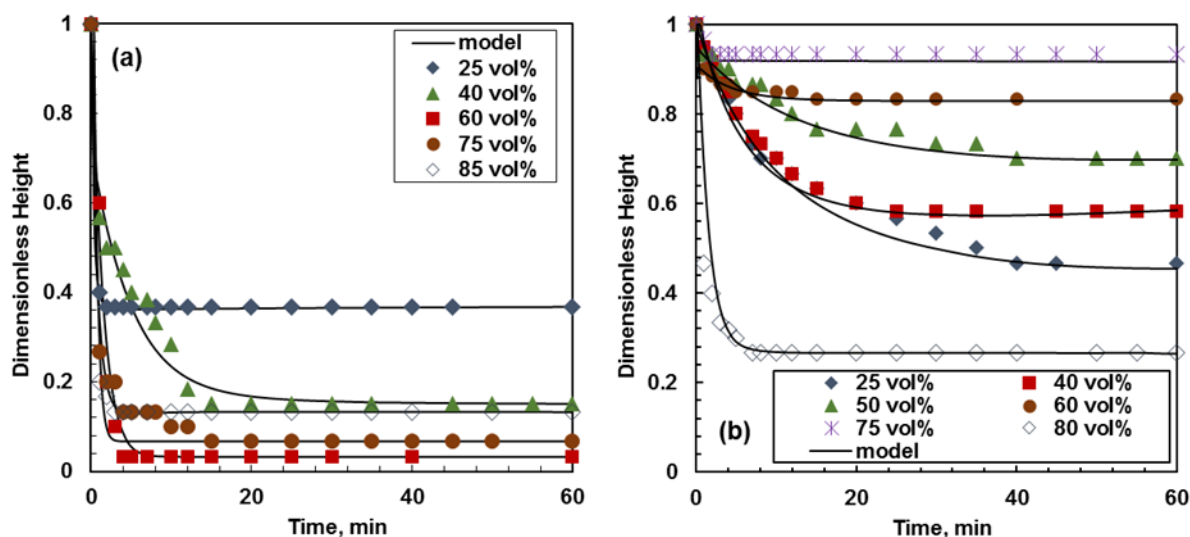


Figure 5.10 Batch emulsion layer height over time for W/O emulsions prepared with initial water volume fraction varying from 0.25 to 0.85 at 60°C for emulsions with organic phases consisting of a) 0.5 g/L of OS asphaltenes in toluene; b) 1.5 g/L of OS asphaltenes in toluene.

Table 5.7 Model parameters used for batch water-in-toluene emulsions stabilized by 0.5 g/L OS asphaltenes and prepared with initial water volume fractions ranging from 0.25 to 0.85.

Parameter	Water Volume Fraction				
	0.25	0.40	0.60	0.75	0.85
h_{lim}/h^o	0.37	0.15	0.03	0.07	0.13
k, min^{-1}	0.02	0.23	0.70	1.0	0.90

Table 5.8 Model parameters used for batch water-in-toluene emulsions stabilized by 1.5 g/L OS asphaltenes and prepared with initial water volume fractions ranging from 0.25 to 0.80.

Parameter	Water Volume Fraction					
	0.25	0.40	0.50	0.60	0.75	0.80
h_{lim}/h^o	0.56	0.74	0.80	0.83	0.95	0.27
k, min^{-1}	0.01	0.005	0.001	0.001	0.001	0.90

5.1.3 Prediction of Continuous Behaviour from Batch Model Parameters

The relative stability of the emulsions is clear in the model parameters. Figure 5.11 shows that as the emulsion stability decreases (OS to CSS to SAGD), the coalescence rate increases and the dimensionless limiting height decreases for both batch and continuous emulsions. Figure 5.12 confirms that the emulsion layer growth rate depends strongly on the fractional bypass which increases as the emulsion stability decreases. While the parameters from each type of experiment differ, they follow the same trends indicating that batch experiments can be used to qualitatively predict trends in continuous separations for asphaltene stabilized emulsions.

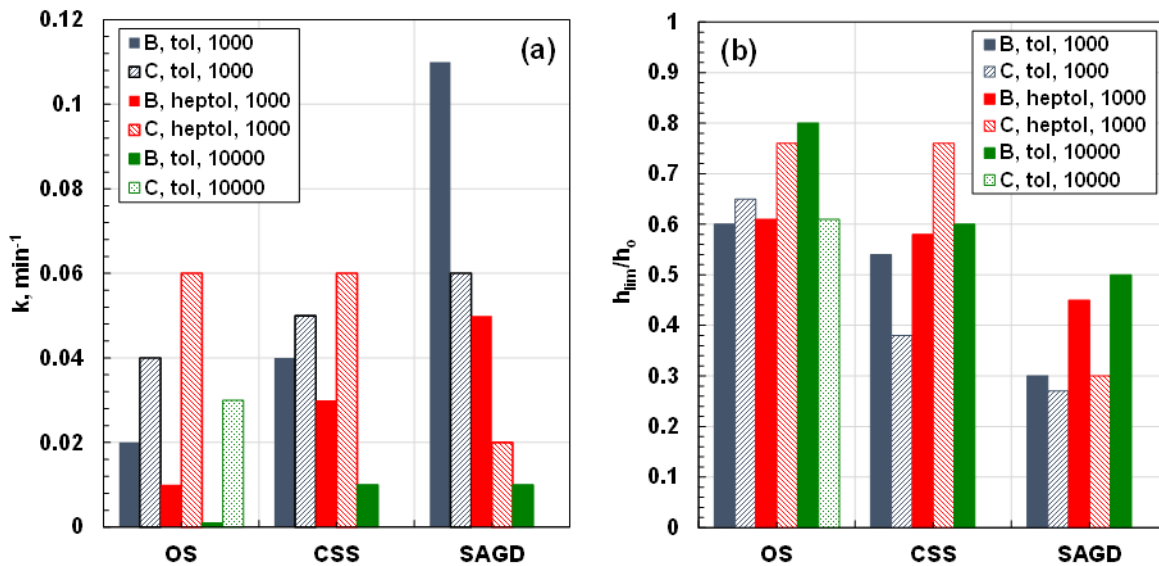


Figure 5.11 Fitted coalescence rate (a) and dimensionless limiting height (b) for batch and continuous tests on W/O emulsions stabilized by OS, CSS, and SAGD asphaltenes. In legend: B=batch, C=continuous; the number indicates the mixing rpm. Note, continuous tests at 10,000 rpm were not performed with the CSS and SAGD asphaltenes due to sample limitations.

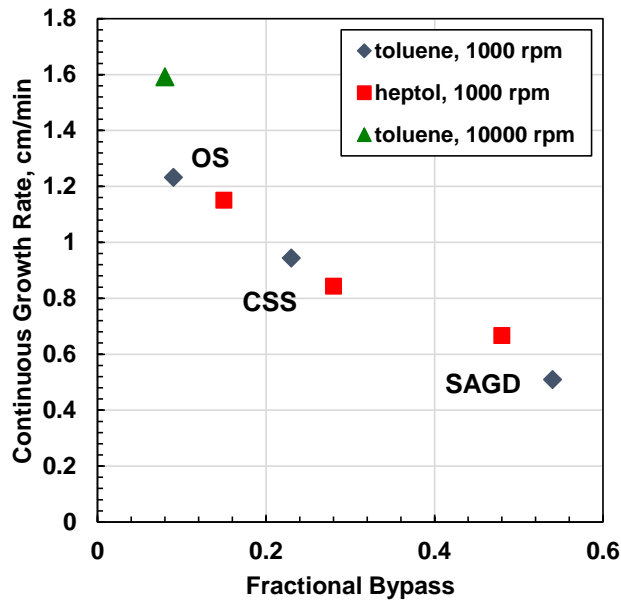


Figure 5.12 Measured emulsion layer growth rate versus fractional bypass for batch and continuous tests on W/O emulsions stabilized by OS, CSS, and SAGD asphaltenes at 60°C.

Figure 5.13 shows that the coalescence rate and dimensionless limiting height from the batch tests correlate well with each other. In other words, more stable emulsion have both lower coalescence rates and higher dimensionless limiting heights. This correspondence also means that only one parameter is required in the attempt to predict continuous emulsion stability. The dimensionless limiting height is the easier value to measure and was selected as the correlating parameter.

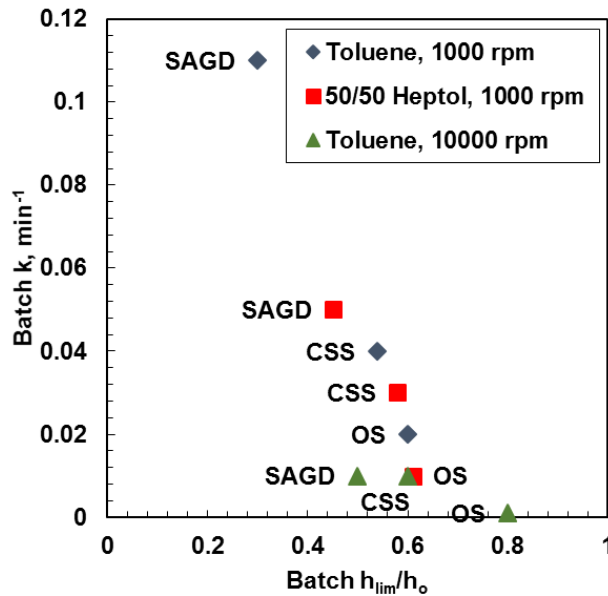


Figure 5.13 Batch model parameters coalescence rate constant and dimensionless limiting height for W/O emulsions stabilized by OS, CSS, and SAGD asphaltenes.

Figure 5.14 shows the correlation of the continuous model parameters with the batch dimensionless limiting height. There is a strong correlation between the fractional bypass and emulsion layer growth rate with the dimensionless limiting height. There is a scattered but consistent correlation between the dimensionless limiting heights from the batch and continuous tests. The correlation for the coalescence rate is poor. As noted previously, the emulsion is altered in its passage through the pump. Fortunately, the coalescence rate is the least important parameter for modeling the growth and decay of the emulsion layer in the continuous separation.

Overall, the dimensionless limiting heights from the batch tests provide a sound qualitative indicator of the emulsion stability in a continuous separation. In general, a high dimensionless limiting height in the batch model predicts a high limiting height and a low fractional bypass parameter in the continuous model. In other words, a stable emulsion in the batch experiment is expected to be stable in continuous separations with fast growth rates at the same conditions. This conclusion supports the use of bottle tests for emulsion assessment in the field, at least when no solids are present in the emulsion. Bottle tests measure the amount of free water resolved after a limited treatment of an emulsion sample (*e.g.*, shaking for a few minutes). The fraction of free

water resolved is equivalent to one minus the dimensionless limiting height. Note, the model cannot be used to predict the time at which complete separation of the emulsion layer into free bulk phases will occur, because the kinematic model will always predict an emulsion layer height equal to the limiting height at infinite time.

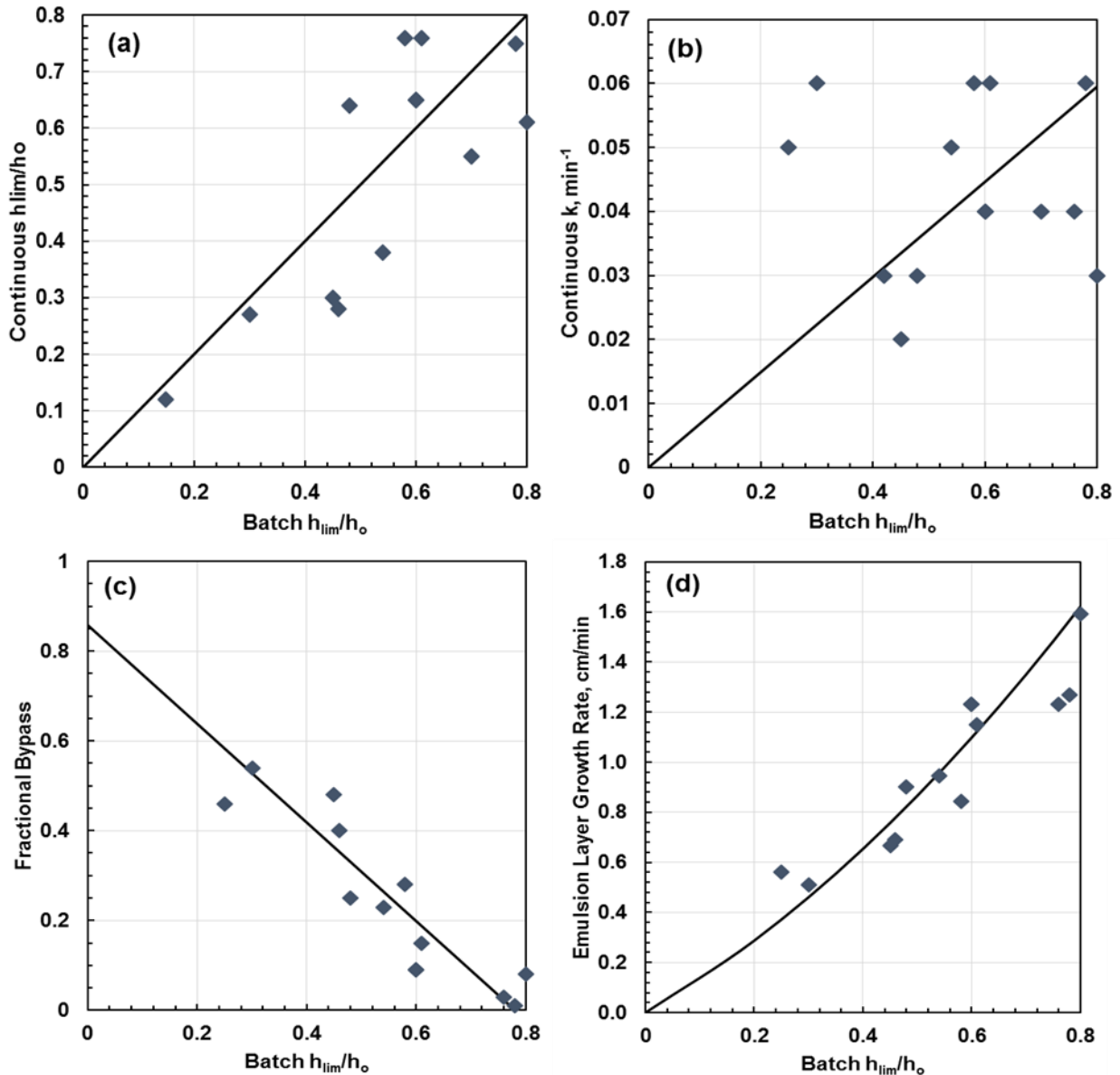


Figure 5.14 Correlation between continuous emulsion model parameters and batch test dimensionless limiting heights for W/O emulsions stabilized by OS, CSS, and SAGD asphaltenes in toluene, 50/50 heptol, at mixing speeds of 1000 and 10,000 rpm at 60°C. The lines are empirical fits to the data.

5.1.4 Selection of Base Case Emulsion for Solids Addition

The main criterion for the base case emulsion is that the emulsions break neither too quickly to observe any emulsion layer growth nor so slowly that the separator filled too rapidly. The target was a 20 minute timeframe before the rag layer filled the separator. The concentration of 1.5 g/L was the minimum concentration that filled the separator within 20 minutes and was selected as the base case for all the experiments with solids performed in this study.

As already noted, the stability of the asphaltene stabilized emulsions was not very sensitive to the type of asphaltenes, the solvent, or the mixing conditions. The OS asphaltenes were selected for the base case simply because more sample was available. Toluene was selected to ensure complete solubilization of the asphaltenes. An initial water fraction of 0.50 was selected to ensure the water-in-oil emulsion layer was comprised only of a dense packed where creaming and/or settling of the emulsified droplets is negligible. The base case mixing condition was originally set as 1000 rpm with the overhead mixer. However, mixing at 10,000 rpm was found to be necessary for the continuous tests with solids and therefore both mixing conditions were considered.

5.2 Solids-Stabilized Emulsions

All solids stabilized emulsions were prepared at the asphaltene stabilized base case conditions of 1.5 g/L OS asphaltenes dissolved in toluene at 60°C. Prior to use in emulsion experiments, the solids were treated, as described in Section 3.1.2, to alter their surface wettability by controlled adsorption of OS asphaltenes. The solids properties of surface wettability and particle size distribution were measured after treatment. In all cases, the treated solids were dispersed in the oil phase prior to mixing. Solids stabilized emulsions were mixed at 10,000 rpm with a homogenizer in order to produce emulsions with measurable stability in the continuous experiments.

The effect of the solids on the batch and continuous emulsion tests is illustrated with 80° contact angle kaolin. The effect of solid type (kaolin and silica), size (12, 18, and 32 μm) and contact angle (75 to 125°) are evaluated with batch tests. Finally, the ability to predict continuous emulsion separation from batch experiments is assessed.

5.2.1 Solids Properties

Properties of the treated solids, including surface wettability and particle diameters were measured prior to use in batch and continuous emulsion separation experiments.

Surface Wettability

The solids used in this study were treated with OS asphaltenes at concentrations from 0 to 1 g/L to obtain a series of wettabilities. Figure 5.15 shows the contact angles on the kaolin and silica solids determined from the compressed disc method and the surface tension measurements from the film floatation method of determining wettability. Kaolin and silica changes from hydrophilic to more hydrophobic as a result of adsorption of asphaltenes. The solids were initially hydrophilic (water wet with contact angles less than 90°). As more asphaltenes adsorbed onto the solids surface, the solids became more hydrophobic or oil wet (contact angle greater than 90°) before reaching a plateau at 135° and 145° for kaolin and silica, respectively, at asphaltene concentrations of 0.5 g/L. The steep increase in contact angle with asphaltene concentration to a plateau suggests that the contact angle is more sensitive at a lower surface coverage of asphaltenes (Wang *et al.*, 2013).

It is not obvious that the wettability of the compressed disc is the same as the wettability of the particles. Therefore, the compressed disc data were compared with the critical surface tensions from the film floatation method. The surface tension of the liquid where 50% of the solids sink is taken as an indicator of wettability and follows the same trend as the compressed disc data. The good correspondence validates the compressed disc wettability measurements.

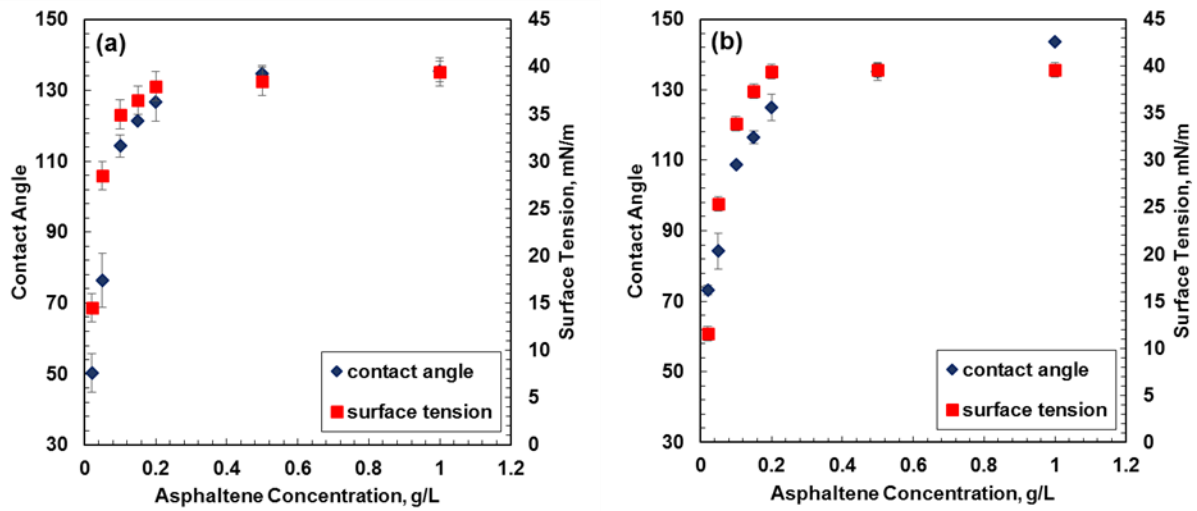


Figure 5.15 Measured contact angles for (a) kaolin and (b) silica solids after treatment with OS asphaltenes in a 50/50 heptol solution.

Particle Size Distribution

The particle size distributions of the treated kaolin and the larger silica particles are shown in Figure 5.16. The average particle diameters were 12 μm and 54 μm respectively for kaolin and silica. The measured kaolin particle diameter is well above the manufacturers specifications of $<0.20 \mu\text{m}$. This discrepancy may be due to the particles clumping together and forming aggregates an order of magnitude greater than the individual particle size. The aggregates could not be broken up by sonication and were therefore assumed to act as individual larger particles.

An average particle diameter of 54 μm for the larger silica particles falls within the range specified by the manufacturer of 32-63 μm . Insufficient quantities of the smaller silica particles were available to measure the particle size distribution in the lab, therefore the particles are assumed to be in the manufacturer specified 18-32 μm particle size range. At these size distributions, all solids considered in this thesis are considered coarse solids with average diameters greater than 1 μm .

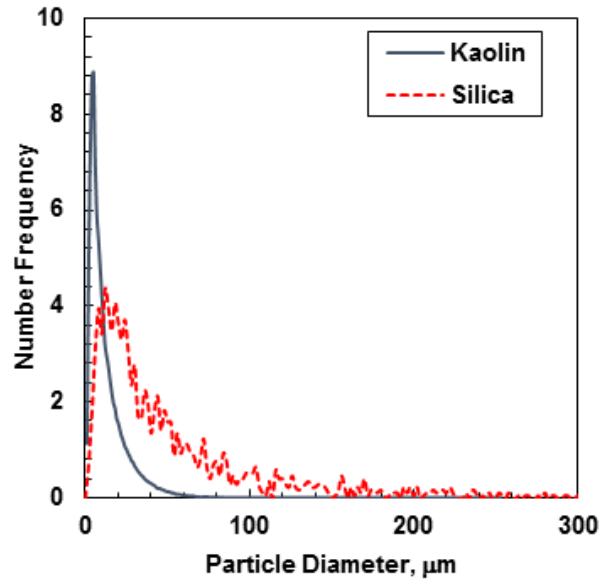


Figure 5.16 Particle size distribution of treated kaolin and silica measured in 50/50 heptol solution.

5.2.2 Effect of Solids Addition in the Batch Experiment

Figure 5.17 shows the effect of adding kaolin (12 μm , 80° contact angle) to the base case batch experiment. The fitted model parameters are provided in Table 5.9. Note that a total volume of only 50 mL was used at kaolin concentrations above 5 g/L in order to minimize the amount of kaolin consumed in each experiment. The emulsions were otherwise prepared as previously described. The presence of solids had a significant impact on the emulsion stability. At solids concentrations below 5 g/L (Figure 5.17a), emulsion stability decreased with increasing solids concentration until a threshold was reached. At solids concentrations above 5 g/L (Figure 5.17b), the trend reversed and emulsion stability began to increase with increasing solids concentration. At kaolin concentrations of 20 g/L, the produced emulsions are more stable than those without solids. Batch model parameters: limiting height and coalescence rate constant are plotted against the concentration of kaolin added to the base emulsion in Figure 5.18. Figure 5.18a confirms that a minimum in the dimensionless limiting heights occurred between 1 and 5 g/L of kaolin. Figure 5.18b shows that a maximum in the coalescence rate also occurred at 5 g/L.

The above trends are consistent with the observations and interpretation from Sztukowski *et al.* (2005) on the impact of coarse solids on emulsion stability. At low solids concentrations (less than 1 g/L), the interface is dominated by asphaltenes and the few solids available to adsorb at the interface as a single layer act as bridges between the droplets, promoting coalescence and resulting in unstable emulsions. At high solids concentrations (greater than 5 g/L), the solids pack in the continuous phase and accumulate around the droplets forming a steric barrier that prevents contact and coalescence between droplets. Stable emulsions form when solids concentrations are sufficient to form a multilayer around all droplets to prevent bridging.

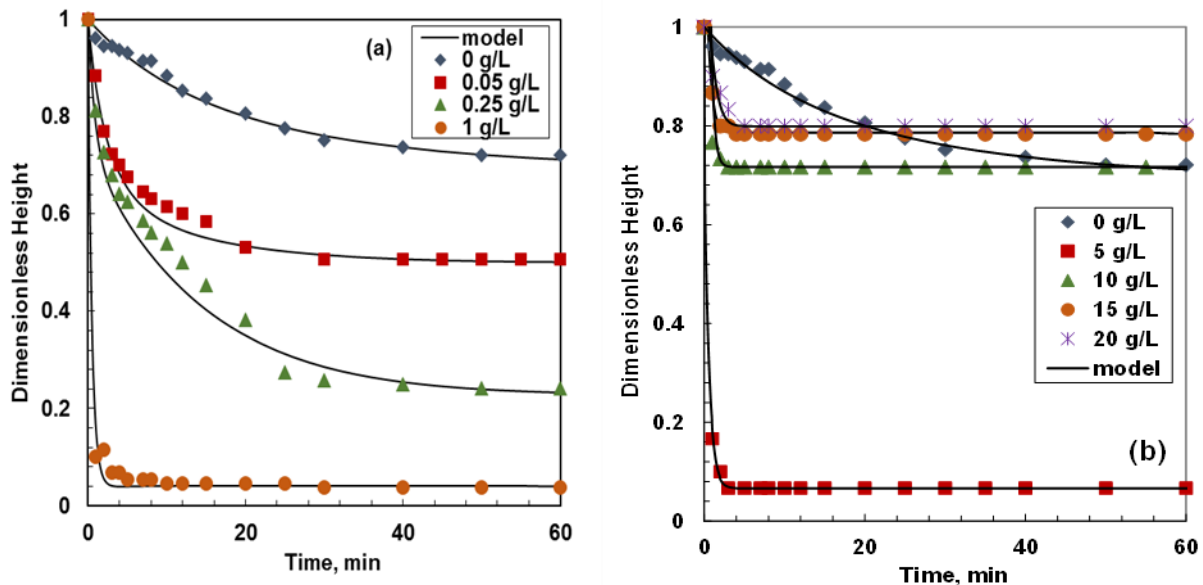


Figure 5.17 Batch separation experiment emulsion layer heights over time for W/O emulsion stabilized by OS asphaltenes with added kaolin with an 80° contact angle at 60°C : a) at low kaolin concentration b) at high kaolin concentration. The emulsions were prepared with 50 vol% aqueous phase and 50 vol% organic phase. The organic phase was 1.5 g/L of OS C7-asphaltenes dissolved in toluene plus added kaolin. Low solids concentration emulsions were prepared with a total volume of 1600 mL and 10,000 rpm mixing speed. High solids concentration emulsions were prepared with a total volume of 50 mL and 10,800 rpm mixing speed.

Table 5.9 Model parameters used for batch experiments for water-in-toluene emulsions stabilized 1.5 g/L OS asphaltenes and 12 μm kaolin particles (contact angle of 80°) at solids concentrations from 0.05 to 20 g/L.

Parameter	Kaolin Concentration (g/L)						
	0.05	0.25	1	5	10	15	20
h_{lim}/h^o	0.50	0.25	0.04	0.07	0.72	0.78	0.80
k, min^{-1}	0.03	0.40	1.00	2.40	2.00	1.80	1.60

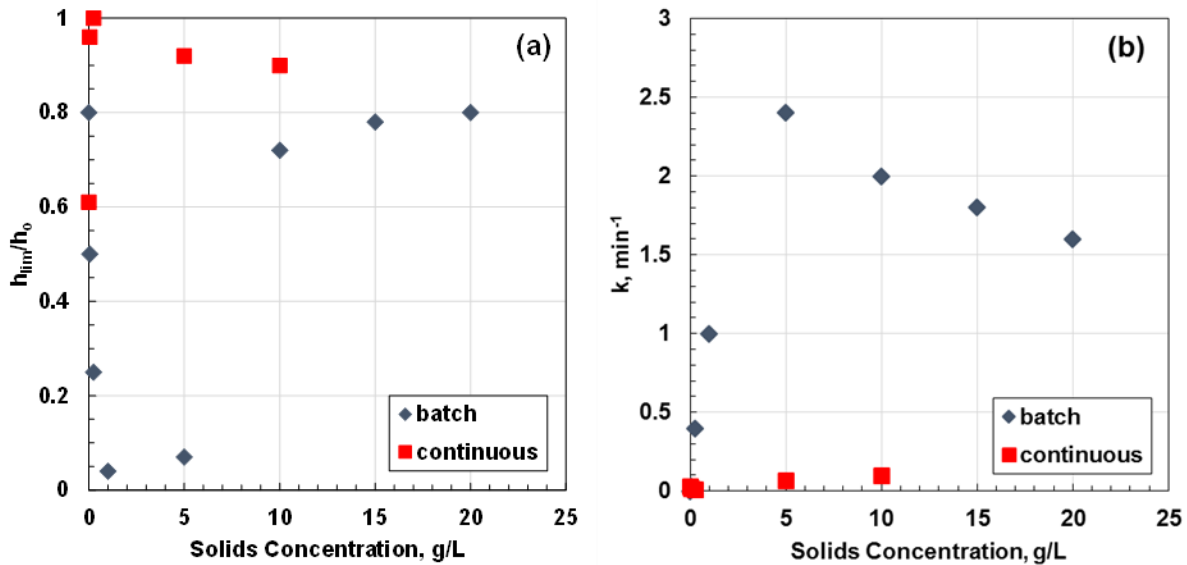


Figure 5.18 Batch and continuous (a) dimensionless limiting height and (b) coalescence rate constant and for W/O emulsions stabilized by OS asphaltenes and kaolin (80° contact angle) in toluene and mixed at 10,000 rpm at 60°C .

5.2.2.1 Effect of Solids Type, Size, and Contact Angle

Additional batch tests were performed with the base case emulsion and the following added solids: 12 μm kaolin with contact angles of 50 and 125° (Figure 5.19), 32 μm silica with contact angles of 75 and 115° (Figure 5.20), and 18 μm silica with a contact angle of 75° (Figure 5.21). All batch tests were performed with a total volume of 50 mL to conserve solids, and mixed at 10,800 rpm with a CAT 520D homogenizer at 60°C in toluene solvent. The corresponding model parameters are provided in Tables 5.10 to 5.14.

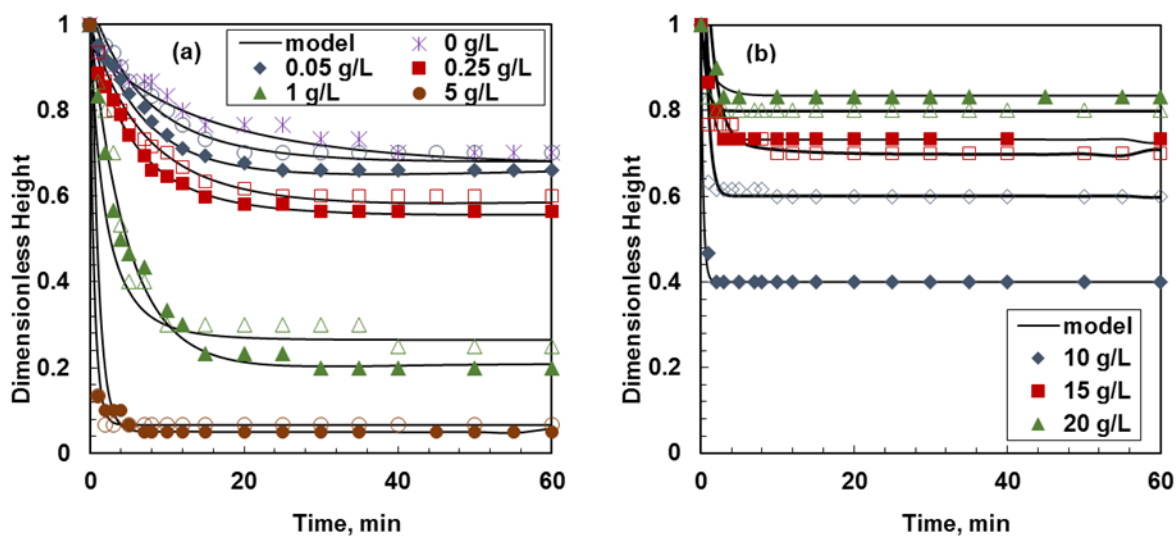


Figure 5.19 Batch separation experiment emulsion layer heights over time for W/O emulsion stabilized by OS asphaltenes with added kaolin (12 μm) with measured contact angles of 50° (closed symbols) and 125° (open symbols) at (a) low concentrations and (b) high concentrations. Emulsions were prepared with 50 vol% aqueous phase and 50 vol% organic phase with a total volume of 50 mL and 10,800 rpm mixing speed. The organic phase was 1.5 g/L of C7-asphaltenes dissolved in toluene plus added kaolin.

Table 5.10 Model parameters used for batch experiments for water-in-toluene emulsions stabilized 1.5 g/L OS asphaltenes and 12 μm kaolin particles (contact angle of 50°) at solids concentrations from 1 to 20 g/L.

Parameter	Kaolin Concentration (g/L)						
	0.05	0.25	1	5	10	15	20
h_{lim}/h^o	0.70	0.57	0.21	0.05	0.40	0.73	0.84
k, min^{-1}	0.01	0.02	0.15	1.0	2.5	1.8	1.6

Table 5.11 Model parameters used for batch experiments for water-in-toluene emulsions stabilized 1.5 g/L OS asphaltenes and 12 μm kaolin particles (contact angle of 125°) at solids concentrations from 0.05 to 20 g/L.

Parameter	Kaolin Concentration (g/L)						
	0.05	0.25	1	5	10	15	20
h_{lim}/h^o	0.70	0.60	0.26	0.07	0.60	0.70	0.80
k, min^{-1}	0.005	0.02	0.14	1.40	1.60	0.80	3.00

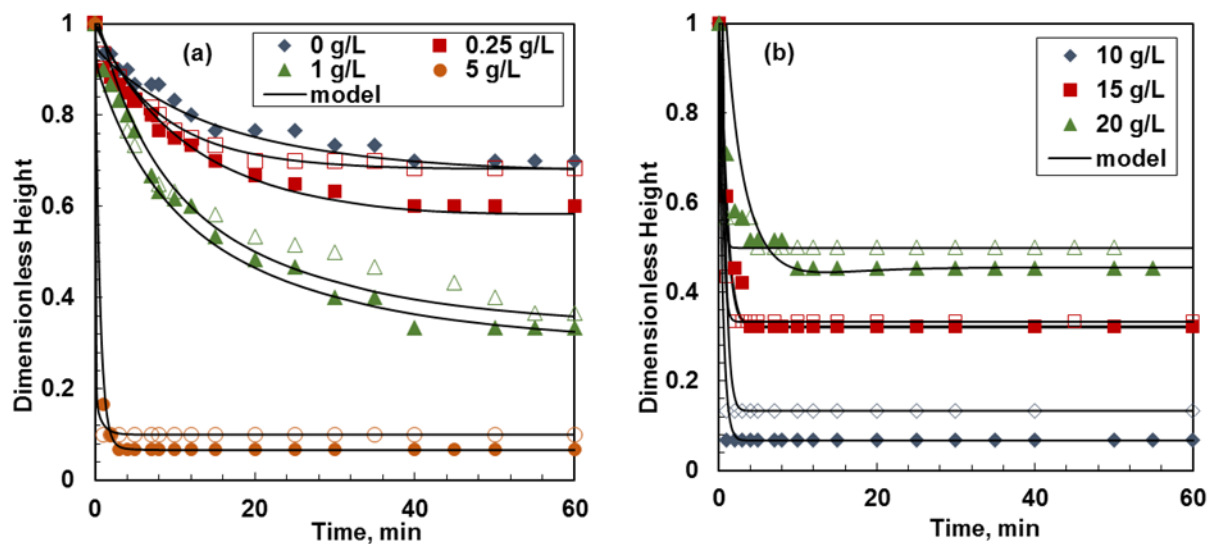


Figure 5.20 Batch separation experiment emulsion layer heights over time for W/O emulsion stabilized by silica (32-63 μm) with measured contact angles of 75° (closed symbols) and 115° (open symbols): a) at low silica concentration; b) at high silica concentration. The emulsions were prepared with 50 vol% aqueous phase and 50 vol% organic phase with a total volume of 50 mL and 10,800 rpm mixing speed. The organic phase was 1.5 g/L of OS C7-asphaltenes dissolved in toluene plus added silica.

Table 5.12 Model parameters used for batch experiments for water-in-toluene emulsions stabilized 1.5 g/L OS asphaltenes and 32 μm silica particles (contact angle of 75°) at solids concentrations from 0.05 to 20 g/L.

Parameter	Silica Concentration (g/L)					
	0.25	1	5	10	15	20
h_{lim}/h^o	0.62	0.28	0.07	0.07	0.32	0.45
k, min^{-1}	0.02	0.03	1.6	2.0	1.65	0.80

Table 5.13 Model parameters used for batch experiments for water-in-toluene emulsions stabilized 1.5 g/L OS asphaltenes and 32 μm silica particles (contact angle of 115°) at solids concentrations from 0.25 to 20 g/L.

Parameter	Silica Concentration (g/L)					
	0.25	1	5	10	15	20
h_{lim}/h^o	0.70	0.32	0.10	0.13	0.33	0.50
k, min^{-1}	0.01	0.02	1.00	2.00	3.00	3.20

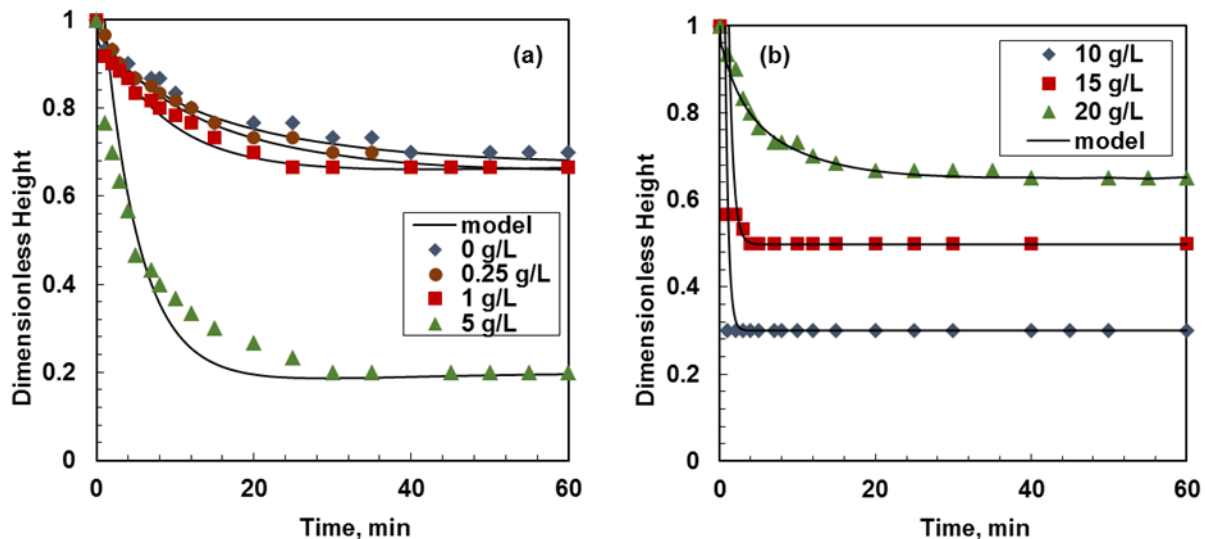


Figure 5.21 Batch separation experiment emulsion layer heights over time for W/O emulsion stabilized by OS asphaltenes with added silica (18-32 μm) with a 75° contact angle; a) at low concentrations, b) at high concentrations. The emulsions were prepared with 50 vol% aqueous phase and 50 vol% organic phase with a total volume of 50 mL and 10,800 rpm mixing speed. The organic phase was 1.5 g/L of C7-asphaltenes dissolved in toluene plus added silica.

Table 5.14 Model parameters used for batch experiments for water-in-toluene emulsions stabilized 1.5 g/L OS asphaltenes and 18 μm silica particles (contact angle of 75°) at solids concentrations from 0.05 to 20 g/L.

Parameter	Silica Concentration (g/L)					
	0.25	1	5	10	15	20
h_{lim}/h^o	0.68	0.67	0.20	0.30	0.50	0.65
k, min^{-1}	0.001	0.05	0.15	2.00	1.50	0.46

Rather than comparing the data versus time in all of the above figures, the batch limiting height parameter can be used as an indicator of emulsion stability at each solids concentration. A higher limiting height value indicates a more stable emulsion. Figure 5.22 shows that, in all cases, the results were similar to the 80° kaolin case described above. The dimensionless limiting height decreased as the solids were added up to a threshold between 5 to 10 g/L and then increased as more solids were added. Some differences were observed with the different solids as noted below.

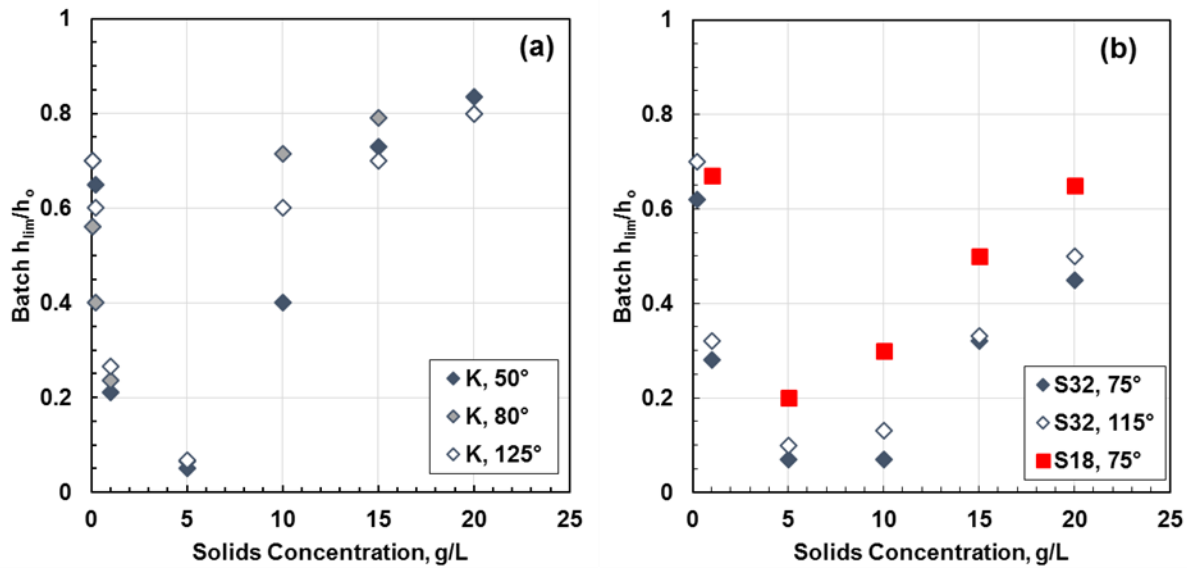


Figure 5.22 Batch dimensionless limiting height for W/O emulsions stabilized by OS asphaltenes and solids in toluene and mixed at 10,000 rpm at 60°C: a) kaolin (K) with contact angles of 50, 80, and 125°; b) 18 μm silica (S18) with a contact angles of 75° and 32 μm silica (S32) with contact angles of 75 and 115°.

Effect of Solids Type

The type of solids has relatively little effect on the destabilization of the emulsions at low solids concentrations. It seems that any coarse particle in the range of wettabilities considered in this study is capable of bridging and coalescing the water droplets. The threshold concentration where emulsion stability increases shifts to a higher concentration of approximately 10 g/L for silica from the 5 g/L threshold for kaolin particles. Kaolin forms a more effective barrier to coalescence than silica at solids concentrations above the threshold. The kaolin aggregates are likely more irregular and pack less efficiently than the spherical silica particles and therefore may create a thicker barrier at the same solid concentration.

Effect of Particle Size

At all concentrations, the 18 μm silica particles produced more stable emulsions than the 32 μm silica particles. In addition, the threshold concentration at which the emulsions became more stable was lower with the smaller particles, approximately 5 g/L versus 10 g/L. Fine particles are expected to stabilize emulsions and it follows that smaller coarse particles are less likely to destabilize emulsions as observed at low solid concentrations. At higher solids concentrations, the smaller particles appear to make a more effective steric barrier.

Effect of Solids Wettability

The effect of contact angle was not strong although the oil-wet solids (high contact angle) produced more stable emulsions at intermediate solids concentrations. The wettability appears to have little effect on the bridging coalescence mechanism that destabilizes the emulsions at low concentrations. It is possible that the wettability only becomes a significant factor for fine solids which typically act as emulsion stabilizers. At intermediate solids concentrations, the contact angle appears to have an effect on the ability the solids to form an effective barrier to coalescence. For kaolin, the intermediate wettability solids form the most effective barrier. This effect is not observed with the silica particles possibly because they are more uniform particles. Note that the reported wettabilities of the solids are the initial wettabilities before contact with the continuous phase. It is possible that the wettability of the solids is altered by contact with the asphaltene toluene solution during emulsion preparation.

5.2.3 Effect of Solids Addition in the Continuous Experiment

Figure 5.23 shows the emulsion layer height versus time when kaolin (12 μm , 80° contact angle) was added to the continuous experiment at 0.05, 0.25, 1, 5 and 10 g/L concentrations. Figure 5.24 shows the continuous results when silica (32 μm , 75° contact angle) was also added at 0.25, 1, 5, 10 and 15 g/L concentrations. The model parameters are provided in Tables 5.15 and 5.16 for kaolin and silica solids addition, respectively.

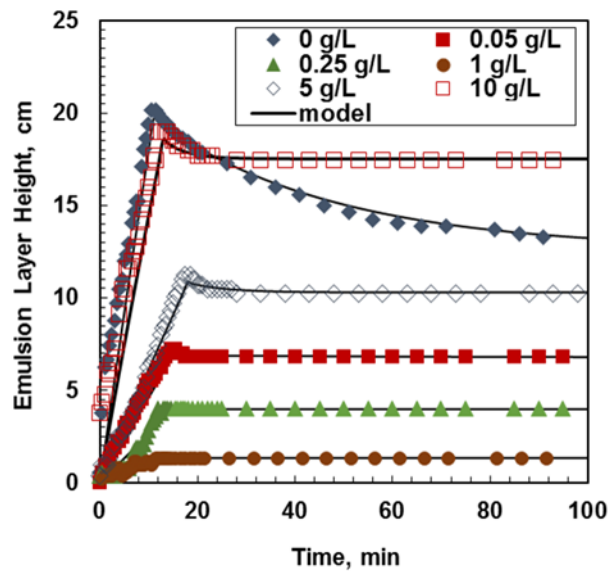


Figure 5.23 Continuous experiment emulsion layer height over time for OS asphaltene stabilized W/O emulsions with added kaolin (80° contact angle) at 60°C. The emulsions were prepared with 50 vol% aqueous phase and 50 vol% organic phase with a 10,000 rpm mixing speed. The organic phase was 1.5 g/L of OS asphaltenes dissolved in toluene plus added kaolin.

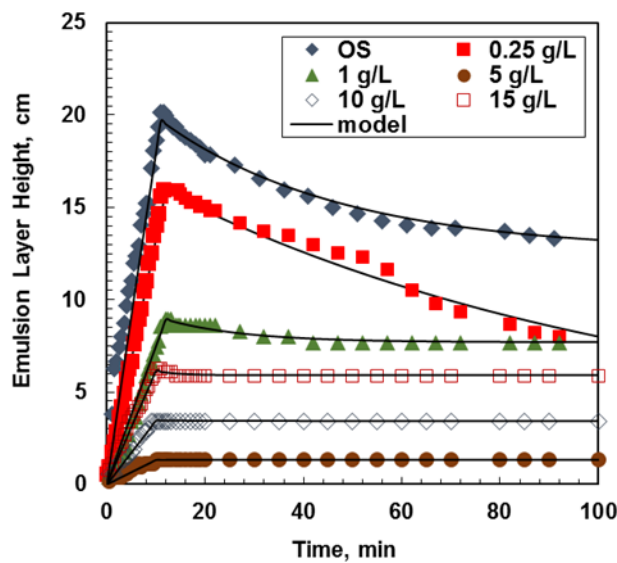


Figure 5.24 Continuous experiment emulsion layer height over time for OS asphaltene stabilized W/O emulsions with added silica (32 μm, 75° contact angle) at 60°C. The emulsions were prepared with 50 vol% aqueous phase and 50 vol% organic phase with a 10,000 rpm mixing speed. The organic phase was 1.5 g/L of OS asphaltenes dissolved in toluene plus added silica.

Table 5.15 Model parameters from continuous experiments for water-in-toluene emulsions stabilized by 1.5 g/L OS asphaltenes and 12 μm kaolin particles with a contact angle of 80° .

Parameter	Kaolin Concentration (g/L)				
	0.05	0.25	1	5	10
dh/dt , cm/min	0.49	0.31	0.08	0.42	1.05
ε	0.67	0.81	0.92	0.69	0.20
h_{lim}	0.96	1.00	1.00	0.92	0.90
k , min^{-1}	0.02	0.01	0.01	0.07	0.10

Table 5.16 Model parameters from continuous experiments for water-in-toluene emulsions stabilized by 1.5 g/L OS asphaltenes and 32 μm silica particles with a contact angle of 75° .

Parameter	Silica Concentration (g/L)				
	0.25	1	5	10	15
dh/dt , cm/min	1.37	0.79	0.12	0.33	0.55
ε	0.01	0.44	0.90	0.75	0.54
h_{lim}	0.15	0.82	1.00	0.99	0.92
k , min^{-1}	0.01	0.06	0.07	0.05	0.02

Rather than comparing the data versus time in all of the above figures, the model parameters can be used as an indicator of emulsion stability at each solids concentration. Figure 5.25 shows that the *emulsion growth rate* followed a trend similar to the trend of the batch experiments. For added kaolin, at solids concentrations below 1 g/L, the emulsion layer growth rate decreased with increasing solids concentration, but the trend reversed at solids concentrations above 5 g/L. For added silica, emulsion layer growth rates initially decreased and then increased for solids concentration above 10 g/L. In both cases the solids concentration at which the trend reversed from decreasing emulsion layer growth rate to increasing growth rate with increasing solids concentration was at the same concentration threshold for emulsion stability in the batch experiments. However, Figure 5.18 showed that the *emulsion stability* (limiting height and coalescence rate) in the continuous experiment was significantly different than the batch test. In the continuous tests, stable emulsions were formed at all solids concentrations. The coalescence rate remained relatively low and the dimensionless limiting height was relatively high at all solids concentrations.

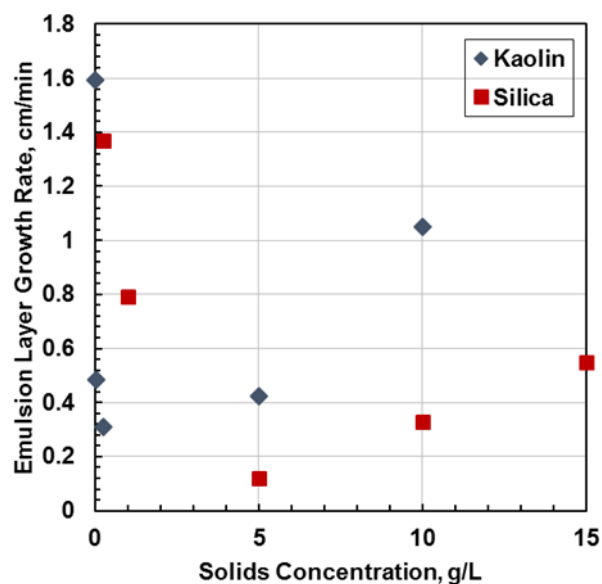


Figure 5.25 Effect of solids content on continuous experiment emulsion layer growth rate for OS asphaltene stabilized W/O emulsions with added kaolin (80° contact angle) and silica (75° contact angle) at 60°C. The emulsions were prepared with 50 vol% aqueous phase and 50 vol% organic phase with a 10,000 rpm mixing speed. The organic phase was 1.5 g/L of OS asphaltenes dissolved in toluene plus added solids.

Emulsions containing solids were found to form stable emulsion layers in the continuous experiment at all initial solids concentrations. These stable emulsions were observed even at low solids concentrations that produced very unstable emulsions in the batch separation experiment. The dimensionless limiting heights in the continuous experiments are near unity, equivalent to almost no coalescence. This observation suggests that solids are accumulating in the residual emulsion layer and preventing coalescence even at low initial solids concentrations. To investigate this hypothesis, the solids content of the emulsion layer at the end of the continuous experiment was measured. The calculated solid concentrations in the emulsion layers are provided in Table 5.17 using Eq. 3.1. The solids concentrations in the emulsion layer are higher than the initial concentration used to prepare the emulsion and above the threshold concentration of 5 g/L for kaolin and 10 g/L for silica for stable emulsions found in the batch experiments. Hence, solids are accumulating in the emulsion layer and forming stabilized emulsions in the decay experiment. Only the addition of 0.25 g/L silica resulted in an unstable emulsion in the decay experiment. In this emulsion, the final solids concentration in the emulsion layer, while greater than the initial

concentration, did not exceed the threshold concentration; thus the emulsion containing 0.25 g/L silica remained unstable as in the batch experiment.

Table 5.17 Calculated kaolin concentrations in the continuous phase of the emulsion layer (using Eq. 3.1) for the continuous experiment water-in-toluene emulsions stabilized by 1.5 g/L OS asphaltenes and 12 μm kaolin particles with a contact angle of 80° or 32 μm silica particles with a contact angle of 75° .

Initial Solids Concentration (g/L)	Kaolin Concentration in Emulsion Layer (g/L)	Silica Concentration in Emulsion Layer (g/L)
0.25	6.5	6.9
1	13.2	13.2
5	16.3	15.3
10	30.1	19.8

5.2.4 Prediction of Continuous Behaviour from Batch Parameters in the Presence of Solids

For asphaltene-stabilized emulsions, relative trends in emulsion stability and growth in the continuous experiment could be predicted from batch model parameters. In the presence of solids, this is no longer the case. Not surprisingly, the accumulation of solids in the continuous experiments compromises the ability to predict the height of the emulsion layer from batch test data. Figure 5.26 shows that while the batch test provides a potential correlation for the growth rate of the emulsion layer, it completely fails to predict the dimensionless limiting height of the continuous emulsion layer. The emulsion layer growth rate in these experiments is not significantly impacted by the dimensionless limiting height, but rather by the fractional bypass. The fractional bypass is generated during continuous flow through the pump where accumulation is not a factor. In a field application, where the emulsion layer will reside in the separator for much longer time frames, the amount of emulsion that does not break (the dimensionless limiting height) will be the key factor. The batch experiments cannot predict the continuous layer height because the accumulation of solids creates a steric barrier that accumulates over time. Hence, batch tests, such as bottle tests, are likely to be unreliable when solids are present in the emulsion.

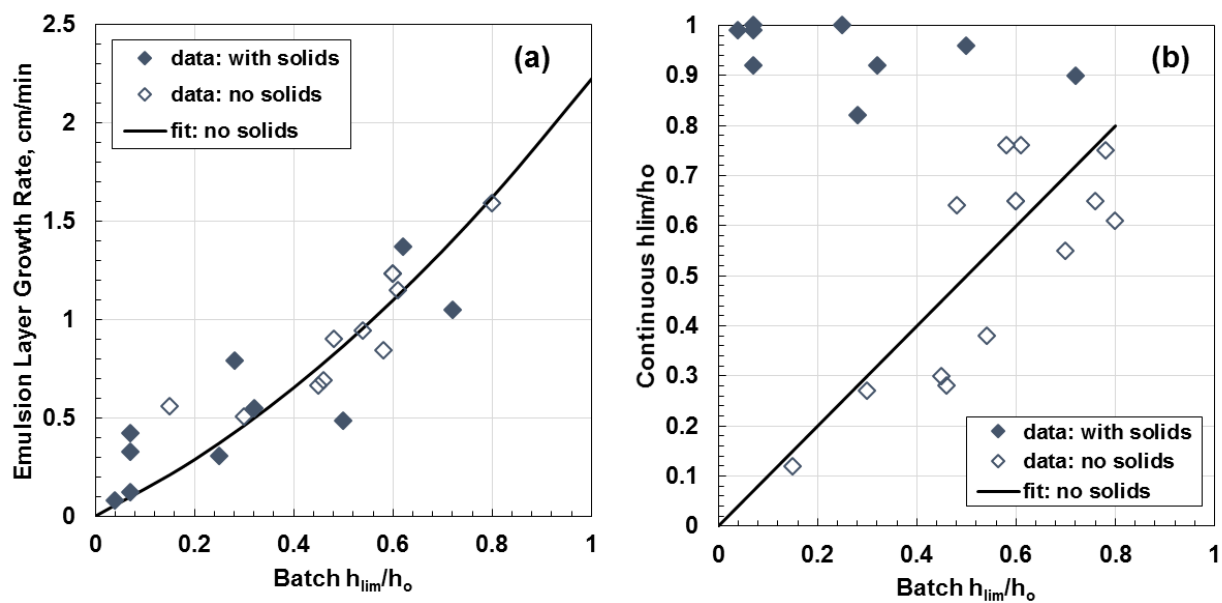


Figure 5.26 Effect of solids on correlation between continuous emulsion model parameters and batch test dimensionless limiting heights for W/O emulsions stabilized by asphaltenes in toluene at 60°C.

CHAPTER 6: CONCLUSIONS AND RECOMMENDATIONS

In this thesis, the effect of solids on emulsion stability and emulsion layer growth for asphaltene-stabilized water-in-oil emulsions was investigated by measuring emulsion layer stability in batch separation experiments and emulsion layer growth in continuous separation experiments. Model emulsions prepared with different asphaltenes, asphaltene concentrations, solvent types, drop size distributions, solids contents, particle size distributions, and solids wettability were studied. Both batch and continuous emulsion separation data for water-in-oil emulsions stabilized by asphaltenes and inorganic solids were modeled with a mass balance based on the rate at which the dispersed phase in the emulsions layer exits the settled emulsion. The model was used to determine coalescence rates, limiting height, and fractional bypass parameter values, which were used to compare emulsions at different conditions and predict emulsion layer behavior in continuous separations from batch model parameters.

6.1 Asphaltene-Stabilized Emulsions

For experiments performed in the absence of solids, water-in-oil emulsions were prepared from an aqueous phase consisting of water and an organic phase consisting of asphaltenes dissolved in toluene and heptane. Asphaltenes from three sources were examined. In these asphaltene-stabilized emulsions, emulsion stability increased with increasing asphaltene concentration, increasing fraction of heptane in the solvent (decreasing solubility of the asphaltenes in the solvent), increasing mixing speed (decreasing drop size distribution) and decreasing dispersed phase volume content in both batch and continuous separations.

When the emulsions were stabilized by asphaltenes alone, the continuous separation parameters correlated well with the dimensionless limiting height obtained in the batch tests. Stable emulsions were found to have high limiting height parameters, and low coalescence rate constants. Low fractional bypass parameters correlated with fast emulsion layer growth rates in the continuous experiment. A high batch limiting height parameter predicted a high continuous limiting height and a low continuous fractional bypass parameter. In other words, an emulsion that is stable in the

batch experiment has similar relative stability in the continuous experiments and more stable emulsions have faster growth rates. Hence, simple batch separations such as bottle tests are good qualitative evaluation tools for this type of emulsion.

6.2 Solids-Stabilized Emulsions

When solids are present in the organic phase, they destabilized the water-in-oil emulsions at concentrations below a threshold ranging from 5 to 10 g/L solids. At low concentrations the solids act as bridges between droplets, promoting coalescence. Above the threshold, the emulsions became more stable with increasing solids concentration. At sufficient concentration, the solids form a steric barrier between the droplets preventing further coalescence. The solids tend to accumulate in the emulsion layer formed in a continuous separation preventing effective long term coalescence. In this case, the batch tests are poor predictors for long term emulsion layer build up. Note, only coarse solids with average diameters ranging from 12 to 32 μm were considered.

Both the batch and continuous separations were less sensitive (compared with the sensitivity to the solids content) to the asphaltene source, solvent type, and emulsion drop size distribution as well as the solid type, size, and contact angle. The asphaltenes that most strongly stabilized batch emulsions also led to faster emulsion layer growth in continuous experiments. Both batch and continuous experiment emulsions were more stable in solvents that more weakly solubilized the asphaltenes, with smaller droplets, and with smaller solids. Kaolin formed a more effective barrier to coalescence than silica.

6.3 Recommendations

Some recommendations for future work are to:

- 1) Repeat some experiments using the original bitumen samples to ensure that the model emulsions are representative of those encountered in the field. In addition, run experiments at the conditions encountered in production facilities, such as higher temperatures, to determine if there are any changes in emulsion layer stability or accumulation behavior.
- 2) Repeat the solids-stabilized emulsion experiments using fine solids (average diameters $<1\text{-}2\ \mu\text{m}$), also considering different wettability, size, and type of solid. Only coarse solids

were considered in this thesis; however, solids most often identified as being contributors to stable rag layers in oil sands processes are fine solids. Iron bearing clays, such as siderite and pyrite should also be considered.

REFERENCES

Agrawala, M., Yarranton, H. W. (2001). Asphaltene Association Model Analogous to Linear Polymerization. *Industrial and Engineering Chemistry Research*, 40, 4664–4672.

Aveyard, R., Binks, B.P., Clint, J.H. (2003). Emulsions Stabilized Solely by Colloidal Particles. *Advances in Colloid and Interface Science*, 100-102, 503-546.

Barnea, E., Mizrahi, J. (1975a) Separation Mechanisms of Liquid-Liquid Dispersions in a Deep-Layer Gravity Settler: Part II- Flow Patterns of the Dispersed and Continuous Phases within the Dispersion Band. *Transactions of the Institution of Chemical Engineers*, 53(2), 70-74.

Barnea, E., Mizrahi, J. (1975b) Separation Mechanisms of Liquid-Liquid Dispersions in a Deep-Layer Gravity Settler: Part III-Hindered Settling and Drop-to-Drop Coalescence in the Dispersion Band. *Transactions of the Institution of Chemical Engineers*, 53(2), 75-82.

Barnea, E., Mizrahi, J. (1975c) Separation Mechanisms of Liquid-Liquid Dispersions in a Deep-Layer Gravity Settler: Part IV- Continuous Settler Characteristics. *Transactions of the Institution of Chemical Engineers*, 53(2), 83-92.

Bensebaa, F., Kotlyar, L., Sparks, B., Chung, K. (2000). Organic Coated Solids in Athabasca Bitumen: Characterization and Process Implications. *Canadian Journal of Chemical Engineering*, 78, 610-616.

Binks, B., Horozov, T. (2006). *Colloidal Particles at Liquid Interfaces*. Cambridge: Cambridge University Press.

Binks, B.P., Kirkland, M. (2002). Interfacial Structure of Solid-Stabilized Emulsions Studied by Scanning Electron Microscopy. *Physical Chemistry Chemical Physics*, 4, 3727-3733.

Binks, B.P., Lumsdon, S.O. (2000). Influence of Particle Wettability on the Type and Stability of Surfactant-Free Emulsions. *Langmuir*, 16, 8622-8631.

Canadian Association of Petroleum Producers'. (2017). Statistical Handbook for Canada's Upstream Petroleum Industry. Calgary, AB.

Chen, Q., Liu, J., Thundat, T., Gray, M.R., Liu, Q. (2017a). Spatially Resolved Organic Coating on Clay Minerals in Bitumen Froth Revealed by Atomic Force Microscopy Adhesion Mapping. *Fuel*. 191, 283-289.

Chen, Q., Stricek, I., Gray, M.R., Liu, Q. (2017b). Influence of Hydrophobicity Distribution of Particle Mixtures on Emulsion Stabilization. *Journal of Petroleum Science and Engineering*, 491, 179-189.

Czarnecki, J., Moran, K. & Yang, X., (2007). On the Rag Layer and Diluted Bitumen Froth Dewatering. *Canadian Journal of Chemical Engineering*, 85(5),748–755.

Czarnecki, J., Tchoukov, P., Dabros, T., Xu, Z. (2013). Role of Asphaltenes in Stabilisation of Water in Crude Oil Emulsions. *The Canadian Journal of Chemical Engineering*, 91(8), 1365-1371.

Dang-Vu, T., Jha, R., Wu, S., Tannant, D.D., Masliyah, J., Xu, Z. (2009). Wettability Determination of Solids Isolated from Oil Sands. *Colloids and Surfaces A: Physicochemical and Engineering Aspects*, 337, 80-90.

Darcovich, K., Kotlyar, L.S., Tse, W.C., Ripmeester, J.A., Capes, C.E., Sparks, B.D. (1989). Wettability Study of Organic-Rich Solids Separated from Athabasca Oil Sands. *Energy Fuels*. 3, 386-391.

Farn, R. (2006). *Chemistry and Technology of Surfactants*. Oxford: Blackwell Publishing Ltd.

Frising, T., Noik, C., Dalmazzone, C. (2006). The Liquid/Liquid Sedimentation Process: From Droplet Coalescence to Technologically Enhanced Water/Oil Emulsion Gravity Separators: A Review. *Journal of Dispersion Science and Technology*, 27, 1035-1057.

Fuerstenau, D.W., Diao, J., Williams, M.C. (1991). Characterization of the Wettability of the Solid Particles by Film Flootation. 1. Experimental Investigation. *Colloids and Surfaces*, 60, 127-144.

Gafonova, O. V., Yarranton, H. W. (2001). The Stabilization of Water-in-Hydrocarbon Emulsions by Asphaltenes and Resins. *Journal of Colloid and Interface Science*, 241(2), 469–478.

Gavrielatos, I., Mohan, R., Shoham, O. (2017). Effect of Intermediate Wettability Nanoparticles on Oil-Water Emulsion Stability. *Journal of Petroleum Science and Engineering*, 152, 664-674.

Gelot, A., Friesen, W., Hamza, H.A. (1984). Emulsification of Oil and Water in the Presence of Finely Divided Solids and Surface-Active Agents. *Colloids and Surfaces*, 12, 271-303.

Golob, J., Modic, R. (1977). Coalescence of Liquid/Liquid Dispersions in Gravity Settlers. *TransIChemE*, 55, 207-211.

Gray, M.R., Tykwinski, R.R., Stryker, J.M., Tan, X. (2011). Supramolecular Assembly Model for Aggregation of Petroleum Asphaltenes. *Energy Fuels*, 25, 3125-3134.

Gu, G., Xu, Z., Nandakumar, K., Masliyah, J.H. (2002). Influence of Water-Soluble and Water-Insoluble Natural Surface Active Components on the Stability of Water-in-Toluene Diluted Bitumen Emulsions. *Fuel*, 81(14), 1859-1869.

Gu G., Zhang, L., Xu, Z., Masliyah, J. (2007). Novel Bitumen Froth Cleaning Device and Rag Layer Characterization. *Energy Fuels*, 21, 3462-3468.

Hannisdal, A., Ese, M.H., Hemmingsen, P.V., Sjoblom, J. (2006). Particle-Stabilized Emulsions: Effect of Heavy Crude Oil Components Pre-adsorbed onto Stabilizing Solids. *Colloids and Surfaces A: Physicochemical and Engineering Aspects*, 276, 45-58.

Hartland, S., Jeelani, S.A.K. (1985). Relationship between Models for Predicting Steady-State Dispersion Height from Batch Settling Data. *Institution of Chemical Engineers Symposium*, 94, 211-223.

Hartland, S., Jeelani, S.A.K. (1987). Choice of Model for Predicting the Dispersion Height in Liquid/Liquid Gravity Settlers from Batch Settling Data. *Chemical Engineering Science*, 42(8), 1927-1938.

Hartland, S., Jeelani, S.A.K. (1988). Prediction of Sedimentation and Coalescence Profiles in a Decaying Batch Dispersion. *Chemical Engineering Science*, 43(9), 2421-2429.

Hartland, S., Vohra, D.K. (1980). Effect of Interdrop Forces on the Coalescence of Drops in Close-Packed Dispersions. *Journal of Colloid and Interface Science*, 77(2), 295-316.

Heath, A.R., Fawell, P.D., Bahri, P.A., Swift, J.D. (2002). Estimating Average Particle Size by Focused Beam Reflectance Measurement (FBRM). *Particle and Particle Systems Characterization*, 19, 84-95.

Hirasaki, G., Jiang, T., Miller, C., Moran, K. (2008). Using Silicate and pH Control for Removal of the Rag Layer Containing Clay Solids Formed during Demulsification. *Energy Fuels*, 22, 4158-4164.

Horozov, T.S., Binks, B.P. (2006). Particle-Stabilized Emulsions: A Bilayer or a Bridging Monolayer. *Angewandte Chemie International Edition*, 45, 773-776.

Jeelani, S.A.K., Hartland, S. (1985). Prediction of Steady State Dispersion Height from Batch Settling Data. *American Institute of Chemical Engineers*, 31(5), 711-720.

Jeelani, S.A.K., Hartland, S. (1986a) Prediction of Dispersion Height in Liquid/Liquid Gravity Settlers from Batch Settling Data. *Chemical Engineering Research and Design*, 64(6), 450-460.

Jeelani, S.A.K., Hartland, S. (1986b). Scale-Up of Industrial Gravity Settlers from Batch Settling Data. *DECHEMA*, 3, 453-460.

Jeelani, S.A.K., Hosig, R., and Windhab, E.J. (2005). Kinetics of Low Reynolds Number Creaming and Coalescence in Droplet Dispersions. *American Institute of Chemical Engineers*, 51, 149-161.

Jiang, T., Hirasaki, G.J., Miller, C.A. (2010). Characterization of Kaolinite ζ Potential for Interpretation of Wettability Alteration in Diluted Bitumen Emulsion Separation. *Energy Fuels*, 24, 2350-2360.

Jiang, T., Hirasaki, G.J., Miller, C.A., Ng, S. (2011). Wettability Alteration of Clay in Solid-Stabilized Emulsions. *Energy Fuels*, 25, 2551-2558.

Kaminsky, H.A.W., Etsell, T.H., Ivey, D.G. (2009). Distribution of Clay Minerals in the Process Streams Produced by the Extraction of Bitumen from Athabasca Oil Sands. *Canadian Journal of Chemical Engineering*, 87, 85-93.

Khatri, N.L. (2010). Measurement and Modeling of Emulsion Layer Growth in Continuous Oil-Water Separations (Master's dissertation). University of Calgary, Calgary, AB.

Khatri, N.L., Andrade, J., Baydak, E.N., Yarranton, H.W. (2011). Emulsion Layer Growth in Continuous Oil-Water Separation. *Colloids and Surfaces A: Physicochemical and Engineering Aspects*, 384, 630-642.

Kiran, S.K., Ng, S., Acosta, E.J. (2011). Impact of Asphaltene and Naphthenic Amphiphiles on the Phase Behaviour of Solvent-Bitumen-Water Systems. *Energy Fuels*, 25, 2223-2231.

Kotlyar, L.S., Sparks, B.D., Woods, J.R., Raymond, S., Le Page, Y., Shelfantook, W. (1998). Distribution and Type of Solids Associated with Bitumen. *Petroleum Science and Technology*, 1, 1-19.

Kotlyar, L.S., Sparks, B.D., Woods, J.R. (1999). Solids Associated with the Asphaltene Fraction of Oil Sands Bitumen. *Energy Fuels*, 13(2), 346-350.

Kupai, M.M., Yang, F., Harbottle, D., Moran, K., Masliyah, J., Xu, Z. (2013). Characterising Rag-Forming Solids. *Canadian Journal of Chemical Engineering*, 91, 1395-1401.

Lebedeva, E.V., Fogden, A. (2011). Wettability Alteration of Kaolinite Exposed to Crude Oil in Salt Solutions. *Colloids and Surfaces A: Physicochemical and Engineering Aspects*, 337, 115-122.

Levine, S., Sanford, E. (1985). Stabilisation of Emulsion Droplets by Fine Powders. *Canadian Journal of Chemical Engineering*, 62, 258-268.

Liu, F., Darjani, S., Akhmetkhanova, N., Maldarelli, C., Banerjee, S., Pauchard, V. (2017). Mixture Effect on the Dilatation Rheology of Asphaltenes-Laden Interfaces. *Langmuir*, 33, 1927-1942.

Liu, J., Zhao, Y., Ren, S. (2015). Molecular Dynamics Simulation of Self-Aggregation of Asphaltenes at an Oil/Water Interface: Formation and Destruction of the Asphaltene Protective Film. *Energy Fuels*, 29, 1233-1242.

Lobo, L., Ivanov, I., Wasan, D. (1993). Dispersion Coalescence: Kinetic Stability of Creamed Dispersion. *American Institute of Chemical Engineers*, 39(2), 322-334.

McLean, J.D., Kilpatrick, P.K. (1997a). Effects of Asphaltene Solvency of Stability of Water-in-Crude Oil Emulsions. *Journal of Colloid and Interface Science*, 189(2), 242-253.

McLean, J.D., Kilpatrick, P.K. (1997b). Effect of Asphaltene Aggregation in Model Heptane-Toluene Mixtures on Stability of Water-in-Oil Emulsions. *Journal of Colloid and Interface Science*, 196, 23-34.

Menon, V.B., Wasan, D.T. (1986). Particle – Fluid Interactions with Application to Solids-Stabilize Emulsions Part I. The Effect of Asphaltene Adsorption. *Colloids and Surfaces*, 19, 89-105.

Menon, V.B., Wasan, D.T. (1988). A Review of the Factors Affecting the Stability of Solids-Stabilized Emulsions. *Separation Science and Technology*, 23(12&13), 2131-2142.

Merino-Garcia, D., Murgich, J., Andersen, S. I. (2004). Asphaltene Self-Association: Modeling and Effect of Fractionation with a Polar Solvent. *Petroleum Science and Technology*, 22(7&8), 735–758.

Mullins, O.C. (2010). The Modified Yen Model. *Energy Fuels*, 24, 2179–2207.

Nadiv, C., Semiat, R. (1995). Batch Settling of Liquid-Liquid Dispersion. *Industrial and Engineering Chemistry Research*, 34(7), 2427-2435.

Natarajan, A., Xie, J., Wang, S., Masliyah, J., Zeng, H., Xu, Z. (2011). Understanding Molecular Interactions of Asphaltenes in Organic Solvents Using a Surface Force Apparatus. *Journal of Physical Chemistry C*, 115(32), 16043–16051.

Ng, Y.M.S., Knapper, B., Cymerman, G., Tran, T., Yeung, A. (2015). *Canada Patent No. 2820040*. Calgary, AB: Canada.

Ortiz, D. P., Baydak, E. N., Yarranton, H. W. (2010). Effect of Surfactants on Interfacial Films and Stability of Water-In-Oil Emulsions Stabilized by Asphaltenes. *Journal of Colloid and Interface Science*, 351(2), 542–555.

Perino, A., Noik, C., Dalmazzone, C. (2013). Effect of Fumed Silica Particles on Water-in-Crude Oil Emulsion: Emulsion Stability, Interfacial Properties and Contribution of Crude Oil Fractions. *Energy Fuels*, 27, 2399-2412.

Pickering, S.U. (1907). Emulsions. *Journal of the Chemical Society*, 91, 2001–2021.

Podgorski, D.C., Corilo, Y.E., Nyadong, L., Lobodin, V.V., Bythell, B.J., Robbins, W.K., McKenna, A.M., Marshall, A.G., Rodgers, R.P. (2013). Heavy Petroleum Composition. 5. Compositional and Structural Continuum of Petroleum Revealed. *Energy Fuels*, 27, 1268–1276.

Pourmohammadbagher, A., Shaw, J.M. (2016). Probing the Impact of Asphaltene Contamination on Kaolinite and Illite Clay Behaviours in Water and Organic Solvents: A Calorimetric Study. *Energy Fuels*, 30, 6561-6569.

Powers, D.P. (2014). Characterization and Asphaltene Precipitation Modeling of Native and Reacted Crude Oils (PhD). University of Calgary.

Rane, J.P., Harbottle, D., Pauchard, V., Couzis, A., Banerjee, S. (2012). Adsorption Kinetics of Asphaltenes at the Oil-Water Interface and Nanoaggregation in the Bulk. *Langmuir*, 28, 9986-9995.

Rocha, J.A., Baydak, E.N., Yarranton, H.W., Sztukowski, D.M., Ali-Marcano, V., Gong, L., Shi, C., Zeng, H. (2016). Role of Aqueous Phase Chemistry, Interfacial Film Properties, and Surface Coverage in Stabilizing Water-in-Bitumen Emulsions. *Energy Fuels*, 30, 5240-5252.

Romanova, U.G., Yarranton, H.W., Schramm, L.L., Shelfantook, W.E. (2004). Investigation of Oil Sands Froth Treatment. *Canadian Journal of Chemical Engineering*, 82, 710-721.

Saadatmand, M., Yarranton, H.W., Moran, K. (2008). Rag Layers in Oil Sand Froths. *Industrial and Engineering Chemistry Research*, 47, 8828-8839.

Sathe, D., Sawant, K., Mondkar, H., Naik, T., Deshpande, M. (2010). Monitoring Temperature Effect on the Polymorphic Transformation of Acitretin Using FBRM-Lasentec. *Organic Process Research and Development*, 14, 1373-1378.

Schramm, L.L. (1992). Petroleum Emulsions, Basic Principles. In *Emulsions: Fundamentals and Applications in the Petroleum Industry*. Washington, D.C.: American Chemical Society.

Schulman, J.H., Leja, J. (1954). Control of Contact Angles at the Oil-Water-Solid Interfaces. Emulsions Stabilized by Solid Particles (BaSO₄). *Transactions of the Faraday Society*, 50, 598-605.

Shi, C., Zhang, L., Xie, L., Lu, X., Liu, Q., He, J., Mantilla, C.A., Van den berg, F.G.A., Zeng, H. (2017). Surface Interaction of Water-in-Oil Emulsion Droplets with Interracially Active Asphaltenes. *Langmuir*, 33, 1265-1274.

Siffert, B., Bourgeois, C., Papirer, E. (1984). Structure and Water-Oil Emulsifying Properties of Asphaltenes. *Fuel*, 63, 834-837.

Singh, B.P. (1994). Chemical Resolution of Petroleum Emulsion. *Chemical Engineering World*, 29(10), 203-209.

Singh, B.P. (1995). Laboratory Test Results on Ultrasound Treated Industrial Emulsion. *Acoustic Letters*, 19(4), 78-82.

Sparks, B.D., Kotlyar, L.S., O'Carroll, J.B., Chung, K.H. (2003). Athabasca Oil Sands: Effect of Organic Coated Solids on Bitumen Recovery and Quality. *Journal of Petroleum Science and Engineering*, 39, 417-430.

Spiecker, P.M., Gawrys, K.L., Kilpatrick, P.K. (2003). Aggregation and Solubility Behaviour of Asphaltenes and Their Subfractions. *Journal of Colloid and Interface Science*, 267, 178-193.

Spiecker, P.M., Kilpatrick, P.K. (2004). Interfacial Rheology of Petroleum Asphaltenes at the Oil-Water Interface. *Langmuir*, 20(10), 4022-4032.

Standal, S., Haavik, J., Blokhus, A.M., Skauge, A. (1999). Effect of Organic Components on Wettability as Studied by Adsorption and Contact Angles. *Journal of Petroleum Science and Engineering*, 24, 131-144.

Strausz, O.P., Mojelsky, T.W., Lown, E.M. (1992). The Molecular Structure of Asphaltene: an Unfolding Story. *Fuel*, 71, 1355-1363.

Sullivan, A.P., Kilpatrick, P.K. (2002). The Effects of Inorganic Solid Particles on Water and Crude Oil Emulsion Stability. *Industrial and Engineering Chemistry Research*, 41, 3389-3404.

Sztukowski, D.M. (2005). Asphaltene and Solids-Stabilized Water-in-Oil Emulsions (Doctoral dissertation). University of Calgary, Calgary, AB.

Sztukowski, D.M., Jafari, M., Alboudwarej, H., Yarranton, H.W. (2003). Asphaltene Self-Association and Water-in-Hydrocarbon Emulsions. *Journal of Colloid and Interface Science*, 265, 179-186.

Sztukowski, D.M., Yarranton, H.W. (2004). Characterization and Interfacial Behaviour of Oil Sands Solids Implicated in Emulsion Stability. *Journal of Dispersion Science and Technology*, 25(3), 299-310.

Sztukowski, D.M., Yarranton, H.W. (2005). Oilfield Solids and Water-in-Oil Emulsion Stability. *Journal of Colloid and Interface Science*, 28, 821-833.

Tadros, T.F. (2009). *Emulsion Science and Technology*. Weinheim: Wiley-VCH Verlag GmbH & Co. KGaA.

Tadros, T.F., Vincent, B. (1983). Emulsion Stability. In *Encyclopedia of Emulsion Technology*. New York: Dekker.

Tambe, D.E., Sharma, M.M. (1993). Factors Controlling the Stability of Colloid-Stabilized Emulsions: 1. An Experimental Investigation. *Journal of Colloid and Interface Science*, 157, 214-253.

Tambe, D.E., Sharma, M.M. (1994). Factors Controlling the Stability of Colloid-Stabilized Emulsions: 2. A Model for the Rheological Properties of Colloid-Laden Interfaces. *Journal of Colloid and Interface Science*, 162, 1-10.

Tchoukov, P., Yang, F., Xu, Z., Dabros, T., Czarnecki, J., Sjoblom, J. (2014). Role of Asphaltene in Stabilizing Thin Liquid Emulsion Films. *Langmuir*, 30, 3024-3033.

Varadaraj, R., Brons, C. (2007). Molecular Origins of Heavy Crude Oil Interfacial Activity Part 2: Fundamental Interfacial Properties of Model Naphthenic Acids and Naphthenic Acids Separated from Heavy Crude Oils. *Energy Fuels*, 21, 199–204.

Vignati, E., Piazza, R., Lockhart, T.P. (2003). Pickering Emulsions: Interfacial Tension, Colloidal Layer Morphology, and Trapped-Particle Motion. *Langmuir*, 19, 6650-6656.

Wang, C., Germain, M., Lui, Q., Ivey, D.G., Estell, T.H. (2015). Comparison of Different Methods to Determine the Surface Wettability of Fine Solids Isolated from Alberta Oil Sands. *Energy Fuels*, 29, 3556-3565.

Wang, S., Liu, Q., Tan, X., Xu, C., Gray, M.R. (2013). Study of Asphaltene Adsorption on Kaolinite by X-ray Photoelectron Spectroscopy and Time-of-Flight Secondary Ion Mass Spectroscopy. *Energy Fuels*, 27, 2465-2473.

Wang, S., Liu, Q., Tan, X., Xu, C., Gray, M.R., (2016), Adsorption of Asphaltenes on Kaolinite as an Irreversible Process. *Colloids and Surfaces A: Physicochemical and Engineering Aspects*, 504, 280-286.

Wen, J., Zhang, J., Wang, Z., Zhang, Z., Zheng, F., Zhu, Y., Han, S. (2014). Full and Partial Emulsification of Crude Oil-Water Systems as a Function of Shear Intensity, Water Fraction, and Temperature. *Industrial and Engineering Chemistry Research*, 53, 9513-9520.

Yaghi, B., Benayoune M. and Al-Bemani, A. (2001). Viscosity of Water-Oil Emulsions with Added Nano-Sized Particles. *Petroleum Science and Technology*, 19 (3&4), 373-386.

Yan, Z., Elliott, J.A.W, Masliyah, J.H. (1999). Roles of Various Bitumen Components in the Stability of Water-in-Diluted-Bitumen Emulsions. *Journal of Colloid and Interface Science*, 220(2), 329-337.

Yan, N., Gray, M.R., Masliyah, J.H. (2001). On Water-in-Oil Emulsions Stabilized by Fine Solids. *Colloids and Surfaces A: Physicochemical and Engineering Aspects*, 193, 97-107.

Yan, Y., Masliyah, J.H. (1993). Effect of Oil Viscosity on the Rheology of Oil-in-Water Emulsions with Added Solids. *The Canadian Journal of Chemical Engineering*, 71, 852-858.

Yan, Y., Masliyah, J.H. (1994). Adsorption and Desorption of Clay Particles at the Oil-Water Interface. *Journal of Colloid and Interface Science*, 168(2), 386-392.

Yang, X., Hamza, H., Czarnecki, J. (2004). Investigation of Subfractions of Athabasca Asphaltenes and Their Role in Emulsion Stability. *Energy Fuels*, 18, 770-777.

Yarranton, H.W., Hussein, H., Masliyah, J.H. (2000). Water-in-Hydrocarbon Emulsions Stabilized by Asphaltenes at Low Concentrations. *Journal of Colloid and Interface Science*, 228, 52-63.

Yarranton, H. W., Masliyah, J. H. (1996). Gibbs - Langmuir Model for Interfacial Tension of Non-Ideal Organic Mixtures over Water. *Journal of Physical Chemistry*, 100, 1786–1792.

Yarranton, H.W., Sztukowski, D.M., Urrutia, P. (2007). Effect of Interfacial Rheology on Model Emulsion Coalescence I. Interfacial Rheology. *Journal of Colloid and Interface Science*, 310, 246-252.

Yekeler, M., Ulusoy, U., and Hiçyilmaz, C. (2004). Effect of Particle Shape and Roughness of Talc Mineral Ground by Different Mills on the Wettability and Floatability. *Powder Technology*, 140, 68.

Yen, T.F., Erdman, J.G., Pollack, S.S. (1961). Investigation of the Structure of Petroleum Asphaltenes by X-Ray Diffraction. *Analytical Chemistry*, 33, 1587–1594.

Zahabi, A., Gray, M.R., Czarnecki, J., Dabros, T. (2010). Flocculation of Silica Particles from a Model Oil Solution: Effect of Adsorbed Asphaltenes. *Energy Fuels*, 24(6), 331-348.

Zhang, J., Tian, D., Lin, M., Tang, Z., Dong, Z. (2016). Effect of Resins, Waxes and Asphaltenes on Water-Oil Interfacial Properties and Emulsion Stability. *Colloids and Surfaces A: Physicochemical and Engineering Aspects*, 507, 1-6.

Zhang, L.Y., Xu, Z., Masliyah, J.H. (2005). Characterization of Adsorbed Athabasca Asphaltene Films at Solvent-Water Interfaces Using a Langmuir Interfacial Trough. *Industrial and Engineering Chemistry Research*, 44, 1160-1174.

APPENDIX A
EMULSIFIED WATER VOLUME FRACTION IN THE EMULSION IN LAYER
DURING BATCH EXPERIMENTS

Figures A.1 to A.12 show the emulsified water volume fraction in the emulsion layer over time for all batch separation experiments presented in Chapter 5. The markers represent the calculated water volume fractions at a given time from experimental data using Eq. 4.8 and the solid lines represent the fitted water fractions over time using Eq. 5.1.

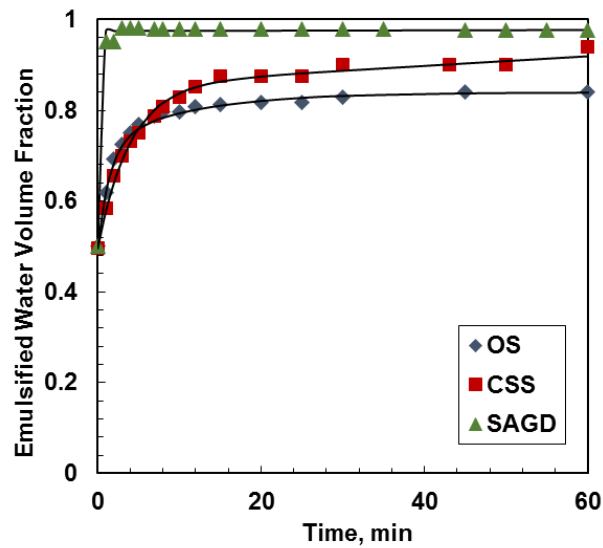


Figure A.1 Batch separation emulsified water volume fractions over time for W/O emulsions stabilized by OS, CSS, and SAGD asphaltenes at 60°C. Model emulsions were prepared with 50 vol% aqueous phase and 50 vol% organic phase. The organic phase was 1.5 g/L of asphaltenes in toluene.

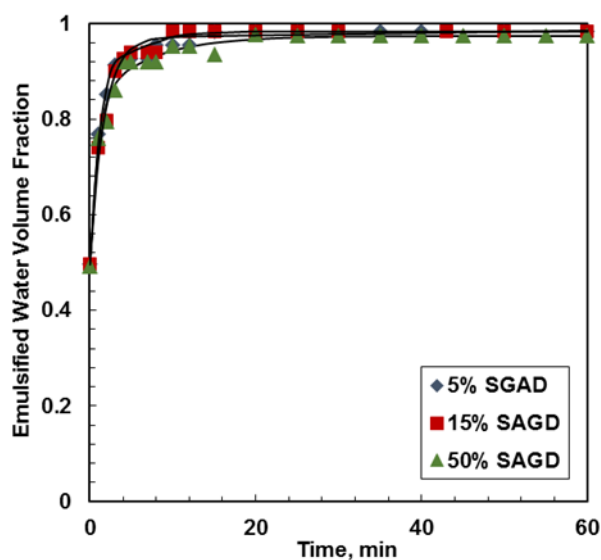


Figure A.2 Batch water volume fractions over time for W/O emulsions stabilized by OS/SAGD asphaltene blends at 60°C. Model emulsions were prepared with 50 vol% aqueous phase and 50 vol% organic phase. The organic phase was 1.5 g/L of C7-asphaltenes in toluene.

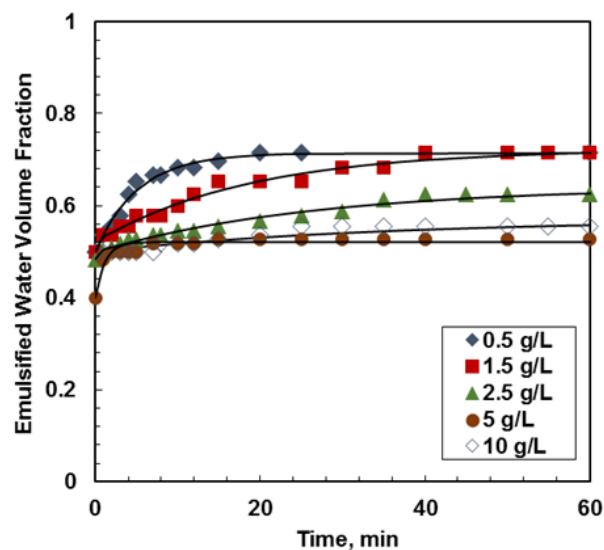


Figure A.3 Batch water volume fractions over time for W/O emulsions stabilized by OS asphaltenes at 21°C and a total volume of 50 mL. Model emulsions were prepared with 50 vol% aqueous phase and 50 vol% organic phase. The organic phases consisted of 0.5, 1.5, 2.5, 5 and 10 g/L of asphaltenes in toluene.

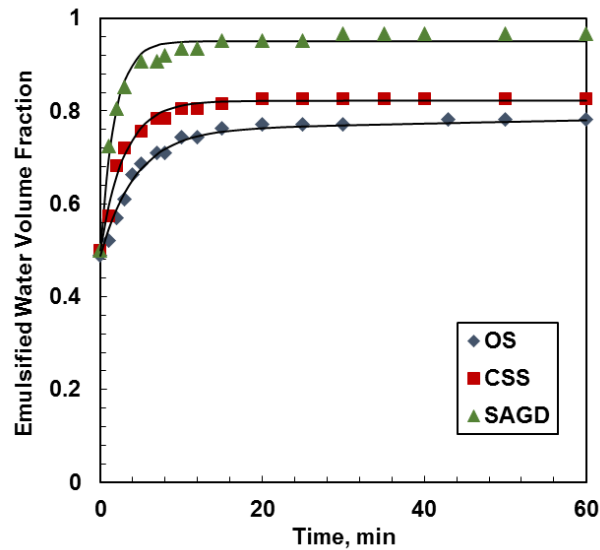


Figure A.4 Batch water volume fractions over time for water-in-50/50 heptol emulsions stabilized by OS, CSS and SAGD asphaltenes at 60°C. Model emulsions were prepared with 50 vol% aqueous phase and 50 vol% organic phase. The organic phases consisted of 1.5 g/L of C7-asphaltenes in 50/50 heptol.

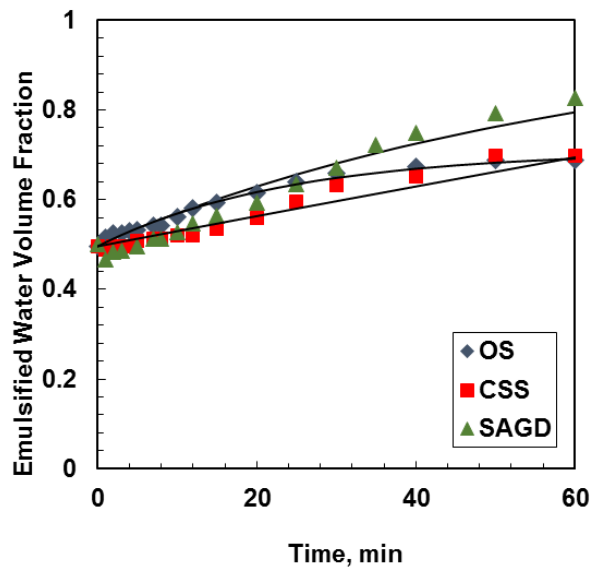


Figure A.5 Batch water volume fractions over time for W/O emulsions stabilized by OS, CSS and SAGD asphaltenes prepared at a mixing speed of 10,000 rpm with a homogenizer. Model emulsions were prepared at 60°C with 50 vol% aqueous phase and 50 vol% organic phase. The organic phase consisted of 1.5 g/L of C7-asphaltenes in toluene.

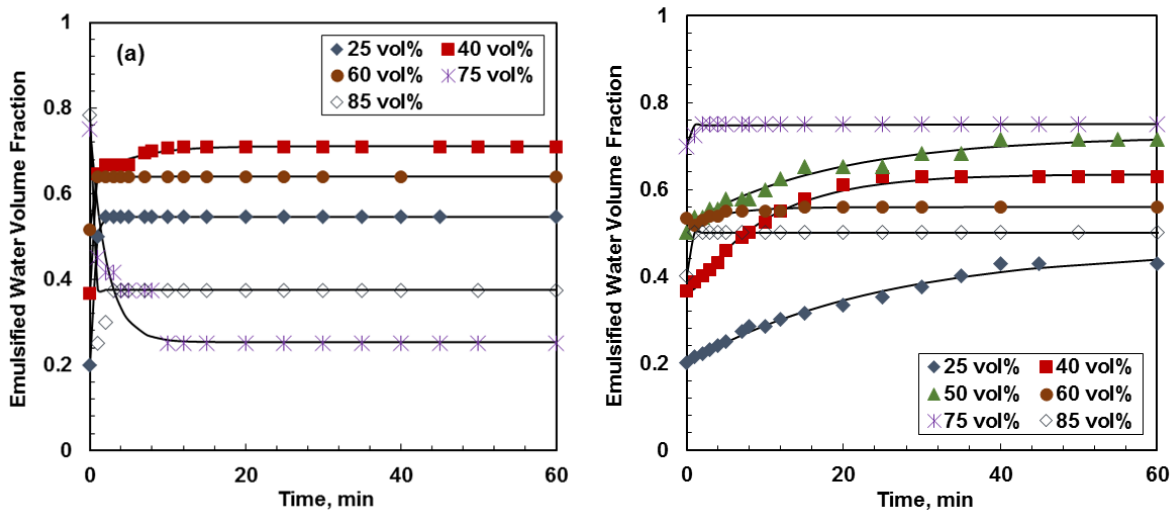


Figure A.6 Batch water volume fractions over time for W/O emulsions stabilized by OS asphaltenes prepared with initial water volume fractions from 0.25 to 0.85. Model emulsions were prepared at 60°C with 50 vol% aqueous phase and 50 vol% organic phase. The organic phases consisted of a) 0.5 g/L; b) 1.5 g/L of C7-asphaltenes in toluene.

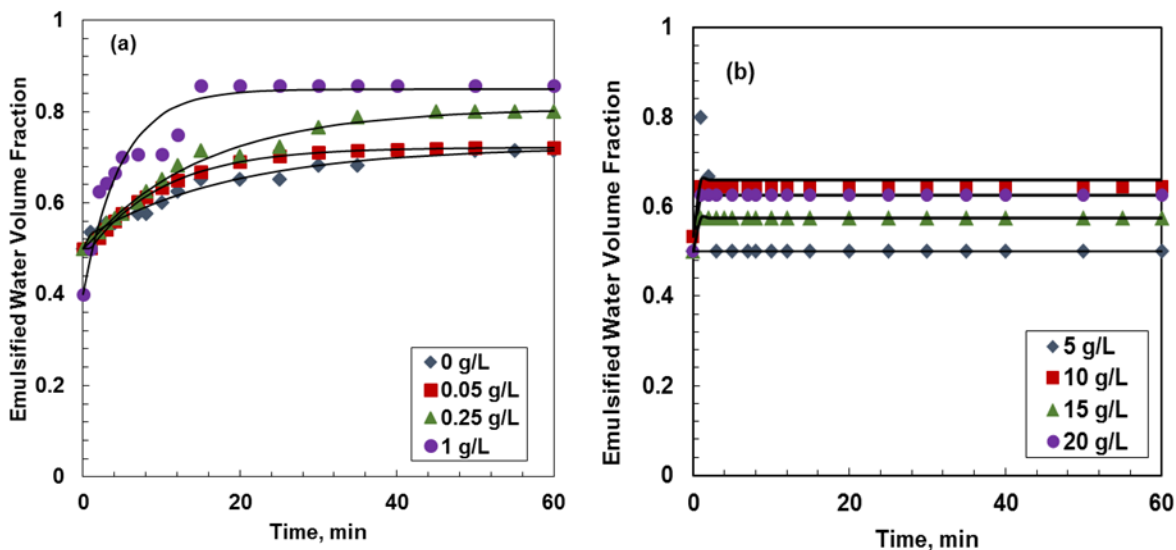


Figure A.7 Batch water volume fractions over time for W/O emulsion stabilized by OS asphaltenes with added kaolin with an 80° contact angle (a) low kaolin concentrations and (b) high kaolin concentrations. The emulsions were prepared with 50 vol% aqueous phase and 50 vol% organic phase. The organic phase was 1.5 g/L of OS C7-asphaltenes dissolved in toluene plus added kaolin.

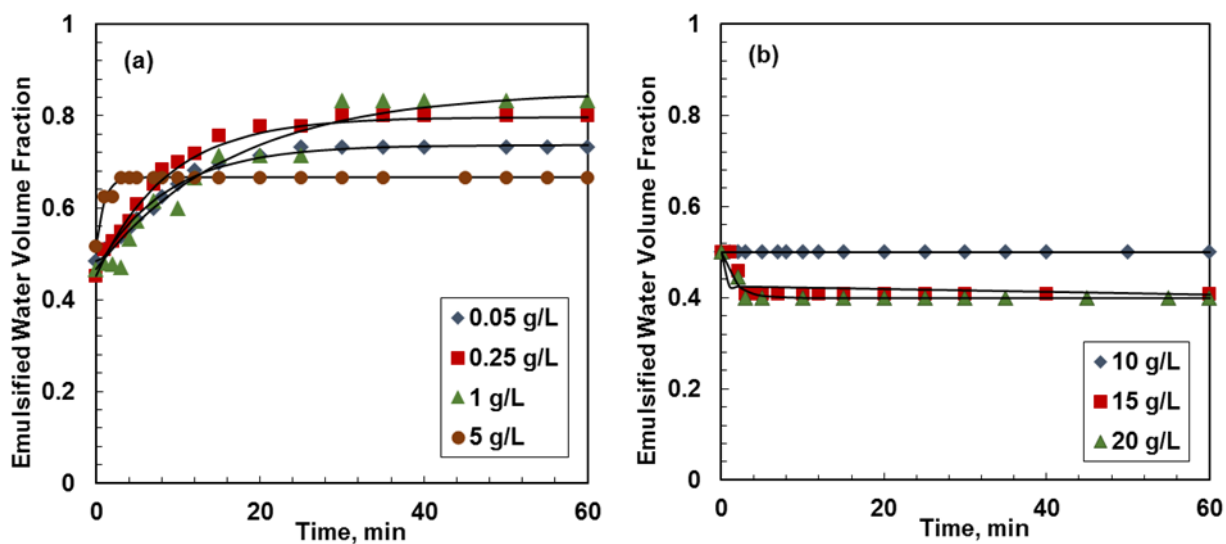


Figure A.8 Batch water volume fractions over time for W/O emulsion stabilized by OS asphaltenes with added kaolin (12 μm) with a measured contact angle of 50° at (a) low concentrations and (b) high concentrations. Emulsions were prepared with 50 vol% aqueous phase and 50 vol% organic phase with a total volume of 50 mL and 10,800 rpm mixing speed. The organic phase was 1.5 g/L of C7-asphaltenes dissolved in toluene plus added kaolin.

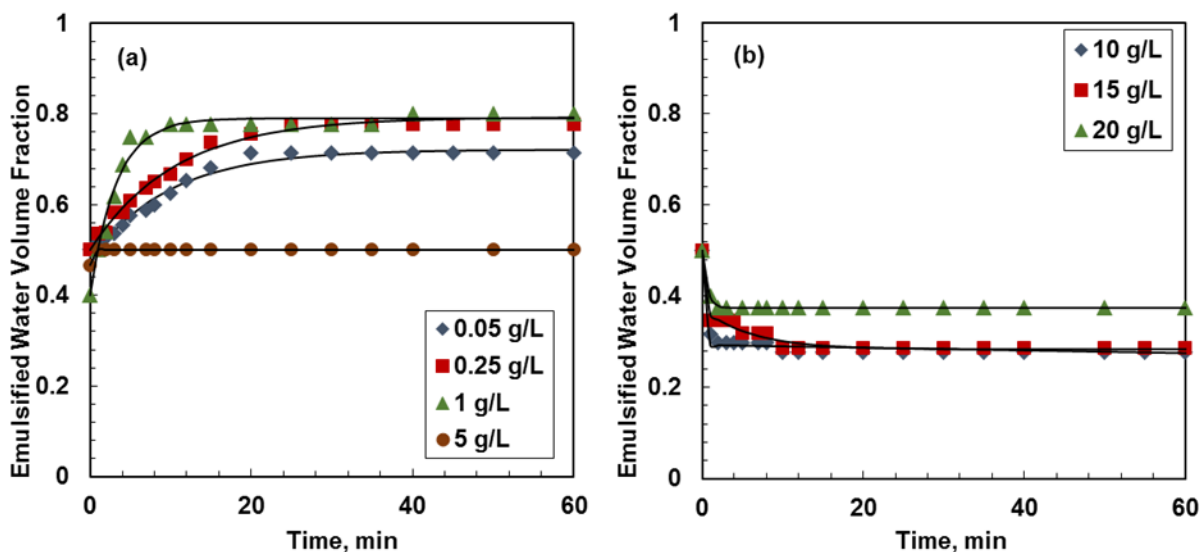


Figure A.9 Batch water volume fractions over time for W/O emulsion stabilized by OS asphaltenes with added kaolin (12 μm) with a measured contact angle of 125° at (a) low concentrations and (b) high concentrations. Emulsions were prepared with 50 vol% aqueous phase and 50 vol% organic phase with a total volume of 50 mL and 10,800 rpm mixing speed. The organic phase was 1.5 g/L of C7-asphaltenes dissolved in toluene plus added kaolin.

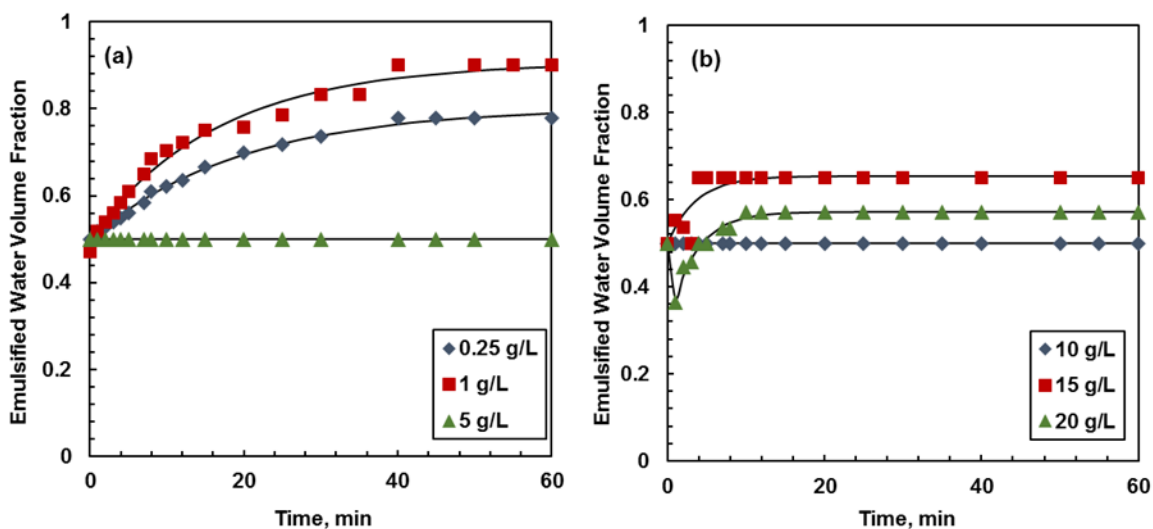


Figure A.10 Batch water volume fractions over time for W/O emulsion stabilized by silica (32-63 μm) with a measured contact angles of 75° : a) at low silica concentration b) at high silica concentration. The emulsions were prepared with 50 vol% aqueous phase and 50 vol% organic phase with a total volume of 50 mL and 10,800 rpm mixing speed. The organic phase was 1.5 g/L of OS C7-asphaltene dissolved in toluene plus added silica.

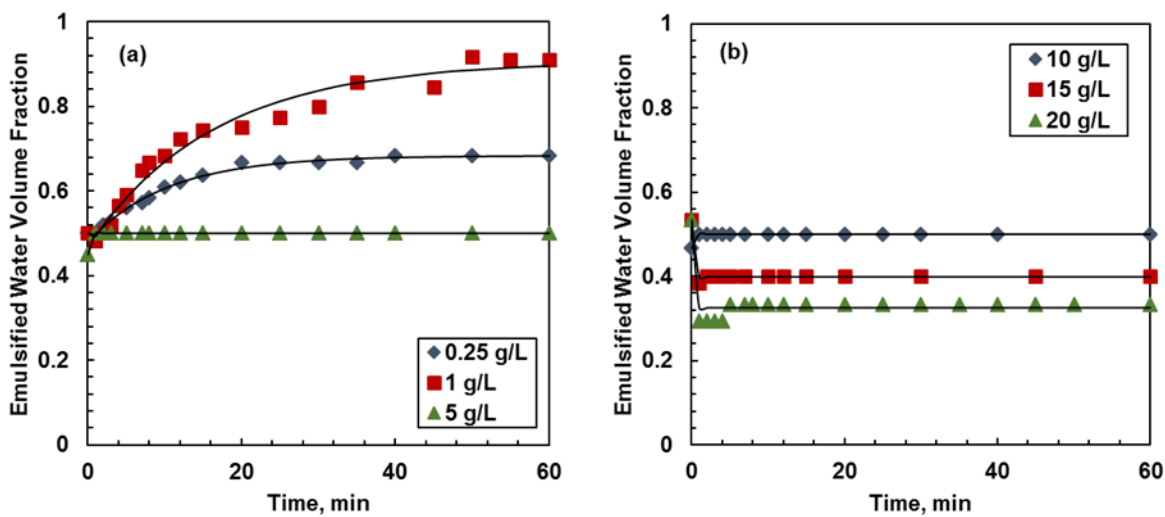


Figure A.11 Batch water volume fractions over time for W/O emulsion stabilized by silica (32-63 μm) with a measured contact angles of 115° : a) at low silica concentration b) at high silica concentration. The emulsions were prepared with 50 vol% aqueous phase and 50 vol% organic phase with a total volume of 50 mL and 10,800 rpm mixing speed. The organic phase was 1.5 g/L of OS C7-asphaltenes dissolved in toluene plus added silica.

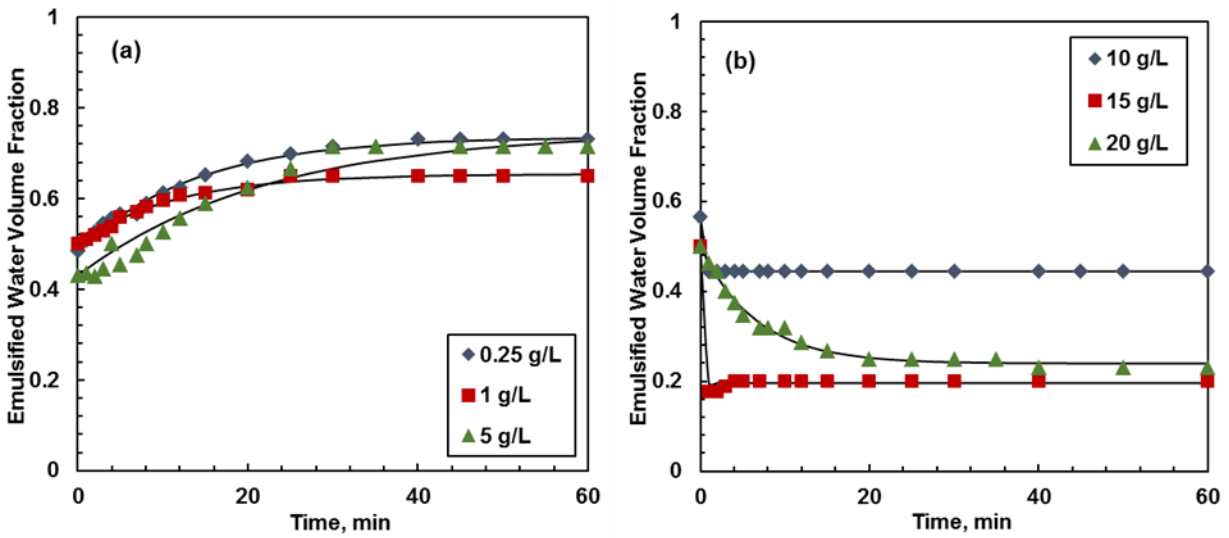


Figure A.12 Batch water volume fractions over time for W/O emulsion stabilized by OS asphaltenes with added silica (18-32 μm) with a 75° contact angle. The emulsions were prepared with 50 vol% aqueous phase and 50 vol% organic phase with a total volume of 50 mL and 10,800 rpm mixing speed. The organic phase was 1.5 g/L of C7-asphaltenes dissolved in toluene plus added silica.

APPENDIX B

EFFECT OF ASPHALTENE CONCENTRATION ON EMULSION STABILITY FOR CSS AND SAGD ASPHALTENE-STABILIZED EMULSIONS

Batch water-in-toluene emulsions stabilized by CSS and SAGD asphaltenes were prepared with a total volume of 1600 mL and mixed at 1000 rpm with the overhead mixer at 60°C and are shown in Figure B.1. The CSS asphaltene-stabilized emulsions were prepared with asphaltene concentrations of 0.5 to 2.5 g/L and the SAGD asphaltene-stabilized emulsions were prepared with asphaltene concentrations of 1.5 to 5 g/L. The emulsified water volume fractions in the emulsion layers are provided in Figure B.2. Model parameters used to fit the data are provided in Table B.1. For both cases, emulsion stability increased slightly with increasing asphaltene concentration. This result is consistent with the OS asphaltene-stabilized emulsions presented in Section 5.1.2.2.

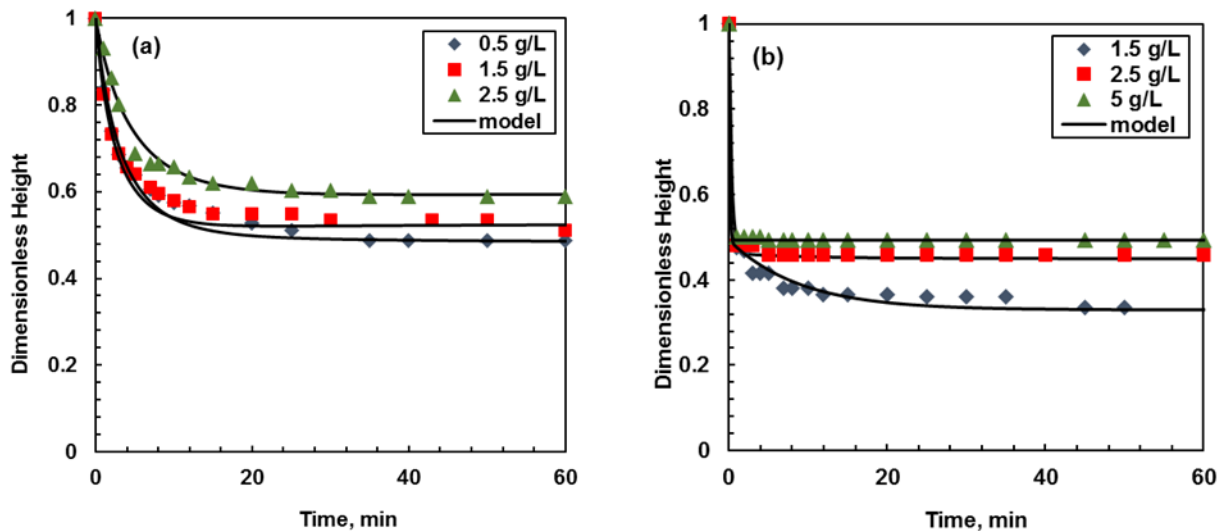


Figure B.1 Emulsion layer height over time for W/O emulsions stabilized a) CSS and b) SAGD asphaltenes for batch experiments at 60°C. Model emulsions were prepared with 50 vol% aqueous phase and 50 vol% organic phase with a total volume of 1600 mL and were mixed a 1000 rpm. The organic phases consisted of 0.5, 1.5, 2.5, and 5 g/L of C7-asphaltene in toluene.

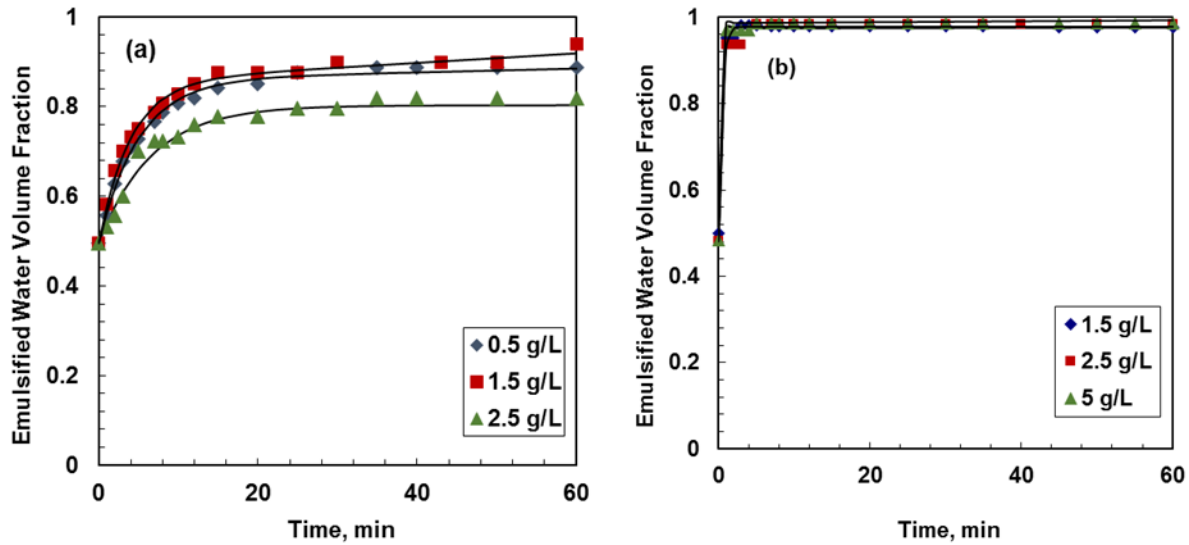


Figure B.2 Batch water volume fractions over time for W/O emulsions stabilized by (a) CSS and (b) SAGD asphaltenes at 60°C. Model emulsions were prepared with 50 vol% aqueous phase and 50 vol% organic phase. The organic phase was 0.5, 1.5, 2.5, and 5 g/L of C7-asphaltenes in toluene.

Table B.1 Model parameters used for batch experiments for water-in-toluene emulsions stabilized by CSS and SAGD asphaltene at concentrations between 0.5 and 5 g/L.

Parameter	CSS Asphaltenes (g/L)			SAGD Asphaltenes (g/L)		
	0.5	1.5	2.5	1.5	2.5	5
h_{lim}/h_o	0.50	0.54	0.60	0.33	0.45	0.50
k, min^{-1}	0.04	0.04	0.01	0.11	0.10	0.30

APPENDIX C

ERROR ANALYSIS

This appendix provides sample error analysis for emulsion layer height in batch continuous and decay experiments, solids contact angle, water volume fraction in the emulsion layer during continuous experiments, mean particle diameter and mean droplet diameter. For repeat measurements made at one experimental condition, confidence intervals were established based on the standard deviations of the sets of repeated measurements using the Student's t -distribution. A 95% confidence level was set for the error assessment for all experiments.

C.1 Error Analysis Theory

C.1.1 Error in Repeated Measurements

The sample mean, \bar{y} , of several repeated measurements made at a single experimental condition is defined as:

$$\bar{y} = \frac{\sum_{i=1}^n y_i}{n} \quad \text{Equation A.1}$$

Where y_i is the i^{th} measured value and n is the number of repeated measurements. The sample standard deviation, s , describes the variability of the data and is defined as:

$$s = \sqrt{\frac{\sum_{i=1}^n (y_i - \bar{y})^2}{n-1}} \quad \text{Equation A.2}$$

It was assumed that the distribution of error was the same for each set of repeated measurements.

The confidence interval is then determined as follows:

$$\bar{y} - t_{\left(\frac{\alpha}{2}, \nu\right)} \frac{s}{\sqrt{n}} \leq \mu \leq \bar{y} + t_{\left(\frac{\alpha}{2}, \nu\right)} \frac{s}{\sqrt{n}} \quad \text{Equation A.3}$$

Where ν is the degrees of freedom in the system equal to $n-1$, and α is the confidence level equal to $(1-\% \text{confidence interval}/100)$. In this study a 95% confidence interval has been selected, therefore $\alpha = 0.05$.

C.1.2 Average Absolute Relative Deviation

The average absolute relative deviation (AARD) of the fit of a model to experimental data is assessed with the following equation:

$$AARD = \frac{\sum_{i=1}^n \left| \frac{\mu_{fit} - \mu_{exp}}{\mu_{exp}} \right|}{n} \quad \text{Equation A.4}$$

where μ_{fit} is the predicted model measurement, μ_{exp} is the experimental measurement and n is the number of measurements.

C.2 Error in Emulsion Layer Height

C.2.1 Batch Experiment

Asphaltene-Stabilized Emulsions

The sample error analysis is presented for water-in-50/50 heptol emulsions stabilized by CSS asphaltenes and summarized in Table C.1. The emulsions were prepared from 50 vol% aqueous phase and 50 vol% organic phase mixed at 1000 rpm at 60°C, where the organic phase was 1.5 g/L CSS asphaltenes in 50/50 heptol. Four repeat experiments were used, therefore $n = 4$ and there are 3 degrees of freedom ($\nu = n - 1 = 3$), for a t-distribution value of 3.182. At a 95% confidence interval the final height of the emulsion layer was 7.5 ± 0.2 cm.

Table C.1 Error analysis for emulsion layer height in the batch experiment for a water-in-50/50 heptol emulsion stabilized by 1.5 g/L CSS asphaltenes, mixed at 1000 rpm at 60°C.

Time, min	Emulsion Layer Height, cm					Standard Deviation, cm
	Run 1	Run 2	Run 3	Run 4	Mean	
2	8.6	9.0	9.1	9.3	9.00	0.29
3	8.1	8.5	8.6	8.8	8.50	0.29
4	8.1	8.3	8.4	8.6	8.35	0.21
5	7.9	8.2	8.2	8.3	8.15	0.17
7	7.7	8.0	7.9	8.1	7.93	0.17
8	7.7	8.0	7.9	7.9	7.88	0.13
10	7.6	7.8	7.7	7.8	7.73	0.10
12	7.6	7.8	7.7	7.8	7.73	0.10
15	7.6	7.8	7.6	7.7	7.68	0.10
20	7.3	7.6	7.5	7.6	7.50	0.14
25	7.3	7.6	7.5	7.6	7.50	0.14
30	7.3	7.6	7.5	7.6	7.50	0.14
40	7.3	7.6	7.5	7.6	7.50	0.14
50	7.3	7.6	7.5	7.6	7.50	0.14
60	7.3	7.6	7.5	7.6	7.50	0.14

Solids-Stabilized Emulsions

The sample error analysis is presented for water-in-toluene emulsions stabilized by kaolin and summarized in Table C.2. The emulsions were prepared from 50 vol% aqueous phase and 50 vol% organic phase mixed at 10,000 rpm at 60°C, where the organic phase was 1.5 g/L OS asphaltenes plus 0.25 g/L kaolin (80° contact angle) in toluene. Four repeat experiments were used, therefore $n = 4$ with 3 degrees of freedom and $t = 3.182$. At a 95% confidence interval the height of the emulsion layer was on average repeatable to ± 0.11 cm.

Table C.2 Error analysis for emulsion layer height in the batch experiment for a water-in-toluene emulsion stabilized by 0.25 g/L kaolin (80° contact angle), mixed at 10,000 rpm at 60°C.

Time, min	Emulsion Layer Height, cm					Standard Deviation, cm
	Run 1	Run 2	Run 3	Run 4	Mean	
2	0.6	0.5	0.4	0.5	0.50	0.08
3	0.6	0.5	0.4	0.5	0.50	0.08
4	0.6	0.5	0.4	0.5	0.50	0.08
5	0.6	0.5	0.4	0.5	0.50	0.08
7	0.6	0.5	0.4	0.5	0.50	0.08
8	0.6	0.5	0.4	0.5	0.50	0.08
10	0.6	0.5	0.4	0.5	0.50	0.08
12	0.6	0.5	0.4	0.5	0.50	0.08
15	0.6	0.5	0.4	0.5	0.50	0.08
20	0.6	0.5	0.4	0.5	0.50	0.08
25	0.5	0.5	0.4	0.5	0.48	0.05
30	0.5	0.5	0.4	0.5	0.48	0.05
40	0.5	0.5	0.4	0.5	0.48	0.05
50	0.5	0.5	0.4	0.5	0.48	0.05
60	0.5	0.5	0.4	0.5	0.48	0.05

C.2.2 Continuous Experiment

The sample error analysis is summarized in Table C.3 for kaolin-stabilized water-in-toluene emulsions. The emulsions were prepared from 50 vol% aqueous phase and 50 vol% organic phase mixed at 10,000 rpm at 60°C, where the organic phase was 1.5 g/L OS asphaltenes plus 0.25 g/L kaolin (80° contact angle) in toluene. Three repeat experimental runs were used, therefore $n = 3$. At a 95% confidence interval the emulsion layer height was repeatable to ± 0.2 cm (or the emulsion layer volume was repeatable to ± 2 mL).

Table C.3 Error analysis for emulsion layer height in the continuous experiment for a water-in-toluene emulsion stabilized by 0.25 g/L kaolin (80° contact angle), mixed at 10,000 rpm at 60°C.

Time, min	Emulsion Layer Volume, cm				Standard Deviation, cm
	Run 1	Run 2	Run 3	Mean	
1	0.2	0.2	0.2	0.2	0
2	0.2	0.2	0.4	0.3	0.14
3	0.8	0.6	0.8	0.7	0.14
4	0.8	0.8	0.8	0.8	0
5	0.8	0.8	0.6	0.7	0.14
6	0.8	1.0	0.6	0.8	0.28
7	1.0	1.0	0.8	0.9	0.14
8	1.4	1.2	1.0	1.1	0.14
9	1.4	1.4	1.4	1.4	0
10	1.4	1.4	1.4	1.4	0

C.2.3 Decay Experiment

The sample error analysis is presented in Table C.4 for kaolin-stabilized water-in-toluene emulsions. The emulsions were prepared from 50 vol% aqueous phase and 50 vol% organic phase mixed at 10,000 rpm at 60°C, where the organic phase is 1.5 g/L OS asphaltenes and 0.25 g/L kaolin (80° contact angle) in toluene. Three repeat experiments were used, therefore $n = 3$ and there are 2 degrees of freedom. At a 95% confidence interval the height emulsion layer was repeatable to ± 0.2 cm.

Table C.4 Error analysis for emulsion layer height in the decay experiment for a water-in-toluene emulsion stabilized by 0.25 g/L kaolin (80° contact angle), mixed at 10,000 rpm at 60°C.

Time, min	Emulsion Layer Height, cm				Standard Deviation, cm
	Run 1	Run 2	Run 3	Mean	
1	1.0	1.2	1.1	1.1	0.1
2	1.0	1.2	1.1	1.1	0.1
3	1.0	1.2	1.1	1.1	0.1
5	1.0	1.2	1.1	1.1	0.1
8	1.0	1.2	1.1	1.1	0.1
10	1.0	1.0	0.8	0.93	0.11
15	1.0	1.0	0.8	0.93	0.11
20	1.0	1.0	0.8	0.93	0.11
30	0.9	1.0	0.8	0.93	0.11
40	0.9	1.0	0.8	0.9	0.1
50	0.9	1.0	0.8	0.9	0.1
60	0.9	1.0	0.8	0.9	0.1
70	0.9	1.0	0.8	0.9	0.1
80	0.9	1.0	0.9	0.93	0.05
100	0.9	1.0	0.9	0.93	0.05

C.3 Error in Solids Contact Angle Measurements

The contact angles of the treated kaolin and silica particles were measured directly by a Drop Shape Analyzer equipped with a camera. To measure the contact angle a water drop was placed on the flat surface of a compacted disc of the treated solids immersed in a 50/50 heptol solution. Measurements were repeated on the same disc.

Kaolin

The error analysis for the three phase contact angle measurements of kaolin-50/50 heptol-water systems are summarized in Table C.5. In this work, the contact angles were measured through the water phase after the solids had been treated with OS asphaltenes at concentrations between 0.02 and 1 g/L, dried and then compressed into flat discs.

Table C.5 Error analysis for contact angle measurements for kaolin-50/50 heptol-water systems, where the kaolin has been treated with 0.02-1 g/L OS asphaltenes.

Asphaltene Concentration, g/L	$\bar{y}, ^\circ$	$s, ^\circ$	n	t	$t_{\left(\frac{\alpha}{2}, v\right)} \frac{s}{\sqrt{n}}, ^\circ$
0.02	50.42	3.04	3	4.30	7.55
0.05	80.34	2.00	4	3.18	3.18
0.10	114.13	0.29	4	3.18	0.45
0.15	123.13	3.36	4	3.18	5.34
0.20	126.04	1.81	5	2.78	2.25
0.50	133.27	1.76	4	3.18	2.80
1.00	135.82	2.95	3	4.30	7.32

Silica

The error analysis for the three phase contact angle measurements of silica-50/50 heptol-water systems are summarized in Table C.6. In this work, the contact angles were measured after the solids had been treated with OS asphaltenes at concentrations between 0.02 and 1 g/L.

Table C.6 Error analysis for contact angle measurements for silica-50/50 heptol-water systems, where the silica has been treated with 0.02-1 g/L OS asphaltenes.

Asphaltene Concentration, g/L	$\bar{y}, ^\circ$	$s, ^\circ$	n	t	$t_{\left(\frac{\alpha}{2}, v\right)} \frac{s}{\sqrt{n}}, ^\circ$
0.02	74.69	2.06	7	2.45	1.91
0.05	84.27	1.04	5	2.78	1.30
0.10	109.27	4.81	6	2.57	5.05
0.15	115.17	0.51	5	2.78	0.63
0.20	124.82	1.88	7	2.45	1.74
0.50	134.01	3.49	6	2.57	3.67
1.00	141.17	1.56	4	3.18	2.49

C.4 Water Volume Fraction in the Emulsion Layer during the Continuous Experiment

The error analysis for the determination of the water volume fraction in the emulsion layer during the continuous experiment is summarized in Table C.7. Water volume fractions were measured at three time intervals (3, 5 and 10 minutes) at two experimental conditions: 1.5 g/L OS and CSS asphaltenes in toluene mixed at 1000 rpm at 60°C. The average water volume fraction was 0.68 ± 0.11 between the two data sets.

Table C.7 Error analysis for the water volume fraction in the emulsion layer.

Experimental Condition	\bar{y}	s	n	t	$t_{\left(\frac{\alpha}{2}, v\right)} \frac{s}{\sqrt{n}}$
CSS Asphaltenes	0.67	0.15	3	4.30	0.37
OS Asphaltenes	0.69	0.02	3	4.30	0.05
Overall	0.68	0.096	6	2.57	0.11

C.5 Particle Size Distribution

The particle size distribution of the treated kaolin and larger silica particles was measured using FBRM methods in the lab, giving average particle diameters of $11.93 \pm 0.02 \mu\text{m}$ and $53.84 \pm 1.71 \mu\text{m}$ respectively. The error analysis for the particle size distributions are summarized in Table C.8.

Table C.8 Error analysis for the particle size distributions.

	$\bar{y}, \mu\text{m}$	$s, \mu\text{m}$	n	t	$t_{\left(\frac{\alpha}{2}, v\right)} \frac{s}{\sqrt{n}}, \mu\text{m}$
Kaolin	11.93	0.07	59	2.00	0.02
Silica	53.84	4.57	30	2.04	1.71

C.6 Droplet Size Distribution.

Droplet size distributions were measured water-in-toluene emulsions stabilized by OS asphaltenes. The emulsions were prepared at two mixing speeds: 1000 rpm with an impeller and 10,000 rpm with a homogenizer. The error in the drop size distributions is summarized in Table C.9, with average droplet diameters of $20.3 \pm 2.5 \mu\text{m}$ and $8.0 \pm 0.3 \mu\text{m}$ for emulsions mixed at 1000 rpm and 10,000 rpm respectively.

Table C.9 Error analysis for the droplet size distributions.

	$\bar{y}, \mu\text{m}$	$s, \mu\text{m}$	n	t	$t_{\left(\frac{\alpha}{2}, v\right)} \frac{s}{\sqrt{n}}, \mu\text{m}$
1000 rpm	20.25	30.73	575	1.96	2.51
10,000 rpm	7.95	5.17	939	1.96	0.33